17/9/76

GRANITIC AND MIGMATITIC ROCKS OF THE COOKE HILL AREA, SOUTH AUSTRALIA AND THEIR STRUCTURAL SETTING

by

SYED ABUL FAZLIL ABBAS

M.Sc. (Karachi)

Department of Geology and Mineralogy

The University of Adelaide

Adelaide

South Australia

August 1975

FIGURES

FIGURE 1

A portion of the Mannum 1 mile Sheet showing the area studied

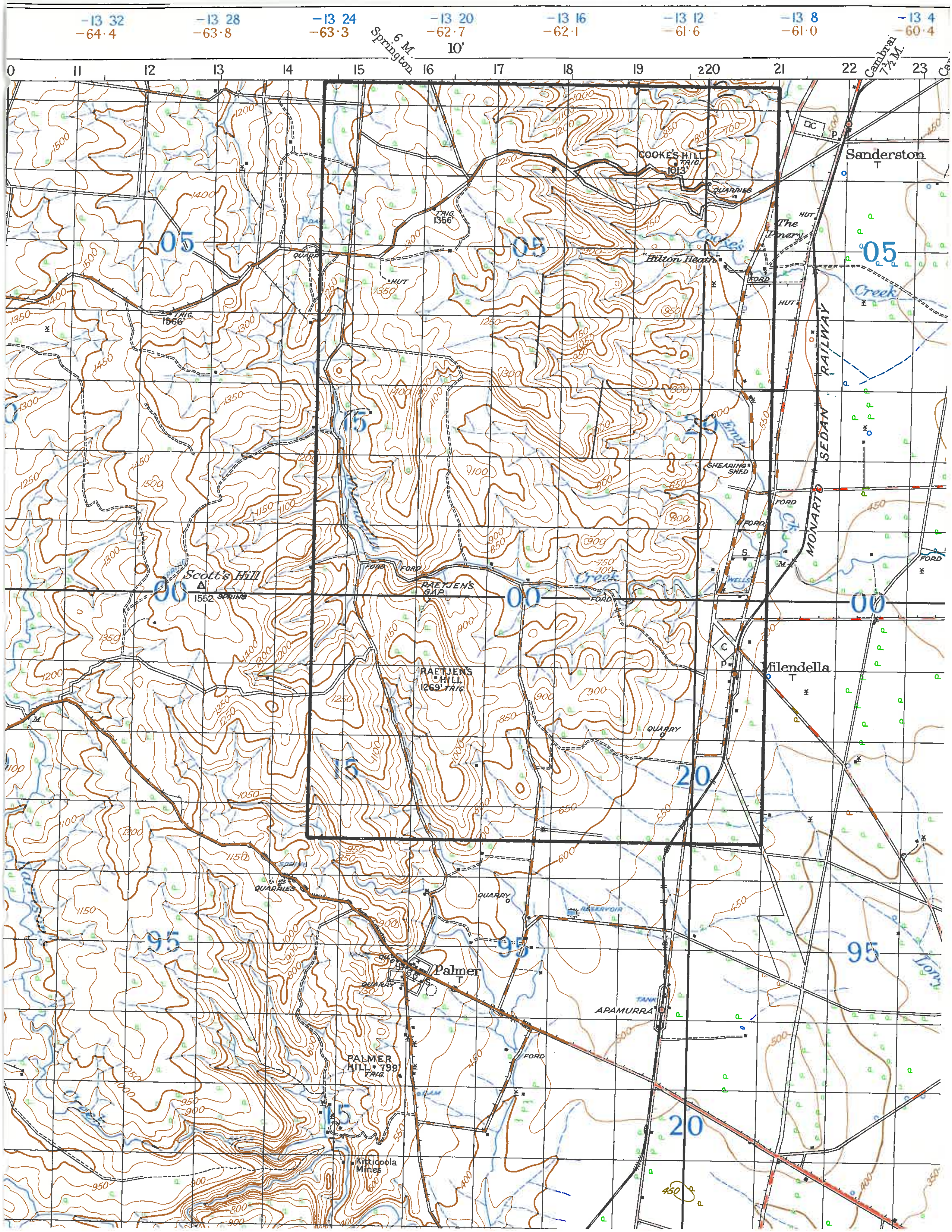

Springton 6 M.
Cambrai 7½ M.
Sanderston
COOKE'S HILL TRIG. 1013'
QUARRIES
The Pinery
"Hilton Heath"
Cooke's Creek
TRIG. 1356'
TRIG. 1566'
Scott's Hill 1552
SPRING
RAETJEN'S GAP
RAETJEN'S HILL 1269' TRIG.
SHEARING SHED
MONARTO SEDAN RAILWAY
Milendella
QUARRY
FORD
WELLS
RESERVOIR
Palmer
APAMURRA
TANK
PALMER HILL 799 TRIG.
Kitticoola Mines
QUARRIES

FIGURE 2

A generalized geological map of the Mt. Lofty Ranges showing the sedimentary and metamorphic rocks of the Archaean, Adelaide Supergroup, Kanmantoo Group and Cainozoic cover. The important limestone beds of the Kanmantoo Group are indicated on the map. The location of the area studied is outlined in the eastern part of the Mt. Lofty Ranges.

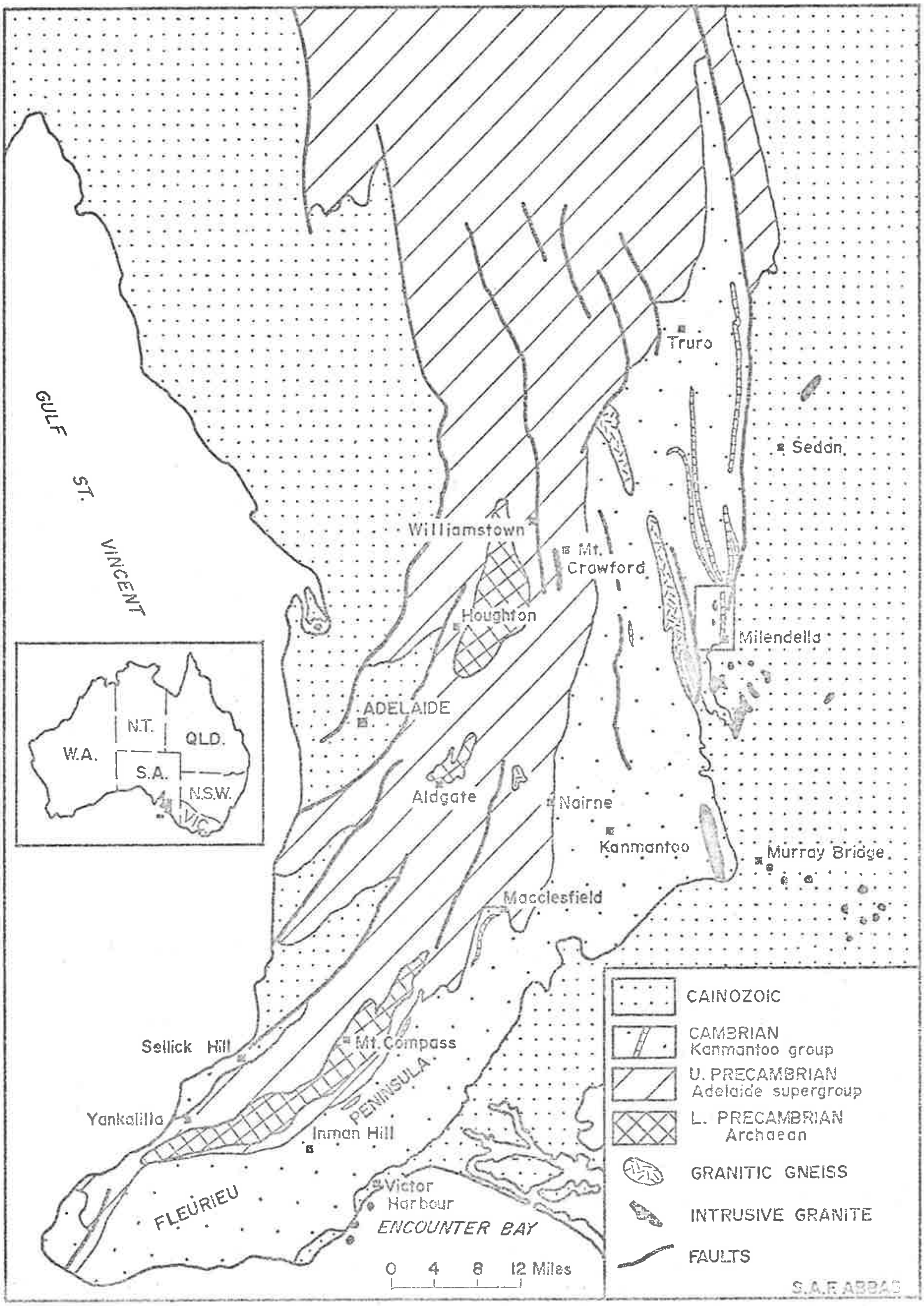
GULF ST. VINCENT
Truro
Sedan
Williamstown
Mt. Crawford
Houghton
Milendella
ADELAIDE
N.T.
QLD.
W.A.
S.A.
N.S.W.
VIC.
Aldgate
Nairne
Kanmantoo
Murray Bridge
Macclesfield
Sellick Hill
Mt. Compass
PENINSULA
Yankalilla
Inman Hill
FLEURIEU
Victor Harbour
ENCOUNTER BAY
0 4 8 12 Miles
CAINOZOIC
CAMBRIAN
Kanmantoo group
U. PRECAMBRIAN
Adelaide supergroup
L. PRECAMBRIAN
Archaean
GRANITIC GNEISS
INTRUSIVE GRANITE
FAULTS
S.A.F. ABBAS

FIGURE 3

Kanmantoo Group sedimentation during the Waitpinga Subsidence

(after Thomson, 1969b)

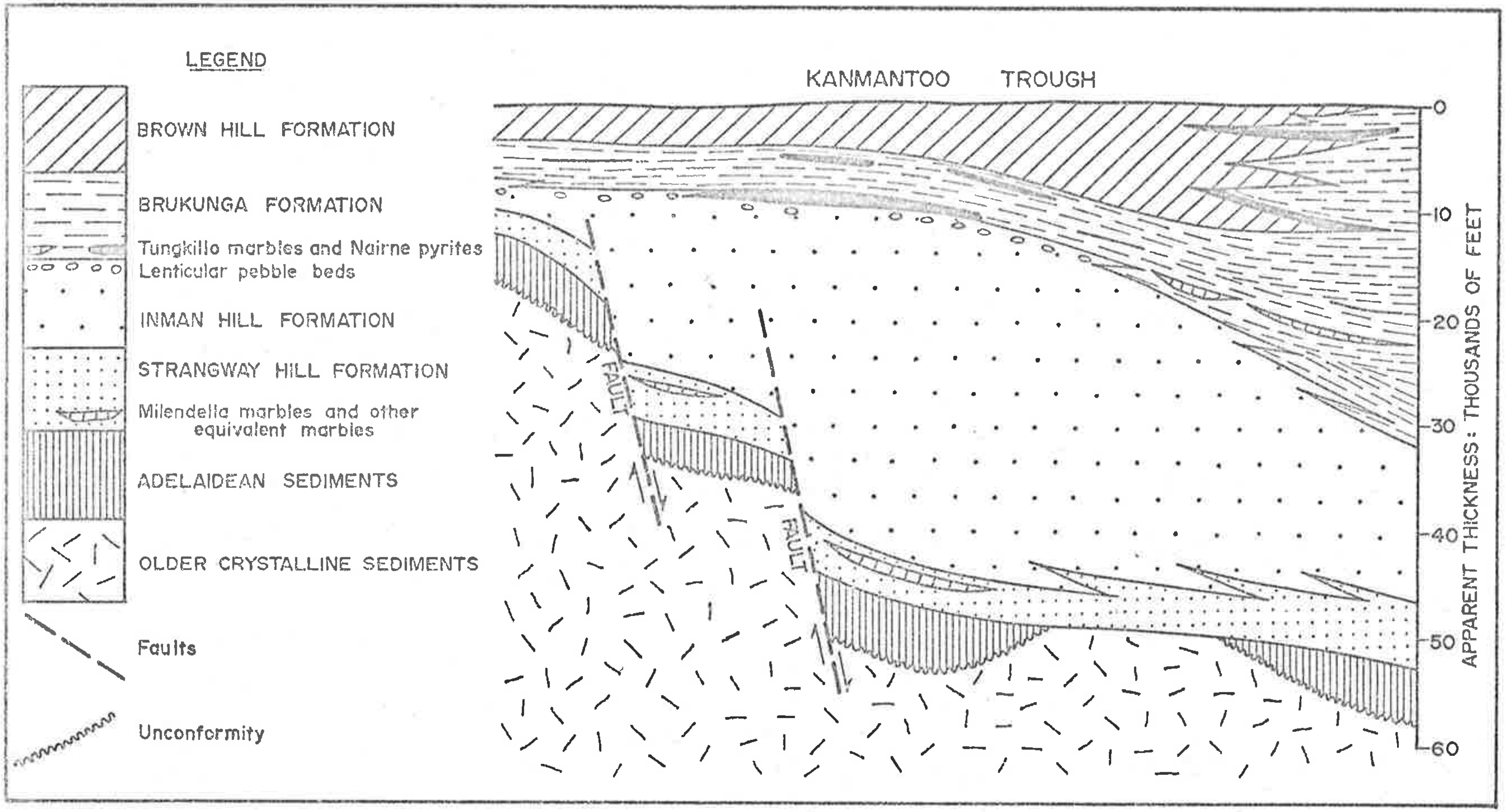

LEGEND
BROWN HILL FORMATION
BRUKUNGA FORMATION
Tungkillo marbles and Nairne pyrites
Lenticular pebble beds
INMAN HILL FORMATION
STRANGWAY HILL FORMATION
Milendella marbles and other equivalent marbles
ADELAIDEAN SEDIMENTS
OLDER CRYSTALLINE SEDIMENTS
Faults
Unconformity
KANMANTOO TROUGH
FAULT
FAULT
0
10
20
30
40
50
60
APPARENT THICKNESS: THOUSANDS OF FEET

FIGURE 4

A generalized geological map showing the grade of metamorphism in the post-Archaean rocks of the Mt. Lofty Ranges. Note the extent of the migmatite zone rocks in the eastern part of the Ranges

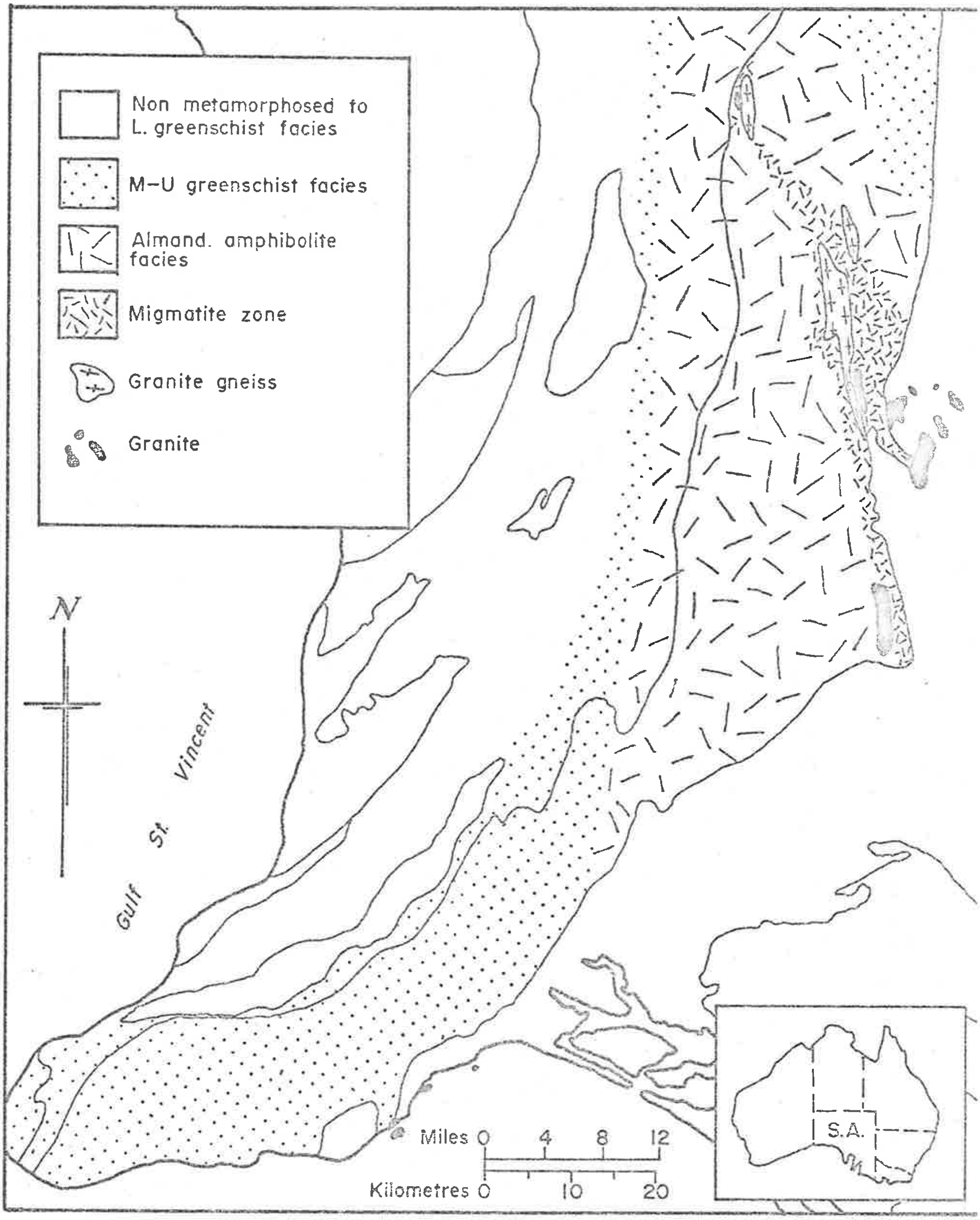
Non metamorphosed to L. greenschist facies
M-U greenschist facies
Almand. amphibolite facies
Migmatite zone
Granite gneiss
Granite
N
Gulf St. Vincent
Miles 0 4 8 12
Kilometres 0 10 20
S.A.

FIGURE 5

PROFILES OF F_1 FOLDS

A F_1 folds in the calc-schist with marked axial plane schistosity (S_1), defined by preferred orientation of actinolite prisms. The actinolite rich layer is shown by stippling.

LOCATION: 169981

B Style of F_1 folding in scapolite rich band (stippled) in the marble. The axial plane schistosity (S_1) is produced by elongation of calcite grains parallel to axial plane of folds.

LOCATION: 197038

C F_1 folds in the thinly laminated quartzo-feldspathic gneiss. The axial plane schistosity (S_1) is well developed and defined by preferred orientation of biotite plates.

LOCATION: 171034

D F_1 folds in the banded quartzo-feldspathic gneiss. The light bands are rich in quartz-feldspar (stippled) and dark bands are rich in biotite (blank).

LOCATION: 170044

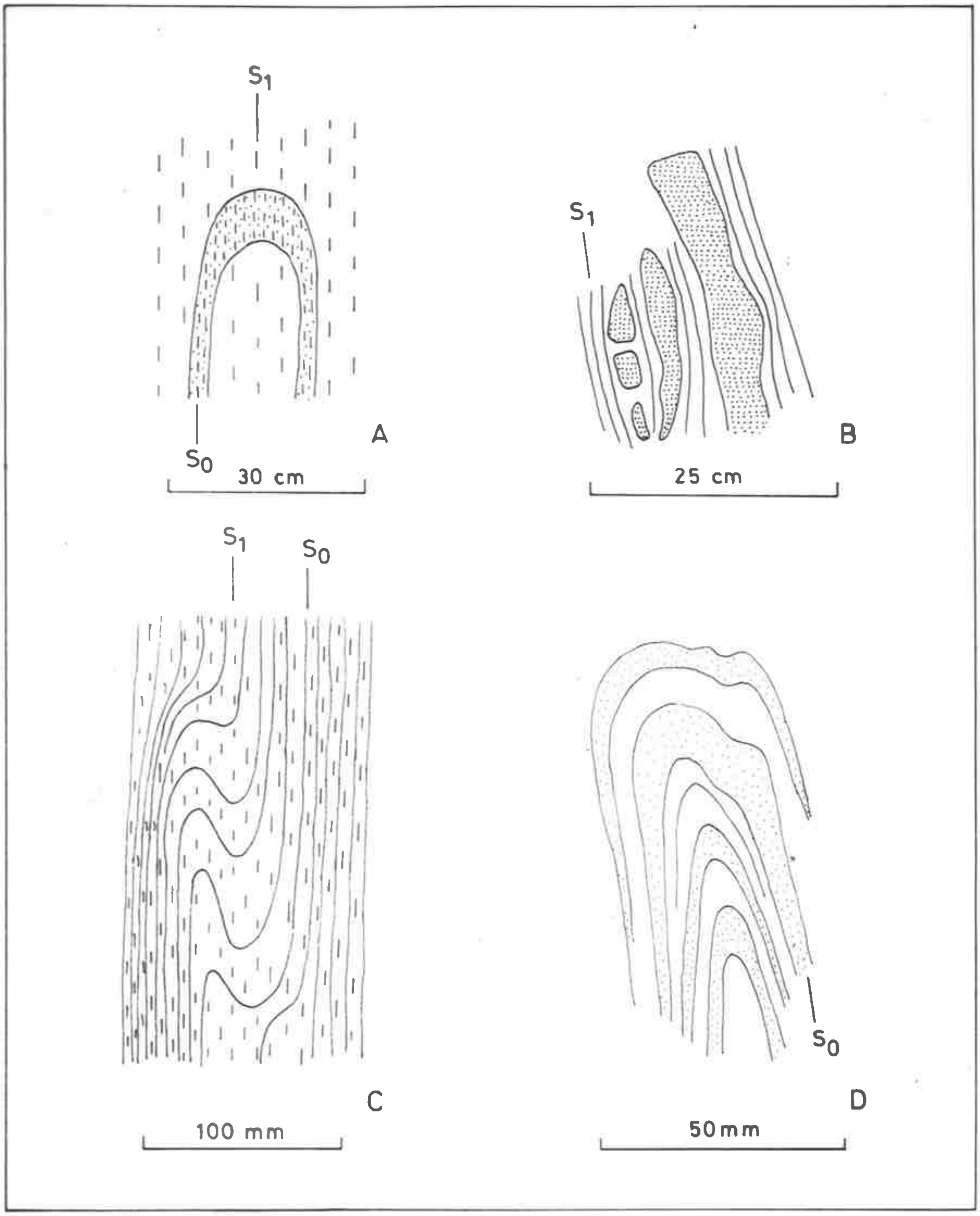
S1
S0
30 cm
A
S1
25 cm
B
S1
S0
100 mm
C
S0
50mm
D

FIGURE 6

PROFILES OF F_2 FOLDS

A F_2 folds in the thinly laminated quartzo-feldspathic gneiss

LOCATION: 179040

B F_2 folds in the migmatite. The leucocratic vein (blank) shows varying thickness in the limbs of folds

LOCATION: 171061

C F_2 folds in the thinly laminated quartzo-feldspathic gneiss. A granitic vein is parallel to the axial plane of the fold.

LOCATION: 179022

D F_2 folds in the banded quartzo-feldspathic and semi-pelitic schists. The axial plane schistosity (S_2) is well developed in the hinges of the folds. A pegmatitic vein is emplaced parallel to axial plane of the folds.

LOCATION: 199059

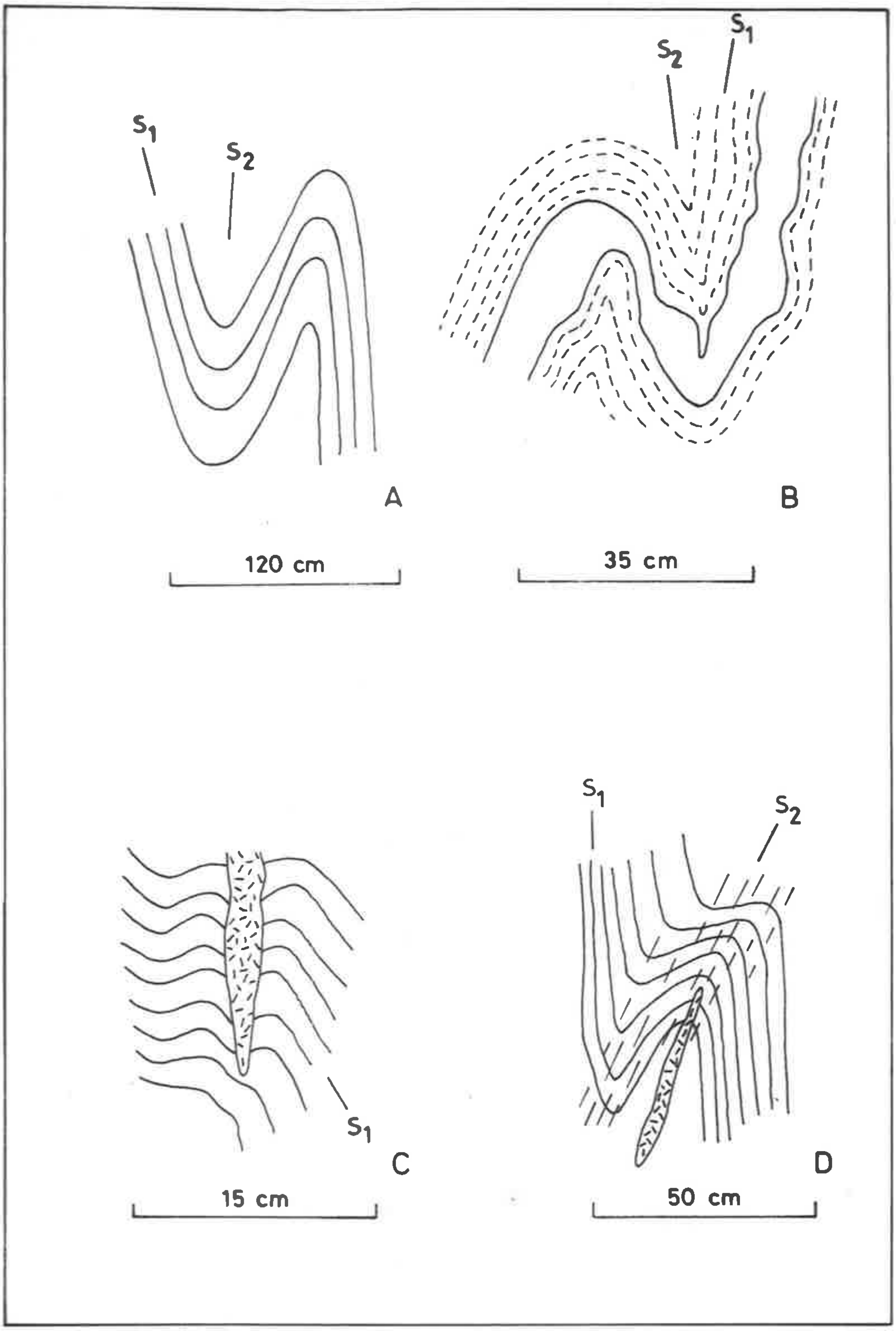
S1
S2
A
120 cm
S2
S1
B
35 cm
S1
C
15 cm
S1
S2
D
50 cm

FIGURE 7

REFOLDED STRUCTURES

A F_1 folds are refolded by F_2 folds in the banded quartzo-feldspathic gneiss. S_2 schistosity is well developed along the axial plane of F_2 folds. The quartzo-feldspathic layers are stippled and the biotite rich layers are blank in this figure.

LOCATION: 166016

B F_1 folds refolded by F_2 folds in the interbedded meta-arkose (the quartzo-feldspathic layers are stippled and biotite rich layers are blank). The S_2 schistosity is well developed parallel to axial plane of F_2 folds in the biotite rich layers. Note small crenulation in the tightly hinged zone of F_2 folds.

LOCATION: 199059

C F_1 folds refolded by F_2 folds in the quartzo-feldspathic gneiss. Note gentle folding in one limb of fold and small crenulation in the other limb.

LOCATION: 185027

D Isoclinal F_1 folds refolded by an open F_2 fold in the quartzo-feldspathic gneiss. S_1 schistosity is well developed parallel to axial plane of F_1 folds.

LOCATION: 182047

E F_1 folds refolded by F_2 folds in the quartzo-feldspathic gneiss.

LOCATION: 168015

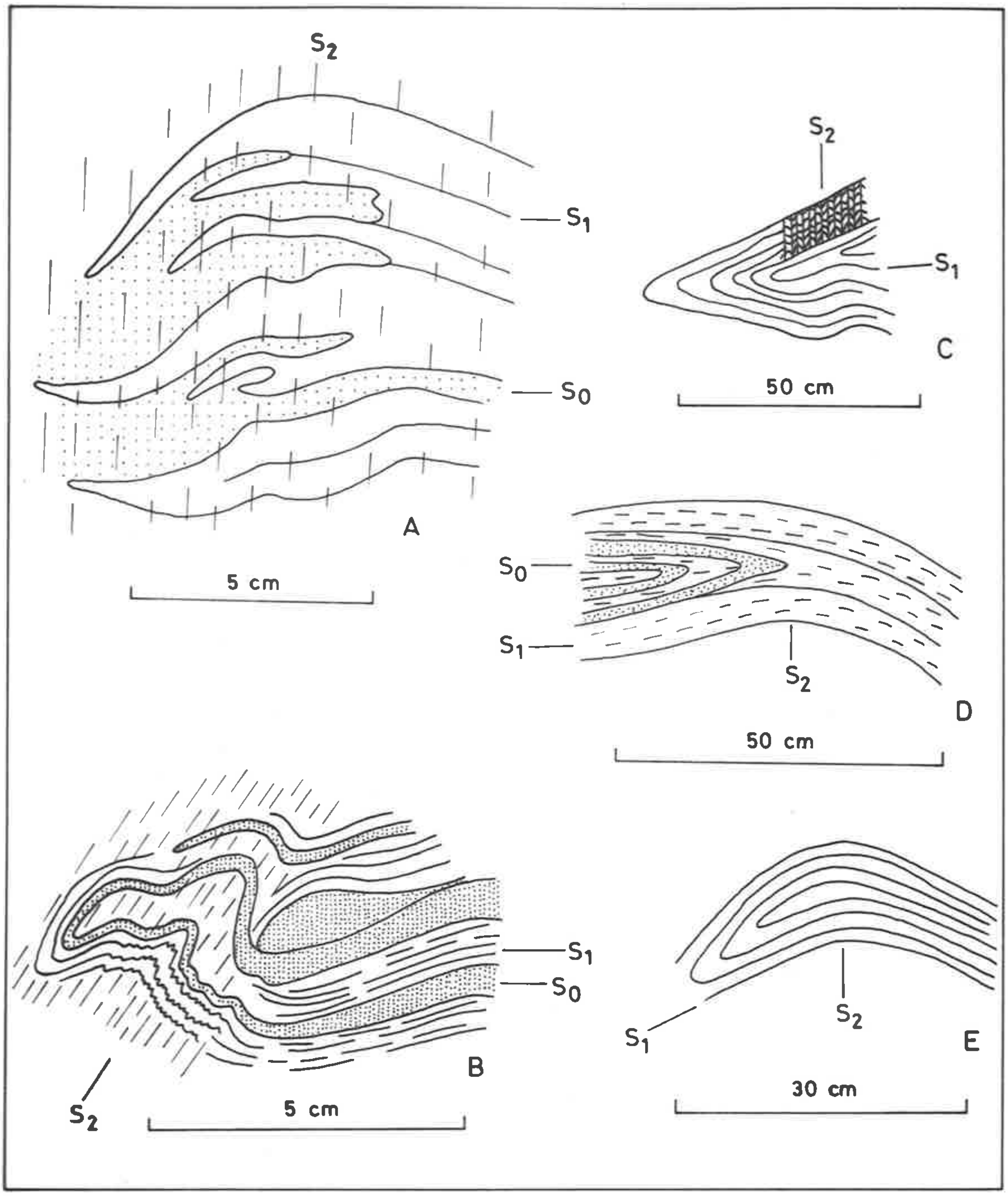

S2
S1
S0
A
5 cm
S2
S1
C
50 cm
S0
S1
S2
D
50 cm
S1
S0
S2
B
5 cm
S1
S2
E
30 cm

FIGURE 8

Dip isogons drawn on F_2 folds in alternate quartzo-feldspathic and biotite rich layers. Note the thickening of hinges in both rock types (drawn and enlarged from a large thin section: A285/473)

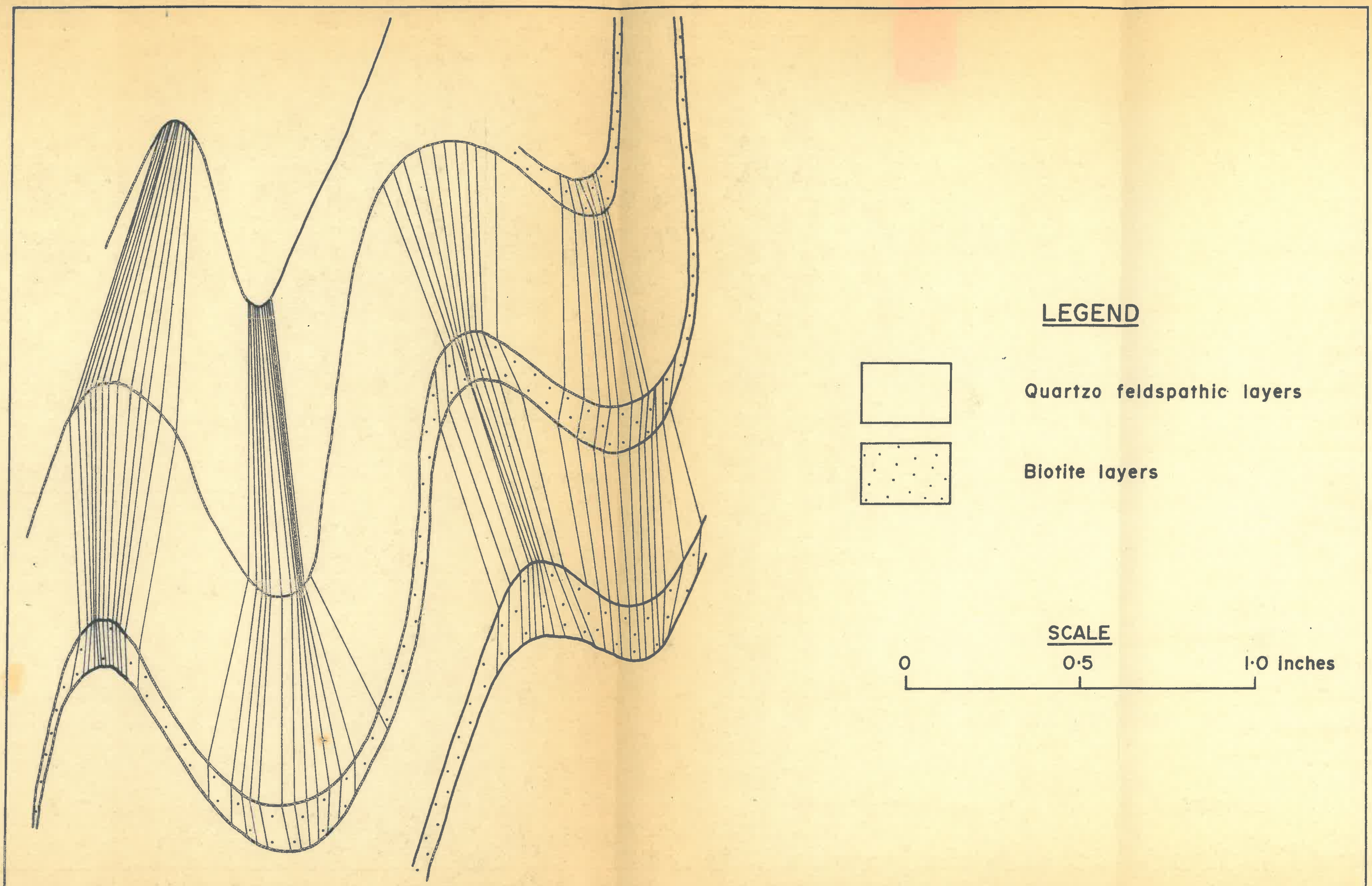
LEGEND
Quartzo feldspathic layers
Biotite layers
SCALE
0
0·5
1·0 inches

FIGURE 9

Structural map showing the trends of F_1 and F_2 major structures in the Cooke Hill and adjacent areas (redrawn from the Adelaide Sheet (1:250,000) after slight modification)

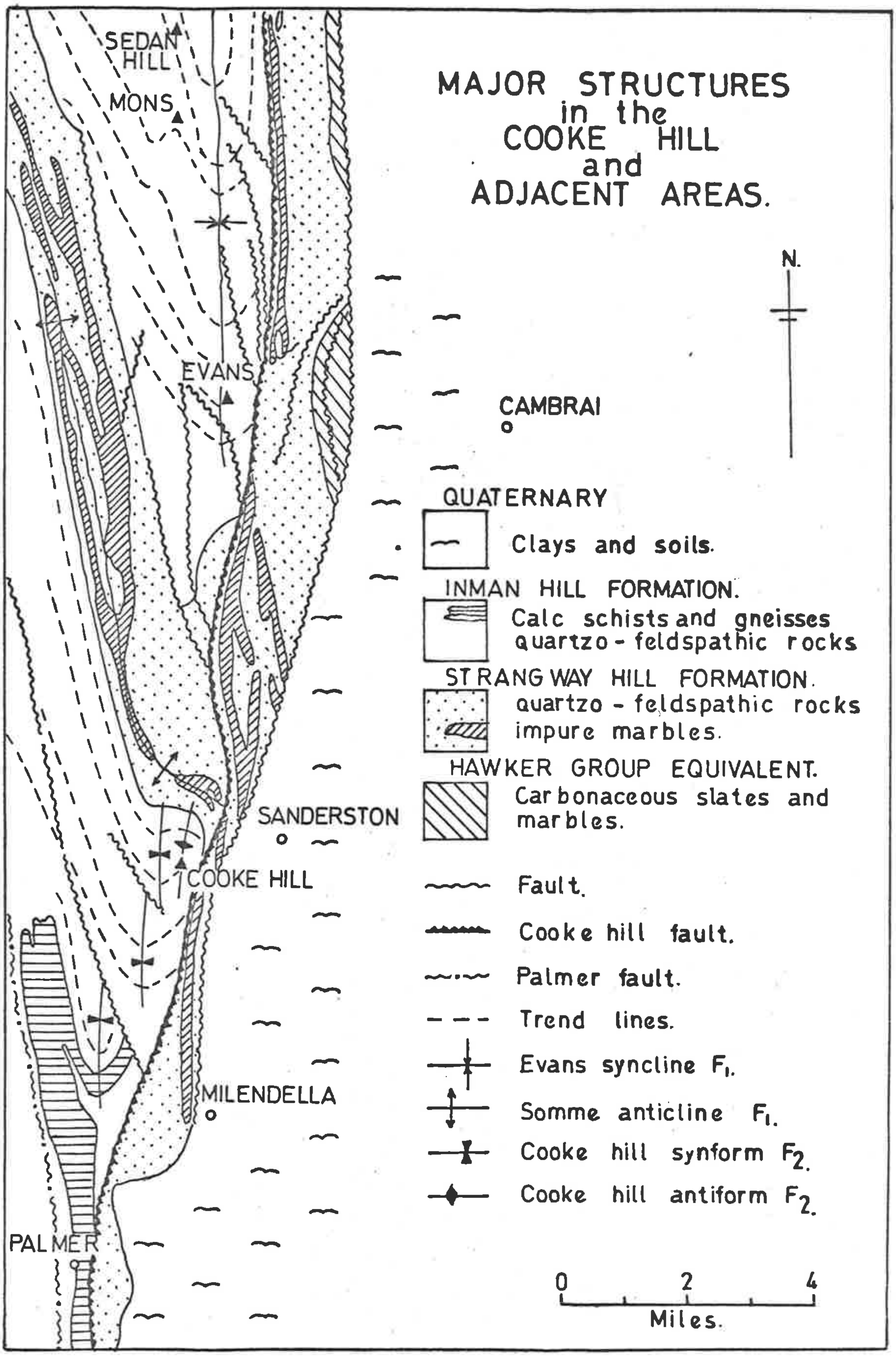

MAJOR STRUCTURES in the COOKE HILL and ADJACENT AREAS.
N.
SEDAN HILL
MONS
EVANS
CAMBRAI
SANDERSTON
COOKE HILL
MILENDELLA
PALMER
QUATERNARY
Clays and soils.
INMAN HILL FORMATION.
Calc schists and gneisses quartzo-feldspathic rocks
STRANG WAY HILL FORMATION.
quartzo-feldspathic rocks
impure marbles.
HAWKER GROUP EQUIVALENT.
Carbonaceous slates and marbles.
Fault.
Cooke hill fault.
Palmer fault.
Trend lines.
Evans syncline F_1.
Somme anticline F_1.
Cooke hill synform F_2.
Cooke hill antiform F_2.
0
2
4
Miles.

FIGURE 10

Collective diagram showing structural elements in the Cooke Hill area.

The figures in brackets represent the contour values expressed as percentage of points per 1 percent area.

A Poles to S_1 (1, 2, 3, 5 & 6%)
600 points

B Poles to S_0(.5, 1, 2, 3, 5, 7, 8 & 10%)
86 points

C Mineral lineation - L (undifferentiated)
(1, 5, 9 & 18%)
287 points

D Fold axes - F_1
43 points

E Mineral lineation - L_2 (1, 5, 10, 15, 20 & 25%)
62 points

F Fold axes - F_2 (1, 5, 10, 13 & 16%)

G Poles to axial planes of F_2 folds
(1, 5, 10, 15, 20 & 25%)
65 points

H Geometry of S_1, F_2 fold axes and maximum of L_2

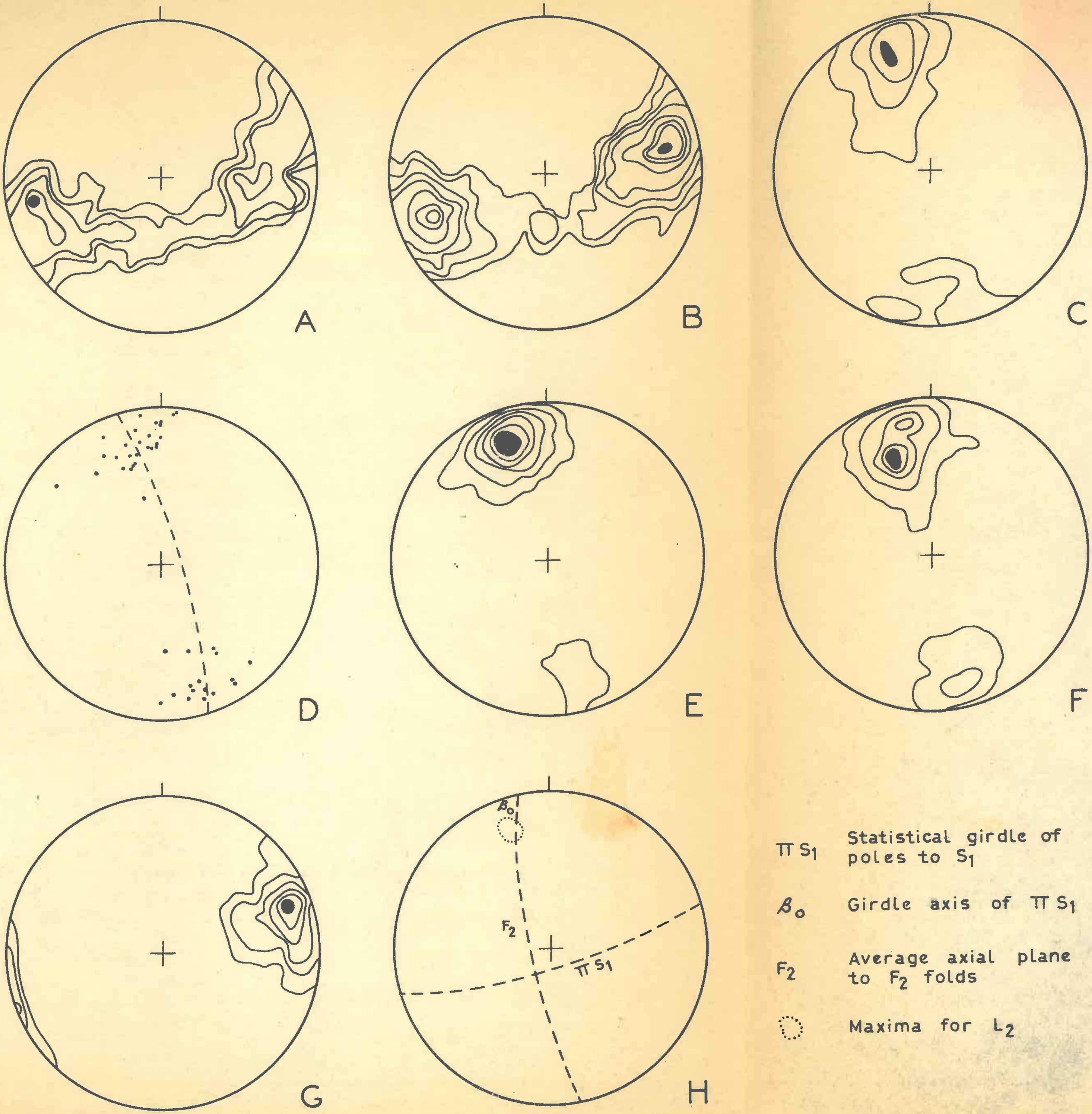
A
B
C
D
E
F
G
β₀
F₂
π S₁
H
π S₁ Statistical girdle of poles to S₁
β₀ Girdle axis of π S₁
F₂ Average axial plane to F₂ folds
Maxima for L₂

FIGURE 11

Stereographic projections showing the relation of the structural elements in the sub-areas of the Cooke Hill area.

Sub-area 1 : Number of poles to S_1 87 points

Sub-area 2 : " " " " " 131 points

Sub-area 3 : " " " " " 109 points

Sub-area 4 : " " " " " 55 points

Sub-area 5 : " " " " " 128 points

Sub-area 6 : " " " " " 94 points

Contour values for S_1 are marked on each diagram

Fig. 11

MESOSCOPIC STRUCTURAL DATA

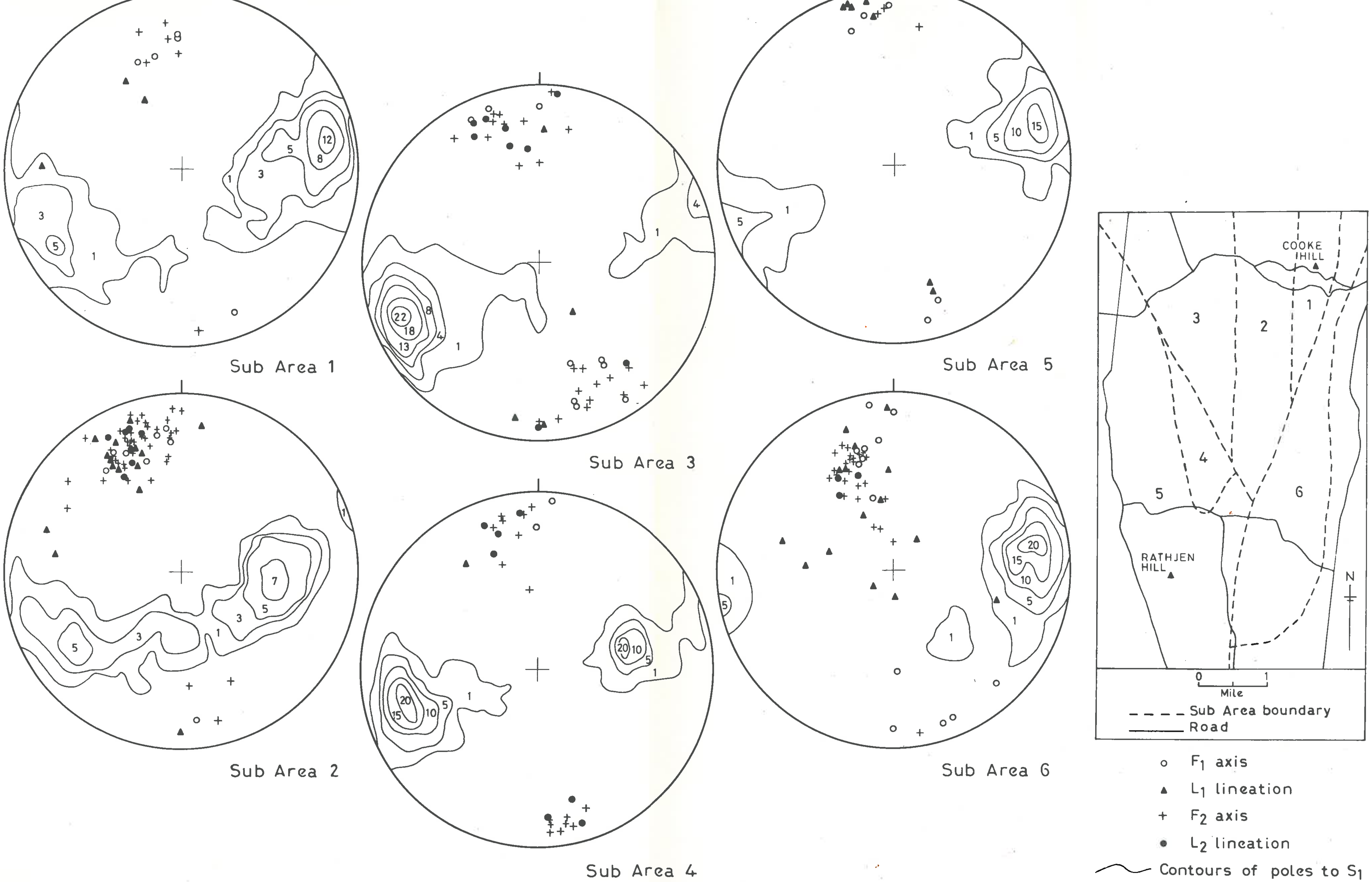

FIGURE 12

Macroscopic geometry of S_1 in the Cooke Hill area. Average girdle of πS_1 for each sub-area (numbered 1 to 6); β - axes of πS_1 (small numbered circles); Maxima for L_2 lineation (dotted circle) and the average axial plane of F_2 folds (marked F_2)

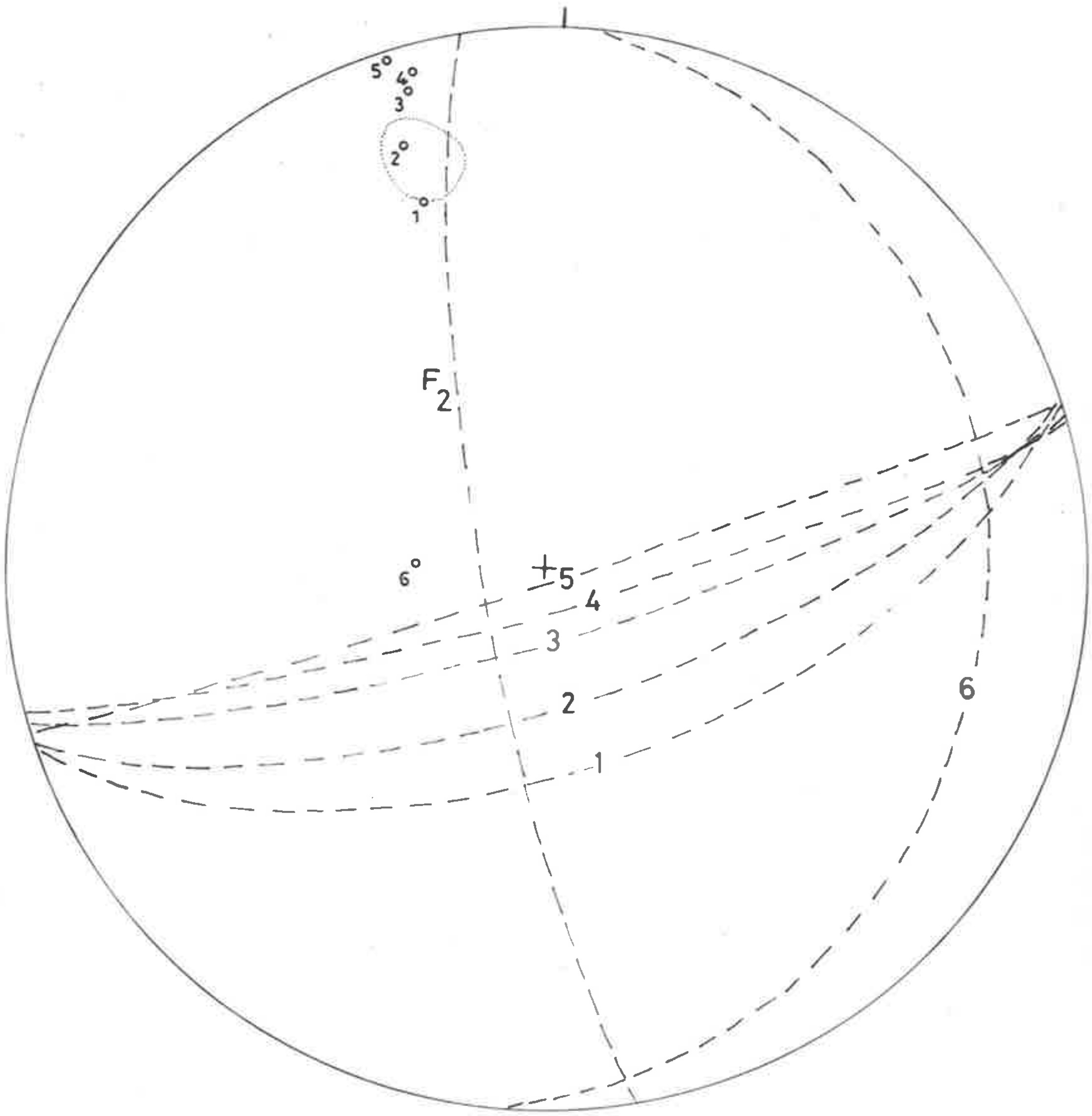

5
4
3
2
1
F2
6
5
4
3
2
1
6

FIGURE 13

Four geological sections showing the stratigraphic sequence of the Strangway Hill and the Inman Hill Formations in the Cooke Hill area (see Map 1)

Fig. 13

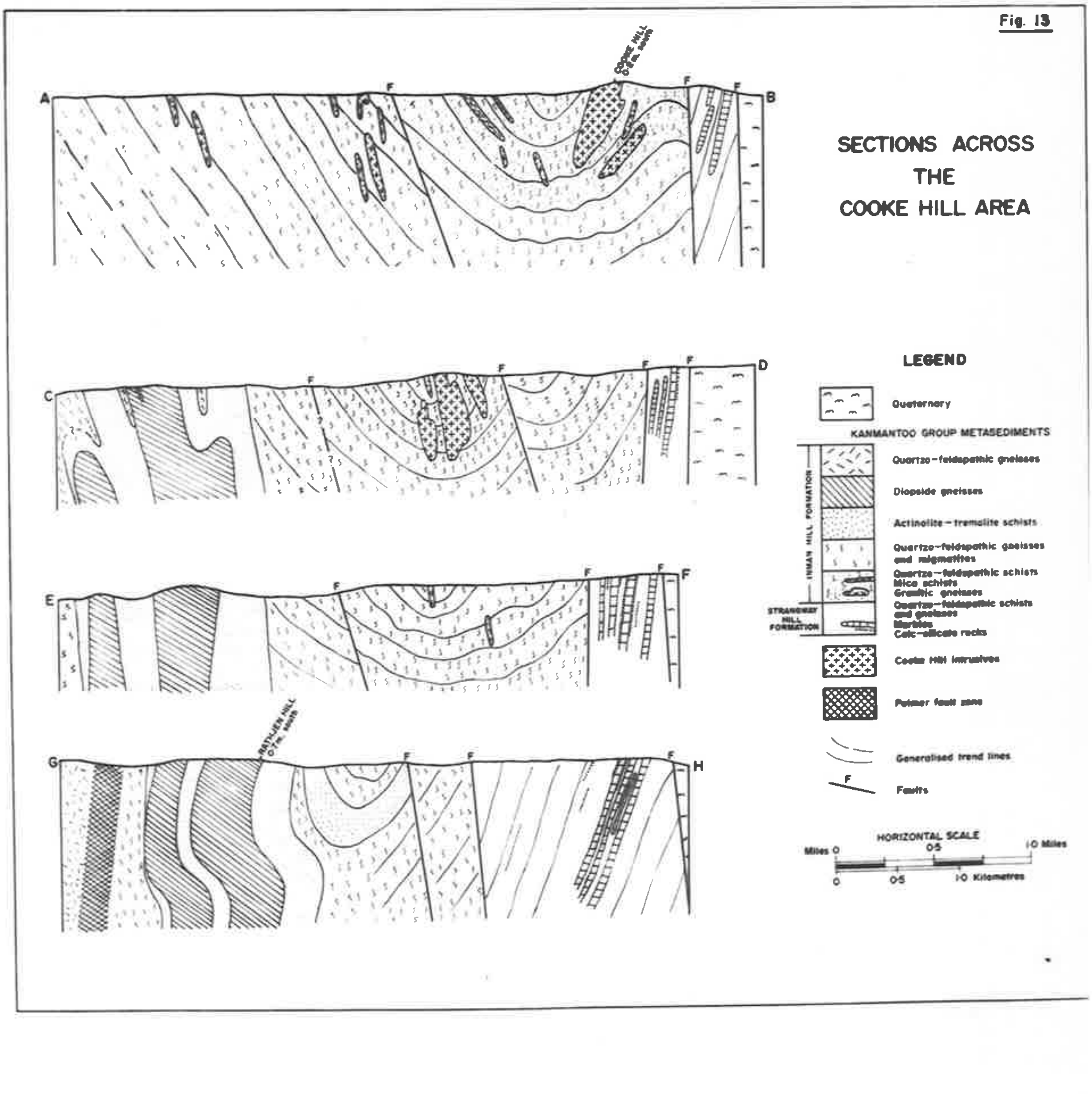
SECTIONS ACROSS THE COOKE HILL AREA
A
B
C
D
E
F
G
H
LEGEND
Quaternary
KANMANTOO GROUP METASEDIMENTS
INMAN HILL FORMATION
Quartzo-feldspathic gneisses
Diopside gneisses
Actinolite-tremolite schists
Quartzo-feldspathic gneisses and migmatites
Quartzo-feldspathic schists
Mica schists
Granitic gneisses
STRANGWAY HILL FORMATION
Quartzo-feldspathic schists and gneisses
Marbles
Calc-silicate rocks
Cooke Hill intrusives
Palmer fault zone
Generalised trend lines
Faults
HORIZONTAL SCALE
Miles 0
0·5
1·0 Miles
0
0·5
1·0 Kilometres

FIGURE 14

Mineralogical composition of the quartzo-feldspathic and semi-pelitic rocks in terms of quartz, feldspar and others (mica and accessories) (diagram after Pettijohn, 1957). Micrometric analyses by White (1966a). Solid circles represent mica content less than 20% and open circles mica content more than 20%

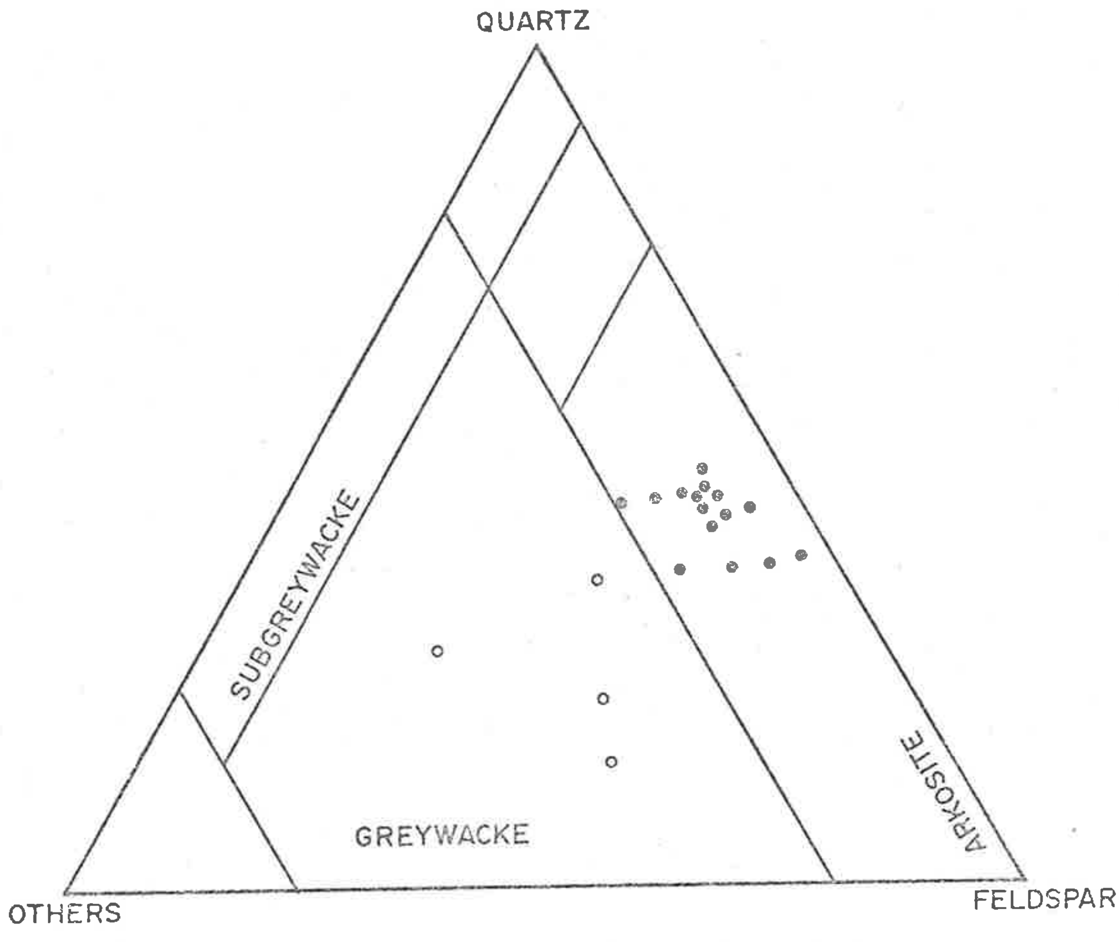
QUARTZ
SUBGREYWACKE
ARKOSITE
GREYWACKE
OTHERS
FELDSPAR

FIGURE 15

A Curves showing limits of stability of muscovite

Curve - A (after B. W. Evans, 1965)

Curve - A' (after H. S. Yoder & H. P. Eugster, 1955)

Curve - A" (after B. Velde, 1966)

B Equilibrium phase diagram for alumino-silicate minerals and stability field of muscovite in presence of quartz in hydrous condition

(1) Stability fields of sillimanite-kyanite-andalusite proposed by Newton (1966b)

(2) Stability curve for the system

muscovite + quartz $\rightleftharpoons$ sillimanite + potash-feldspar + water (after Evans, 1965)

(3) Beginning of melting curve for granite (Luth, Jahns & Tuttle, 1964)

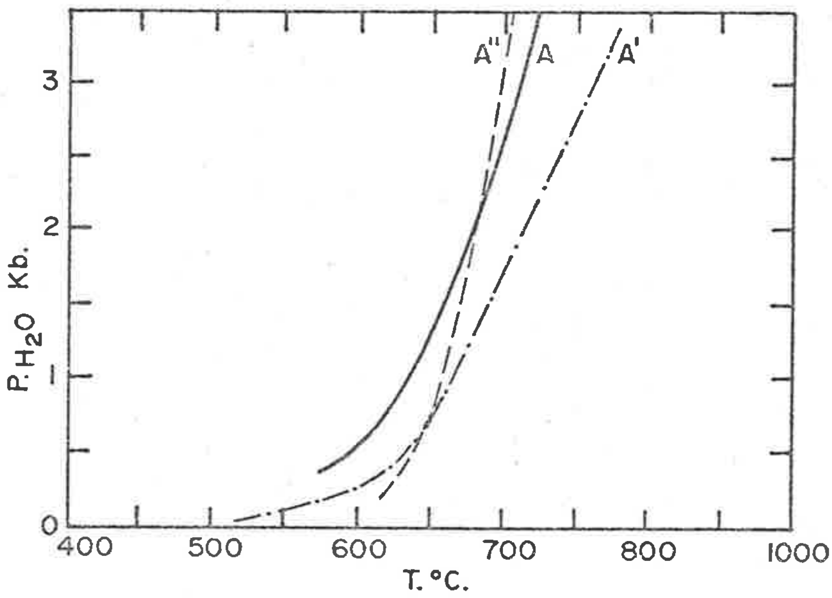
A''
A
A'
3
2
1
0
P. H_2O Kb.
400
500
600
700
800
1000
T. °C.

A

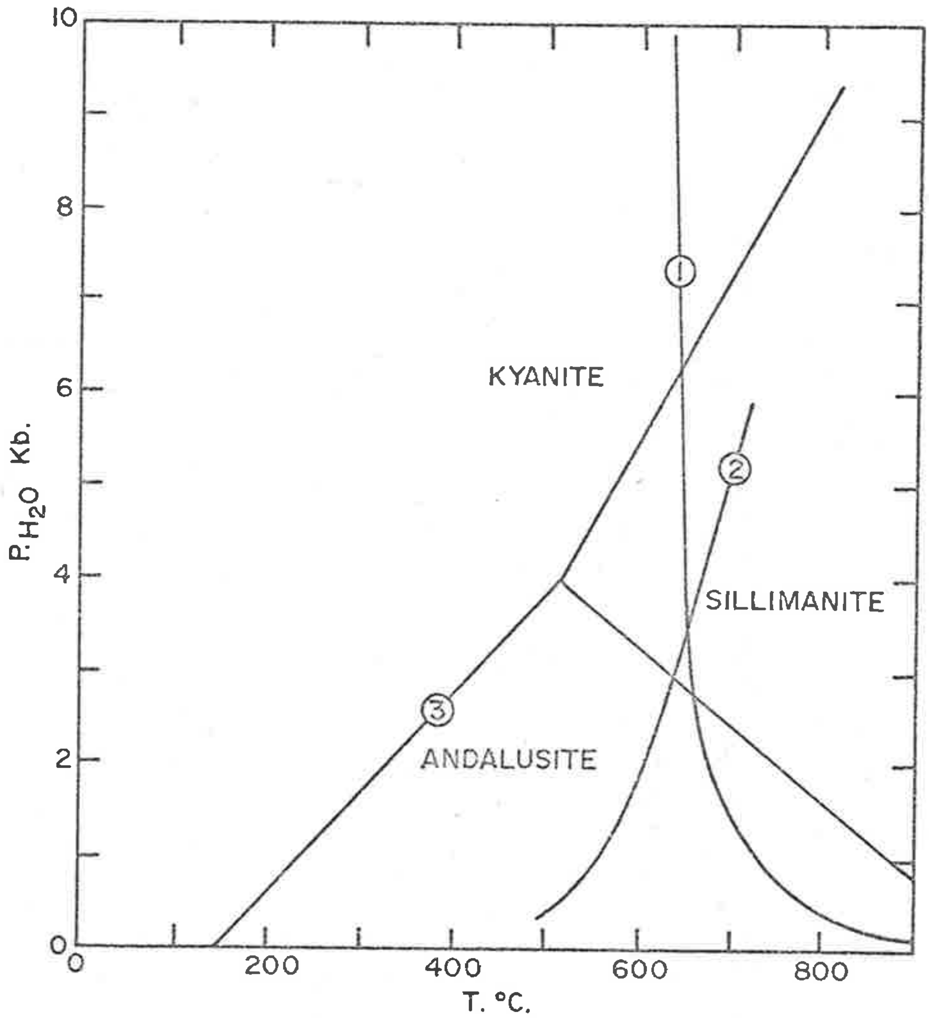
10
8
6
4
2
0
P. H_2O Kb.
0
200
400
600
800
T. °C.
KYANITE
SILLIMANITE
ANDALUSITE
1
2
3

B

FIGURE 16

Mineralogical composition of leucocratic veins (open circles) and host rock (filled circles) of migmatite expressed in terms of quartz, feldspar and biotite (Fig. 16A) and quartz, plagioclase and potash feldspar (Fig. 16B)

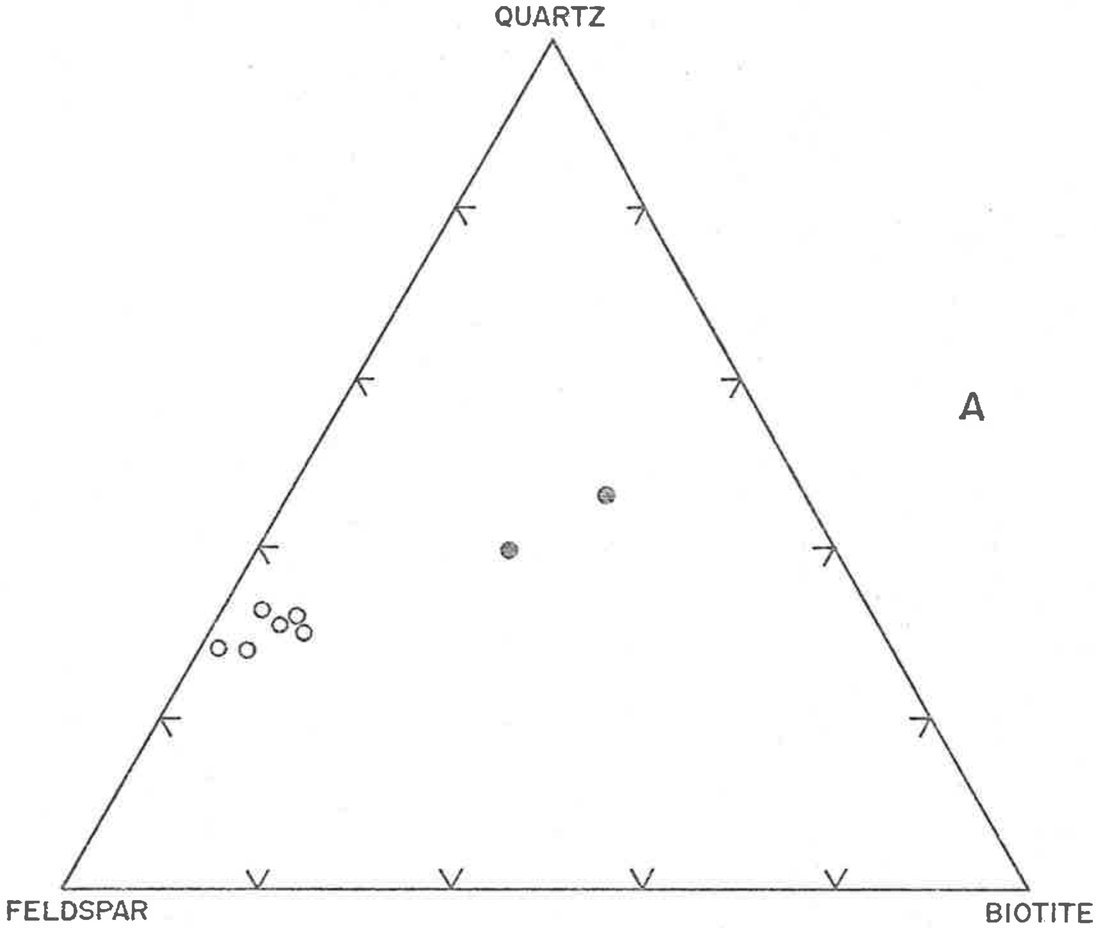

A

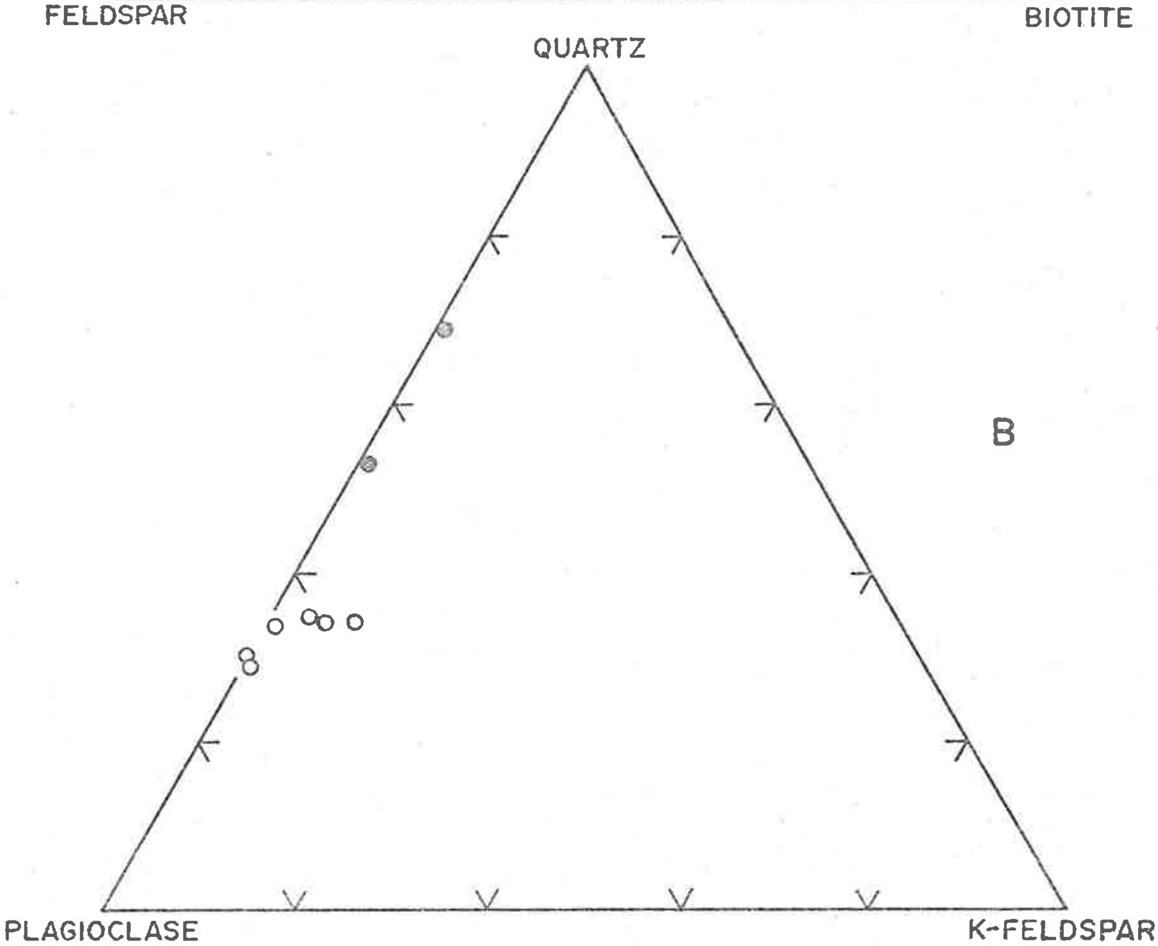

B

FIGURE 17

Mineralogical assemblages of the silica deficient marble (stippled area) represented on a tetrahedral diagram (after Burnham, 1959)

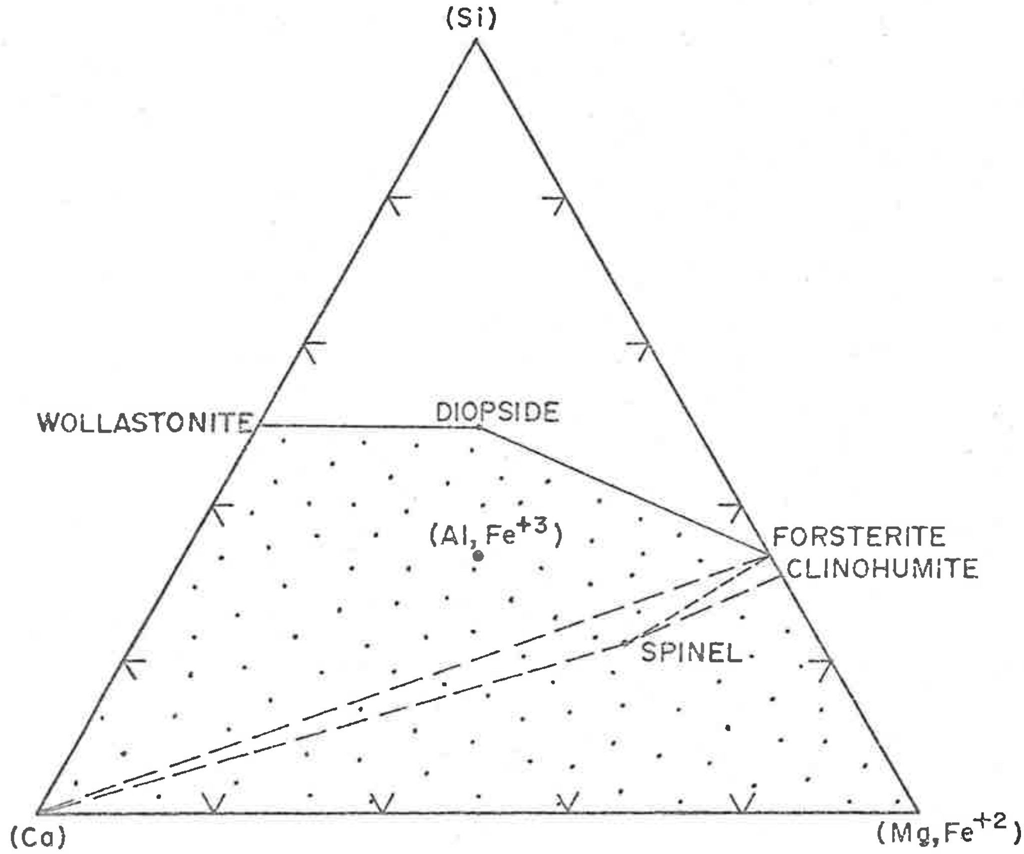
(Si)
WOLLASTONITE
DIOPSIDE
(Al, Fe+3)
FORSTERITE
CLINOHUMITE
SPINEL
(Ca)
(Mg,Fe+2)

FIGURE 18

A triangular plot of weight % CaO, Na_2O and K_2O of the migmatite veins, host rock, the Cooke Hill intrusives, the Massive granodiorite and the metasediments of the present area. The arrow connects the points representing the leucocratic vein and its host rock - specimens 285/372 & /372AG. The field of common igneous rocks (Nockolds, 1954) is shown by broken lines

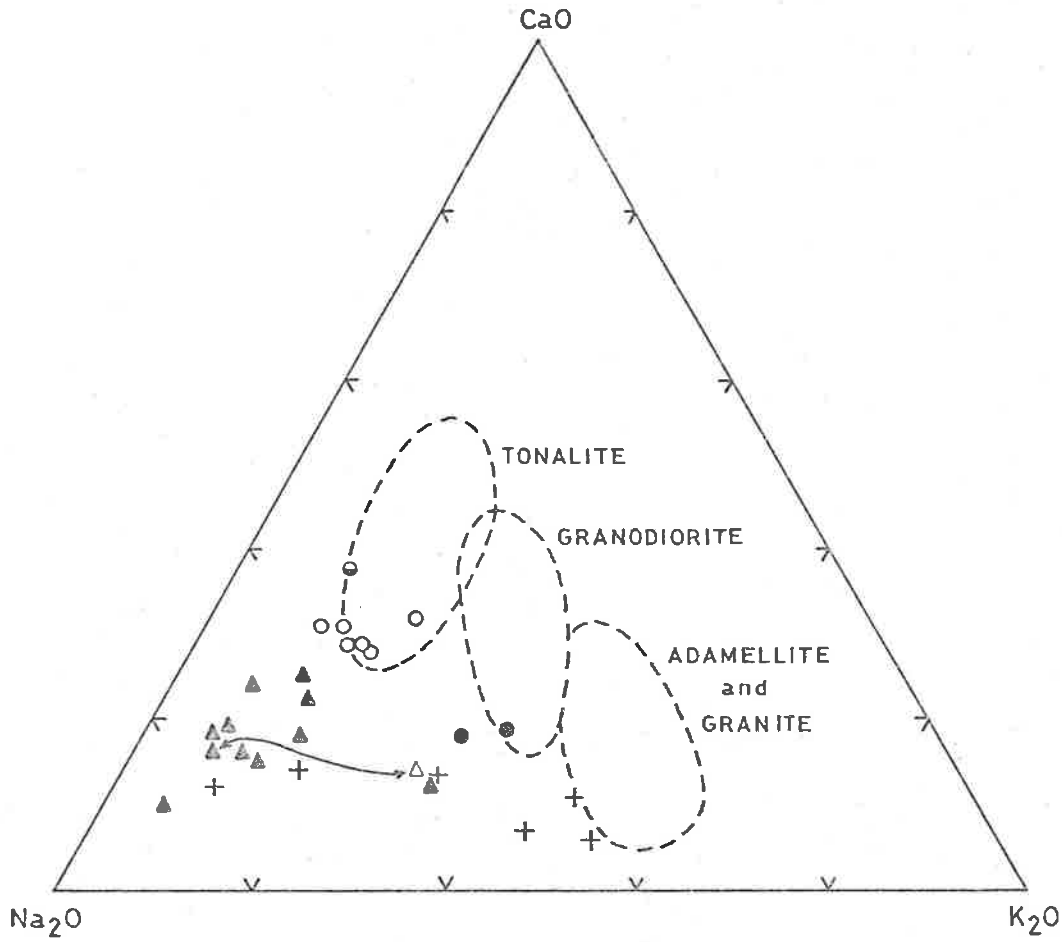

▲ Migmatitic veins

△ Migmatitic host rock

○ Cooke Hill tonalite

● Cooke Hill granodiorite

◒ Massive granodiorite

\+ Metasediments

FIGURE 19

A plot of ionic percentages of Fe^2 and Fe^3 of the migmatite veins, the host rock, the Cooke Hill intrusives, the Massive granodiorite and the metasediments of the present area. Symbols as for Figure 18

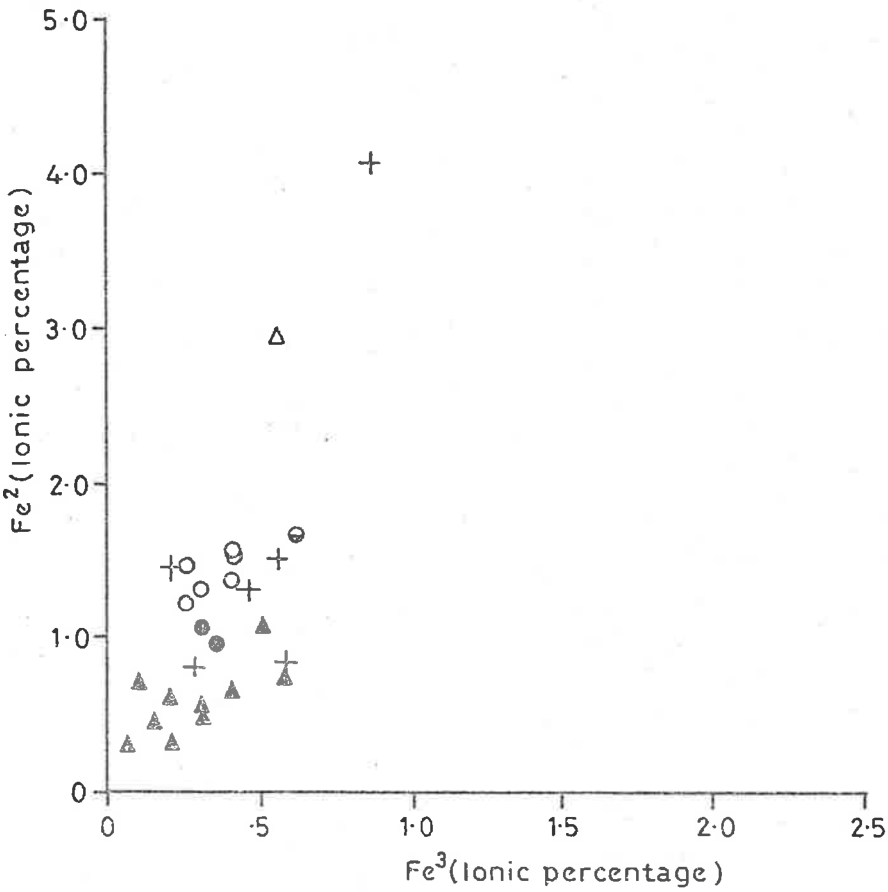

5·0
4·0
3·0
2·0
1·0
0
Fe2(Ionic percentage)
0
·5
1·0
1·5
2·0
2·5
Fe3(Ionic percentage)

FIGURE 20

A plot of weight % of total iron as FeO and MgO of the migmatite veins, the Cooke Hill intrusives and the metasediments of the present area. The host rock of migmatite is not plotted as it lies outside the limits of the diagram. Symbols as for Figure 18

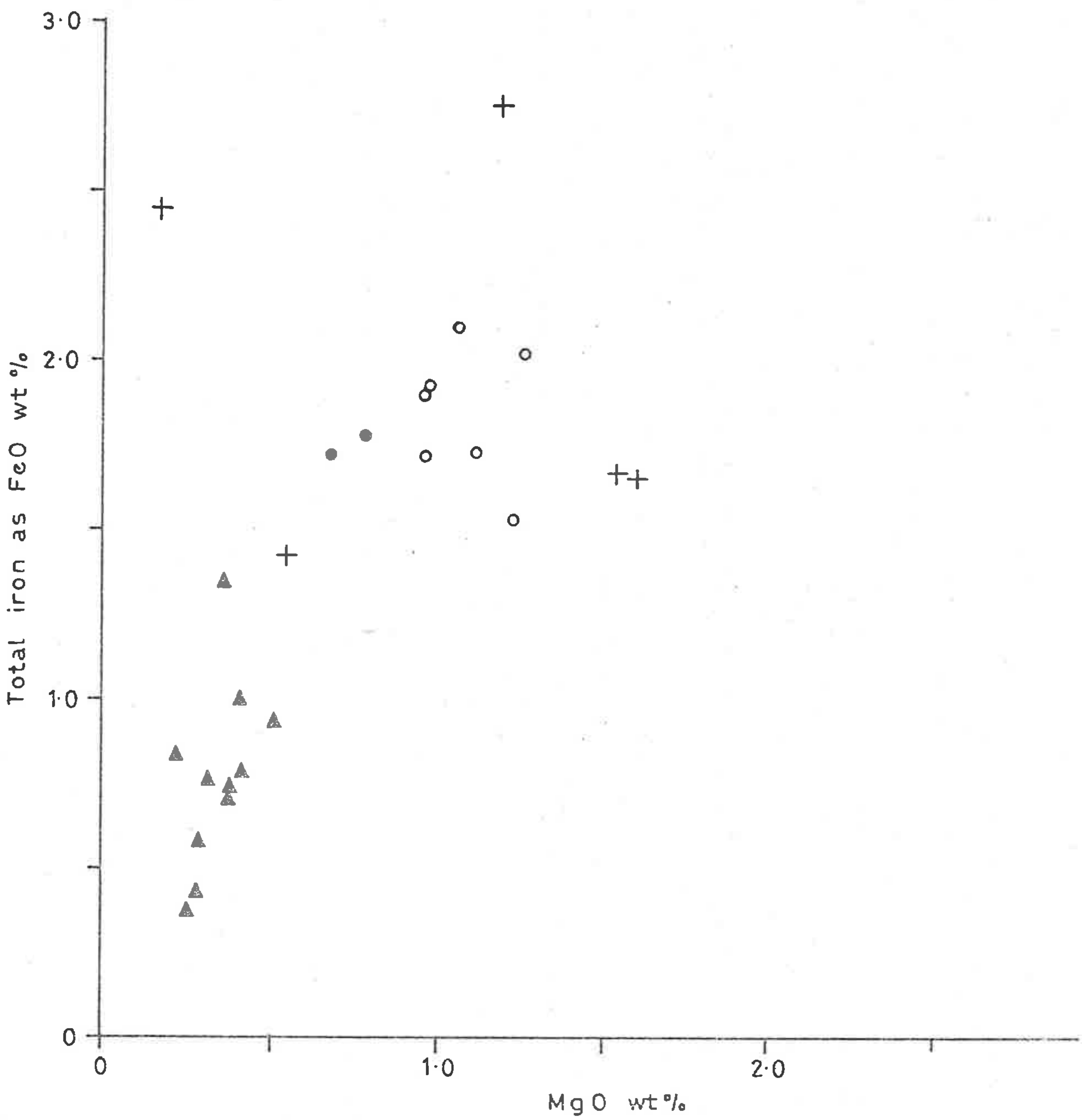
3·0
2·0
1·0
0
Total iron as FeO wt %
0
1·0
2·0
MgO wt %

FIGURE 21

A plot of ionic percentages of Ti and Fe (total) of the migmatite veins, the host rock, the Cooke Hill intrusives, the Massive granodiorite and the metasediments of the present area. Symbols as for Figure 18

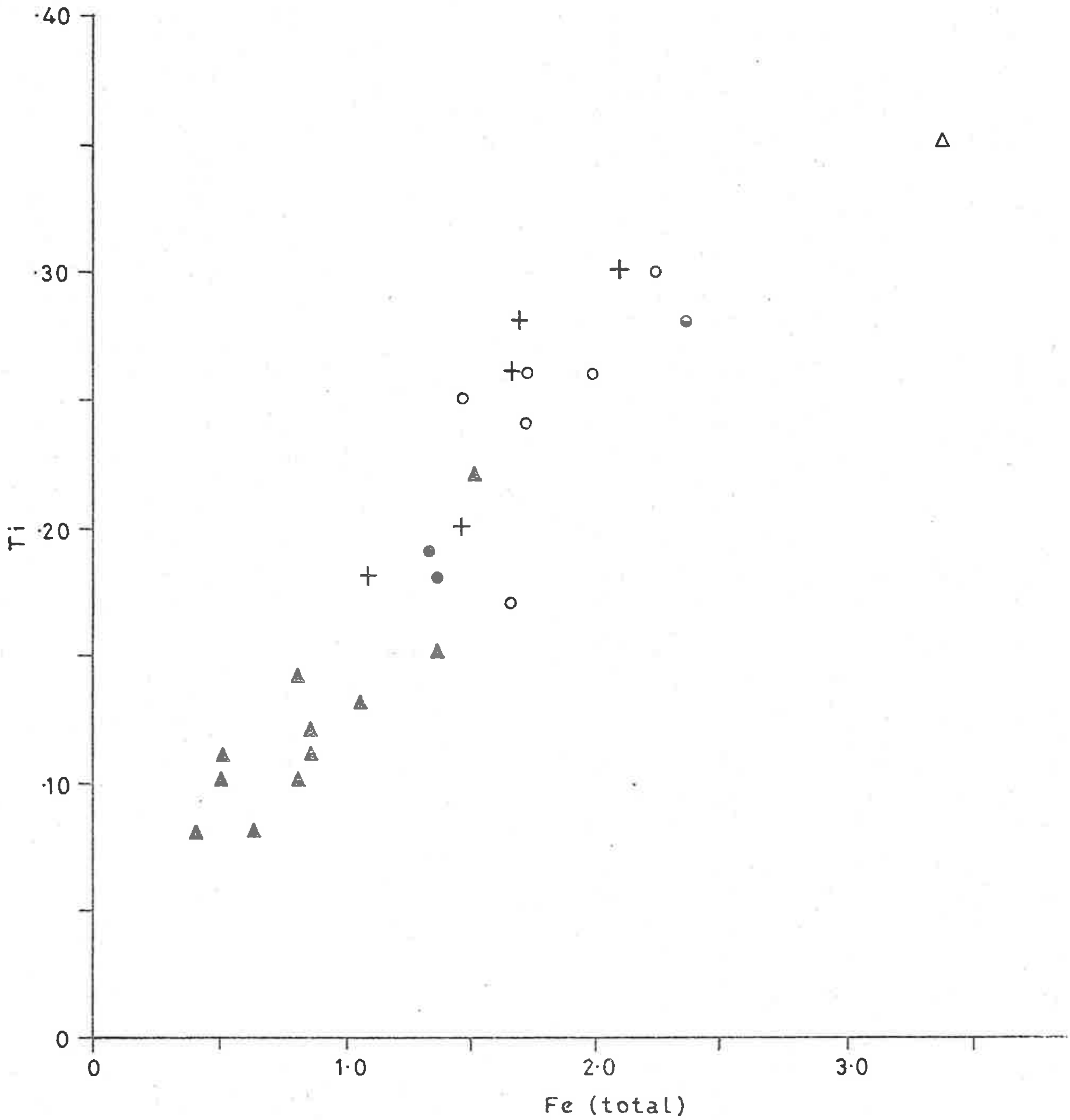

·40
·30
·20
·10
0
Ti
0
1·0
2·0
3·0
Fe (total)

FIGURE 22

Ca-Sr relationships for the Cooke Hill migmatite veins, the Cooke Hill intrusives, the Massive granodiorite, the Cooke Hill metasediments, the Palmer migmatites, the Rathjen granite gneisses, the Murray Bridge granites and the Palmer quartzo-feldspathic schists. The arrow connects the points representing the leucocratic vein and its host rock - specimens 285/372 & /372AG. Symbols as for Figure 22A. Logarithmic scale

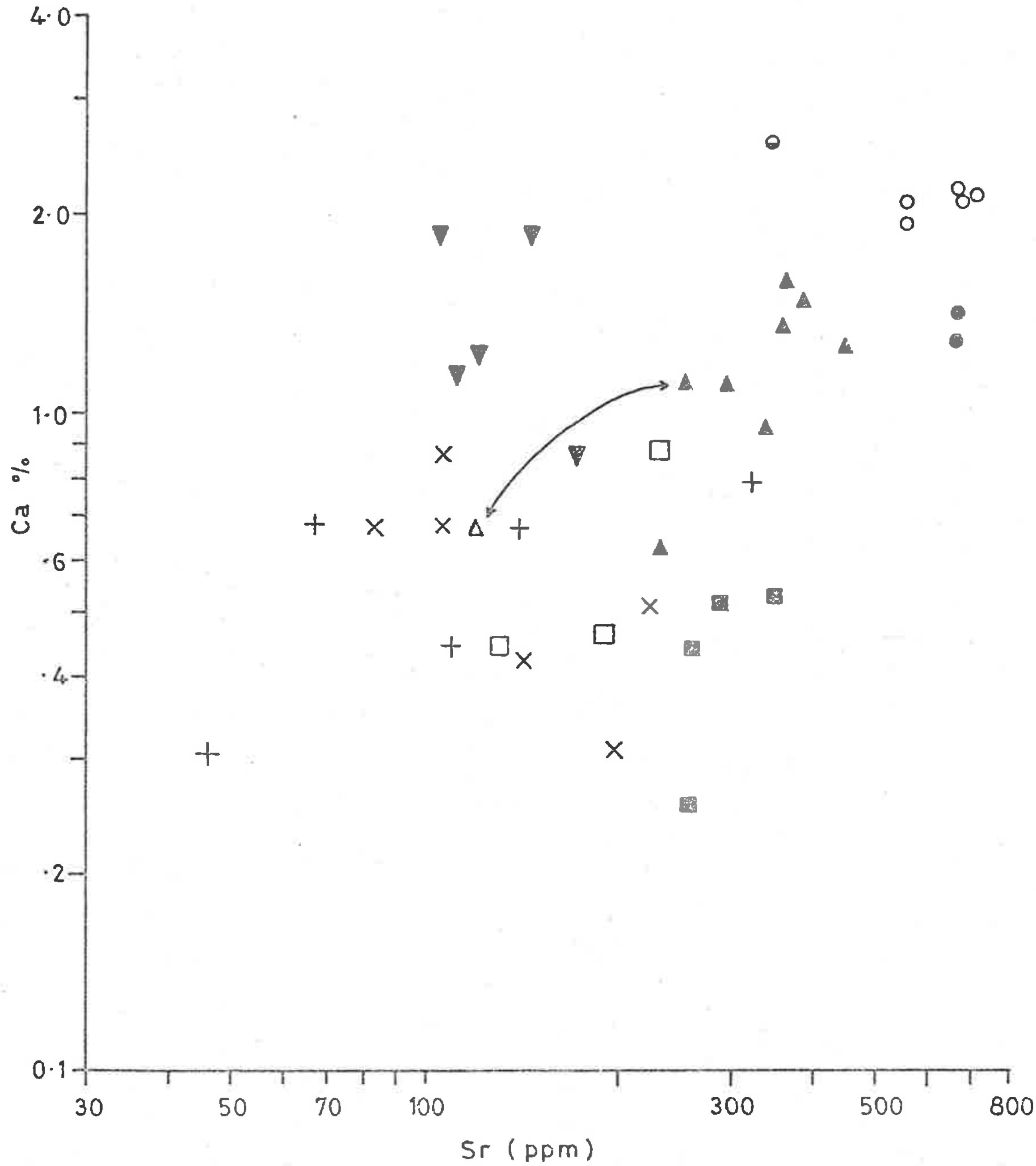

4·0
2·0
1·0
·6
·4
·2
0·1
Ca %
30
50
70
100
300
500
800
Sr (ppm)

Fig. 22A.

Legend

▲	Migmatitic veins
△	Migmatitic host rock
○	Cooke Hill tonalite
●	Cooke Hill granodiorite
◒	Massive granodiorite
+	Metasediments
×	Palmer quartzo-feldspathic schists
□	Palmer total rock migmatite
■	Palmer migmatitic vein
▼	Rathjen granite gneiss
▽	Murray Bridge granite

FIGURE 23

K-Rb relationships for the Cooke Hill vein migmatites, the Cooke Hill intrusives, the Massive granodiorite, the Cooke Hill metasediments, the Palmer migmatites, the Rathjen granite gneisses, the Murray Bridge granites and the Palmer quartzo-feldspathic schists. The arrow connects the points representing the leucocratic vein and its host rock - specimens 285/372 & /372AG. Symbols as for Figure 22A. Logarithmic scale

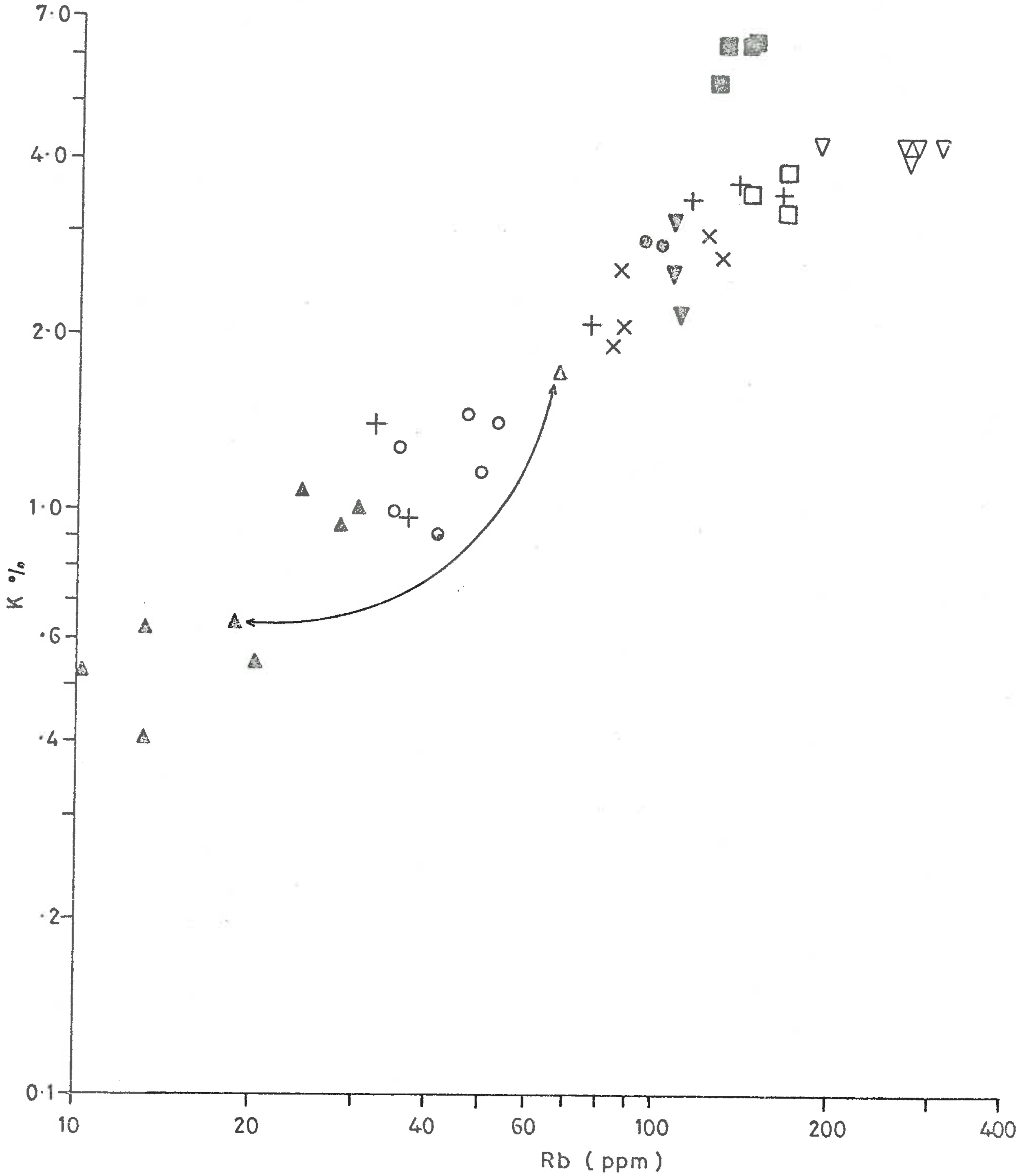

7·0
4·0
2·0
1·0
·6
·4
·2
0·1
K %
10
20
40
60
100
200
400
Rb (ppm)

FIGURE 24

Ba-Rb relationships for the Cooke Hill migmatite veins and migmatite host rock, the Cooke Hill intrusives, the Massive granodiorite, the Cooke Hill metasediments, the Palmer migmatites, the Rathjen granite gneisses and the Palmer quartzo-feldspathic schists. The arrow connects the points representing the leucocratic vein and its host rock - specimens 285/372 & /372AG. Symbols as for Figure 22A. Logarithmic scale

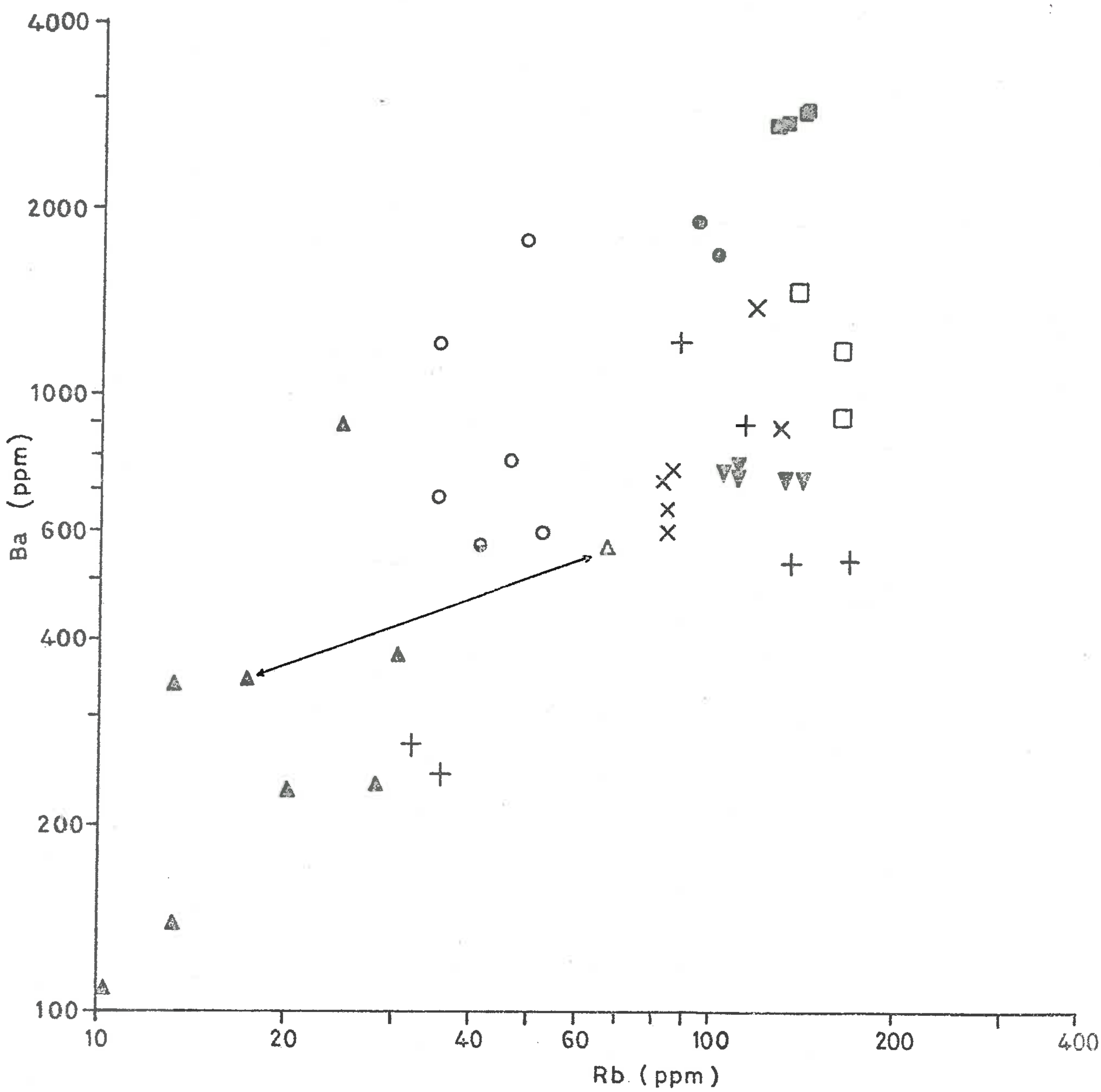

4000
2000
1000
600
400
200
100
Ba (ppm)
10
20
40
60
100
200
400
Rb (ppm)

FIGURE 25

K-Ba relationships for the Cooke Hill vein migmatites, the Cooke Hill intrusives, the Massive granodiorite, the Cooke Hill metasediments, the Palmer migmatites, the Rathjen granite gneisses and the Palmer quartzo-feldspathic schists. The arrow connects the points representing the leucocratic vein and its host rock - specimens 285/372 & /372AG. Symbols as for Figure 22A.

Logarithmic scale

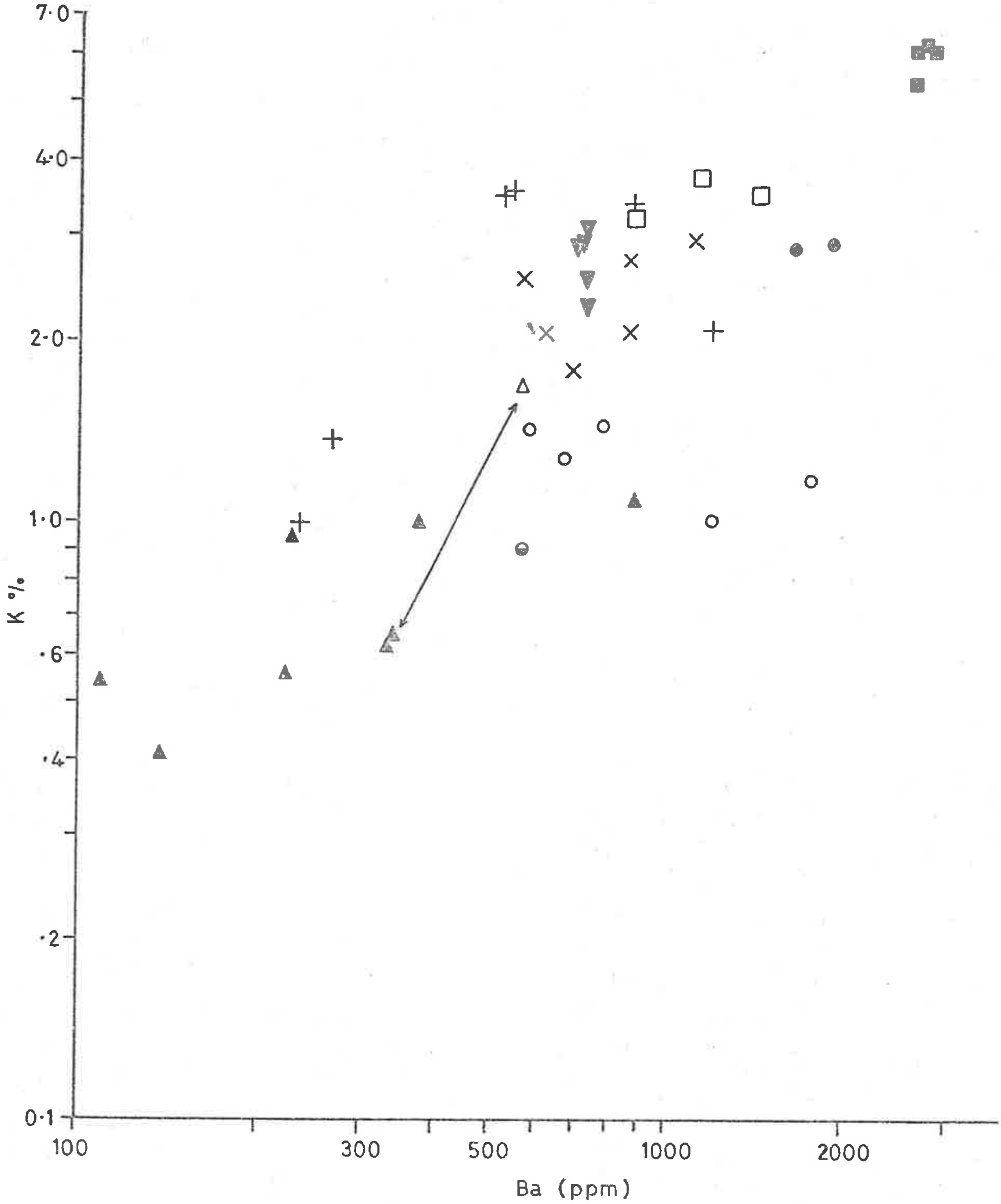
7·0
4·0
2·0
1·0
K %
·6
·4
·2
0·1
100
300
500
1000
2000
Ba (ppm)

FIGURE 26

A plot of biotite compositions on a triangular diagram representing octahedral groups of Al-Fe^{3}-Ti, Fe^{2}-Mn and Mg. The compositional fields of biotites from granite and schist-gneiss are taken from Foster's (1960) diagram. Symbols for biotites from the migmatite veins and migmatite host, the Cooke Hill intrusives, the Massive granodiorite and the Cooke Hill metasediments are the same as those used for the total rocks in Figure 22A

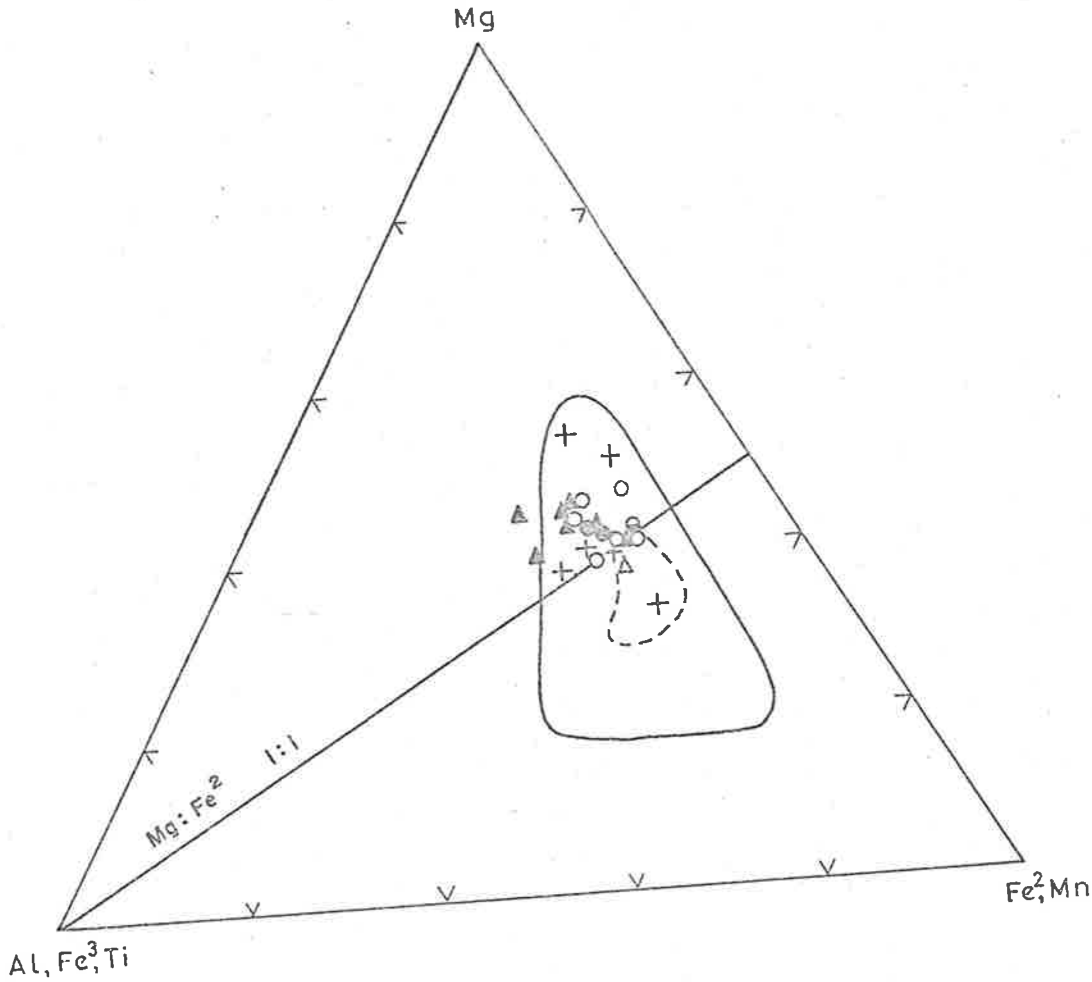

——— Field of granite

----- Field of schist and gneiss

FIGURE 27

Mineralogical compositions of the leucocratic veins and host rock of the Cooke Hill migmatites expressed in terms of quartz (SiO_2), plagioclase (Ab + An) and K-feldspar (Or) after recalculation from the analysed samples. Symbols as for Figure 22A

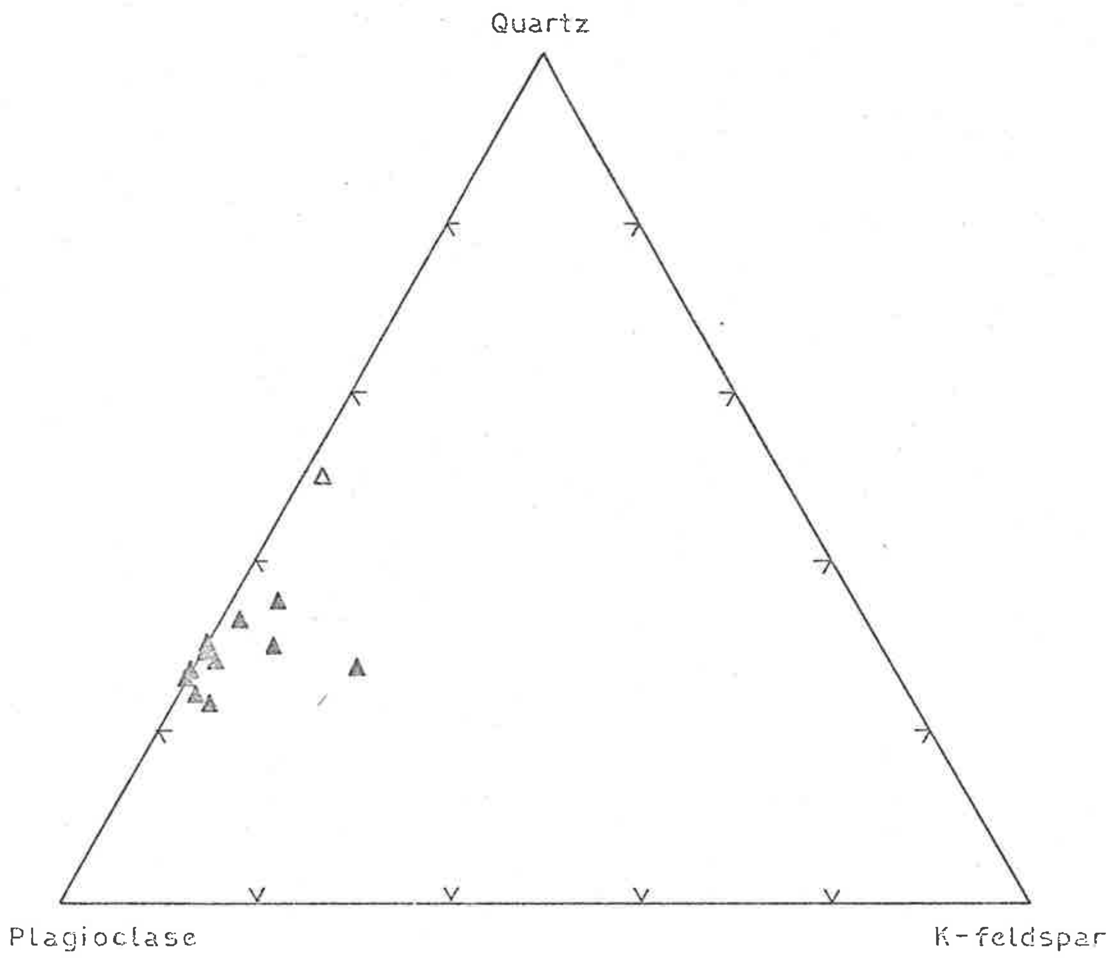

Quartz
Plagioclase
K-feldspar

FIGURE 28

Normative percentages of Q, Ab and Or projected on to the diagram representing the $NaAlSi_3O_8$-$KAlSi_3O_8$-SiO_2-H_2O system at water pressures of 500-10,000 bars (after Tuttle & Bowen, 1958; Luth et al., 1964). Figure 28A is a plot of the Barth mesonorms and Figure 28B is the C.I.P.W. norms for the Cooke Hill migmatite veins and migmatite host rock, the Cooke Hill intrusives, the Massive granodiorite and the Cooke Hill metasediments. Symbols as for Figure 22A.

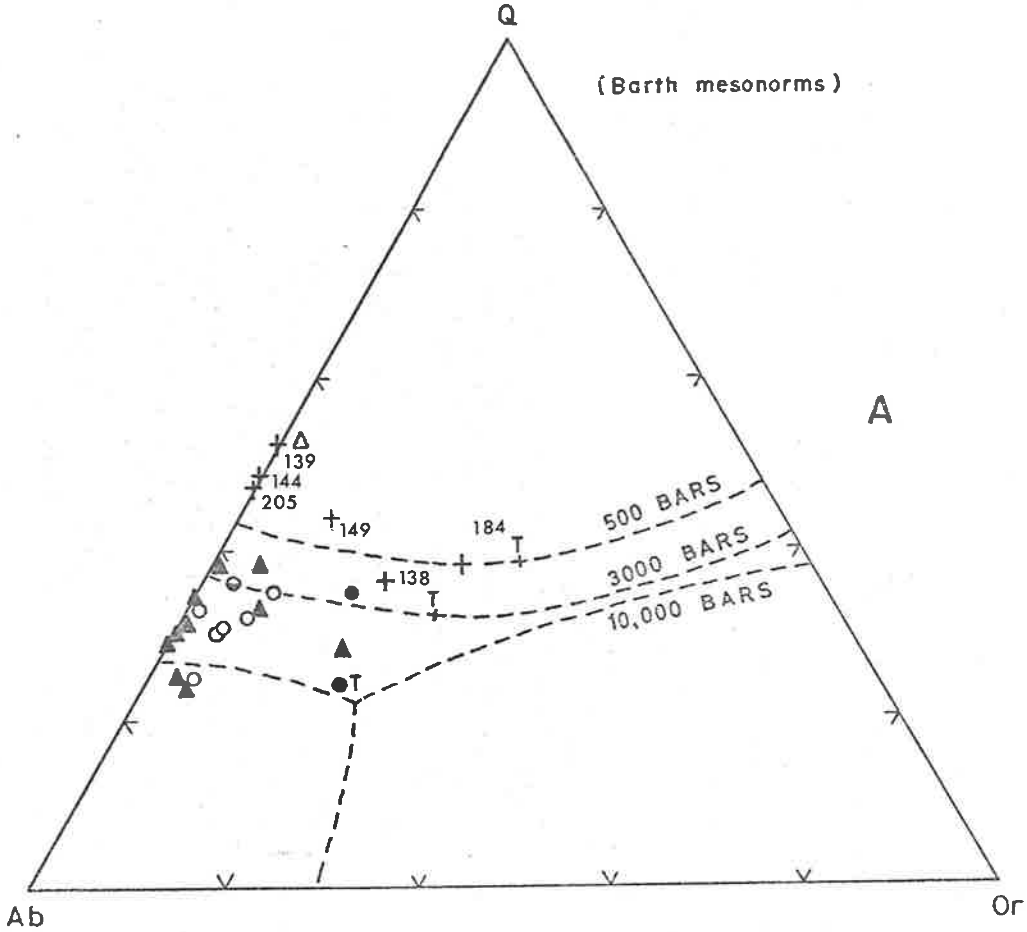
Q
(Barth mesonorms)
139
144
205
149
184
138
T
500 BARS
3000 BARS
10,000 BARS
Ab
Or

A

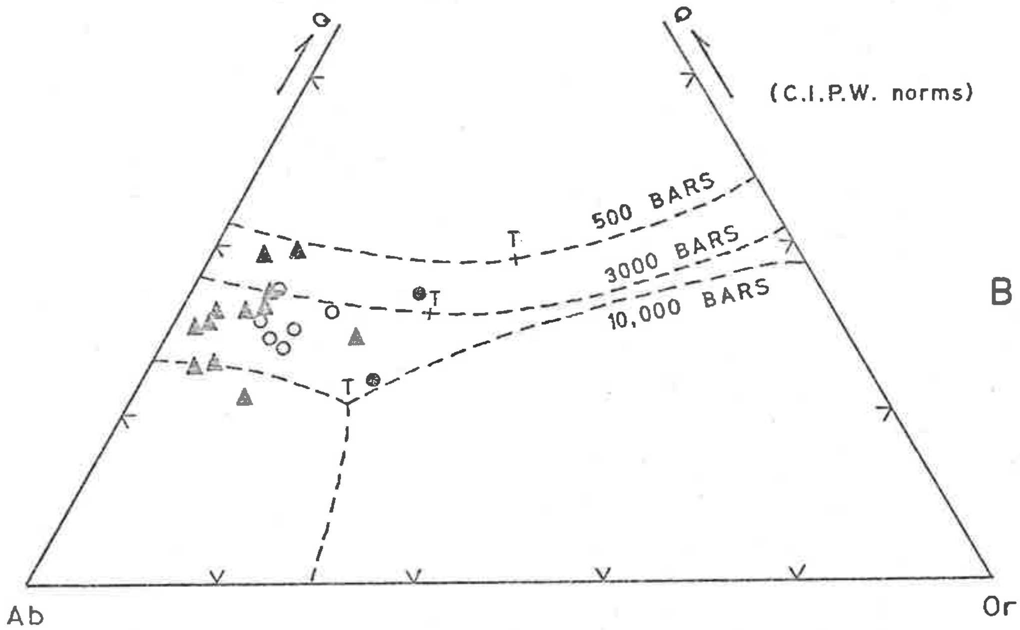
Q
Q
(C.I.P.W. norms)
500 BARS
3000 BARS
10,000 BARS
T
Ab
Or

B

FIGURE 29

Normative percentages of An, Ab and Or are projected on to a diagram representing the $KAlSi_3O_8$-$NaAlSi_3O_8$-$CaAl_2Si_2O_8$-SiO_2-H_2O system with 5,000 bar low temperature trough (after Kleeman, 1965). Figure 29A is the plot of the Barth mesonorms and Figure 29B is the C.I.P.W. norms for the Cooke Hill migmatite veins and migmatite host rock, the Cooke Hill intrusives and the Massive granodiorite. Symbols as for Figure 22A

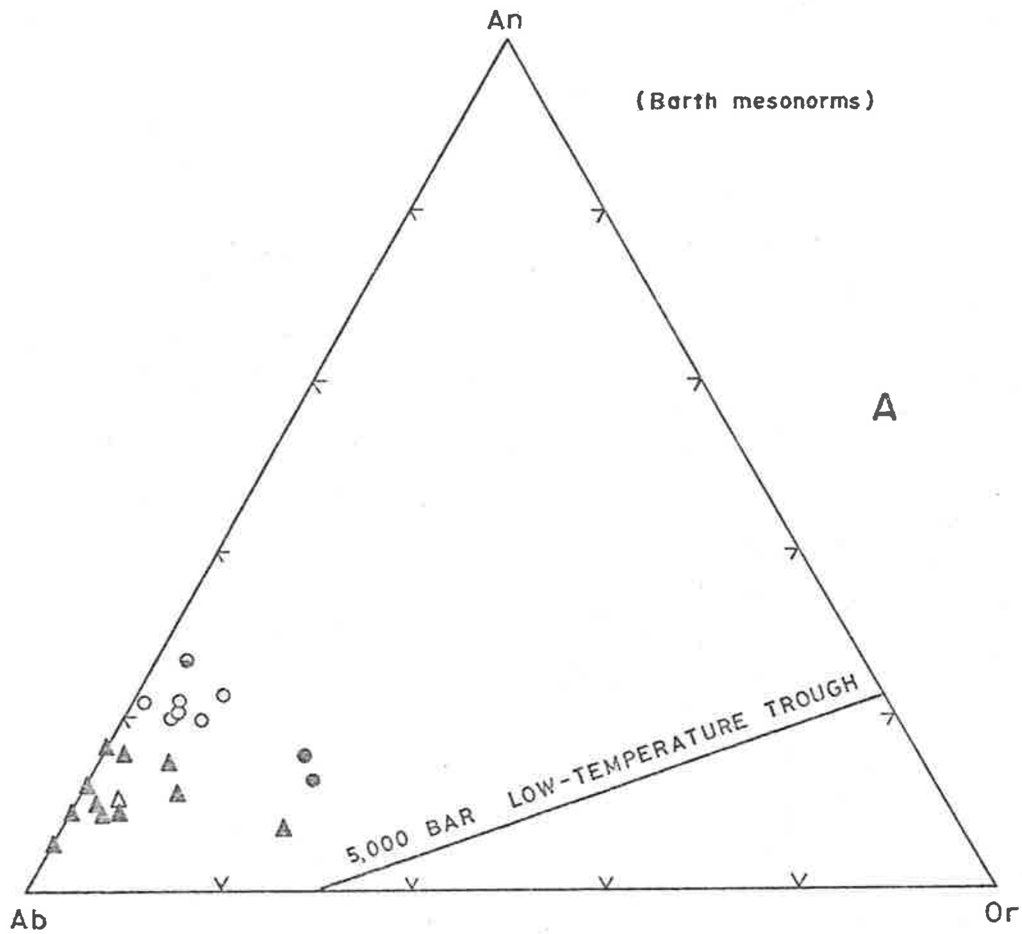
An
(Barth mesonorms)
A
5,000 BAR LOW-TEMPERATURE TROUGH
Ab
Or

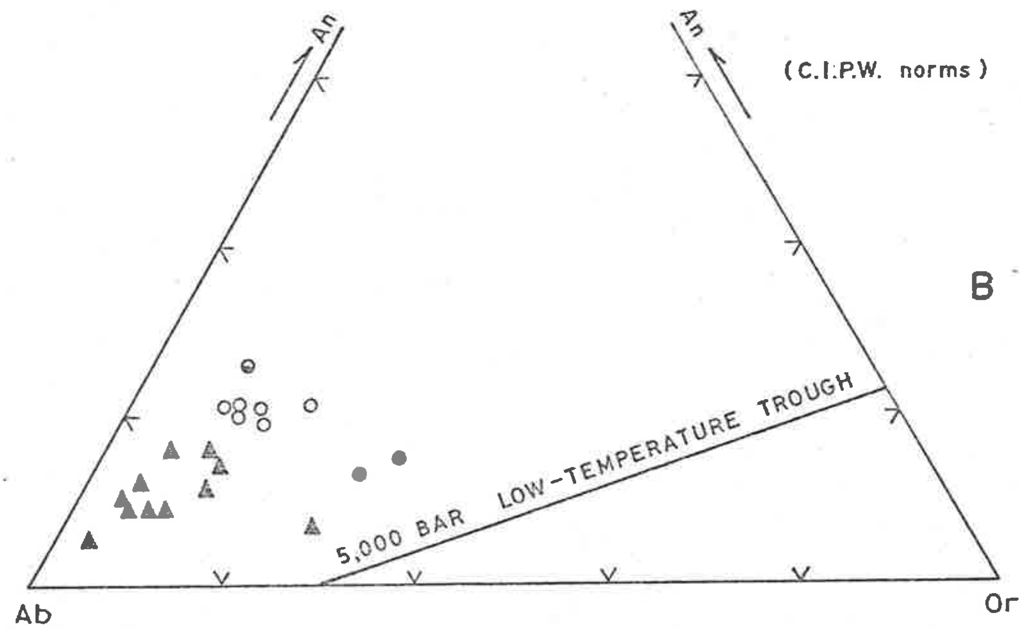
An
An
(C.I.P.W. norms)
B
5,000 BAR LOW-TEMPERATURE TROUGH
Ab
Or

FIGURE 30

Plot of K_2O versus Na_2O for the Cooke Hill tonalites, Cooke Hill granodiorites and the Massive granodiorite. Symbols as for Figure 30A

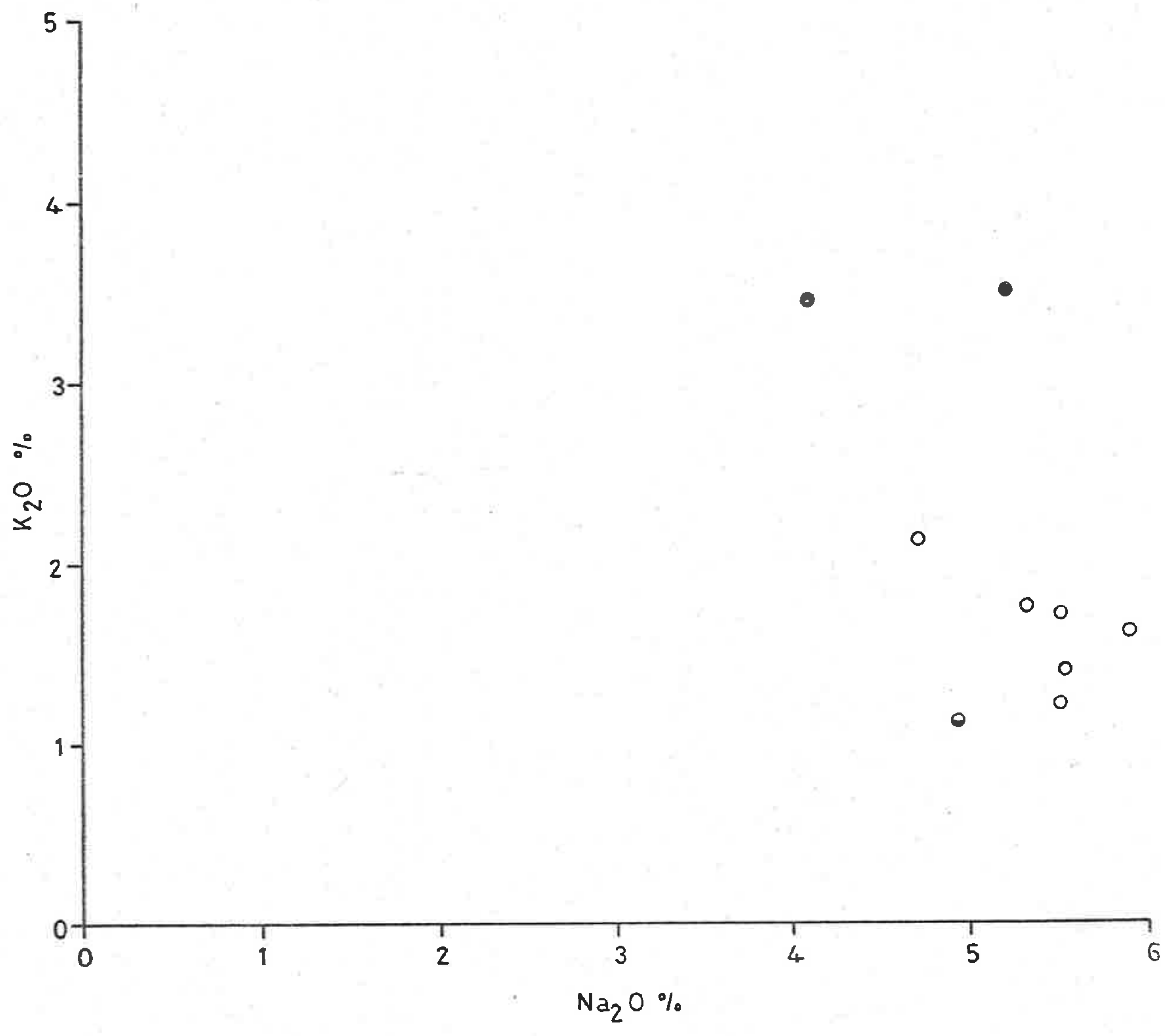

5
4
3
2
1
0
K_2O %
0
1
2
3
4
5
6
Na_2O %

Fig. 30A.

Legend

○	Cooke Hill tonalite
●	Cooke Hill granodiorite
◒	Massive granodiorite
△	Mannum aplite
▲	Mannum granite
◩	Monarto granite
⊙	Reedy Creek tonalite
□	Swanport granite
▣	Palmer granite
▽	Murray Bridge granite
▼	Rathjen granite gneiss

FIGURE 31

Plot of total iron as FeO versus MgO for the Cooke Hill tonalites, Cooke Hill granodiorites and the Massive granodiorite. Symbols as for Figure 30A

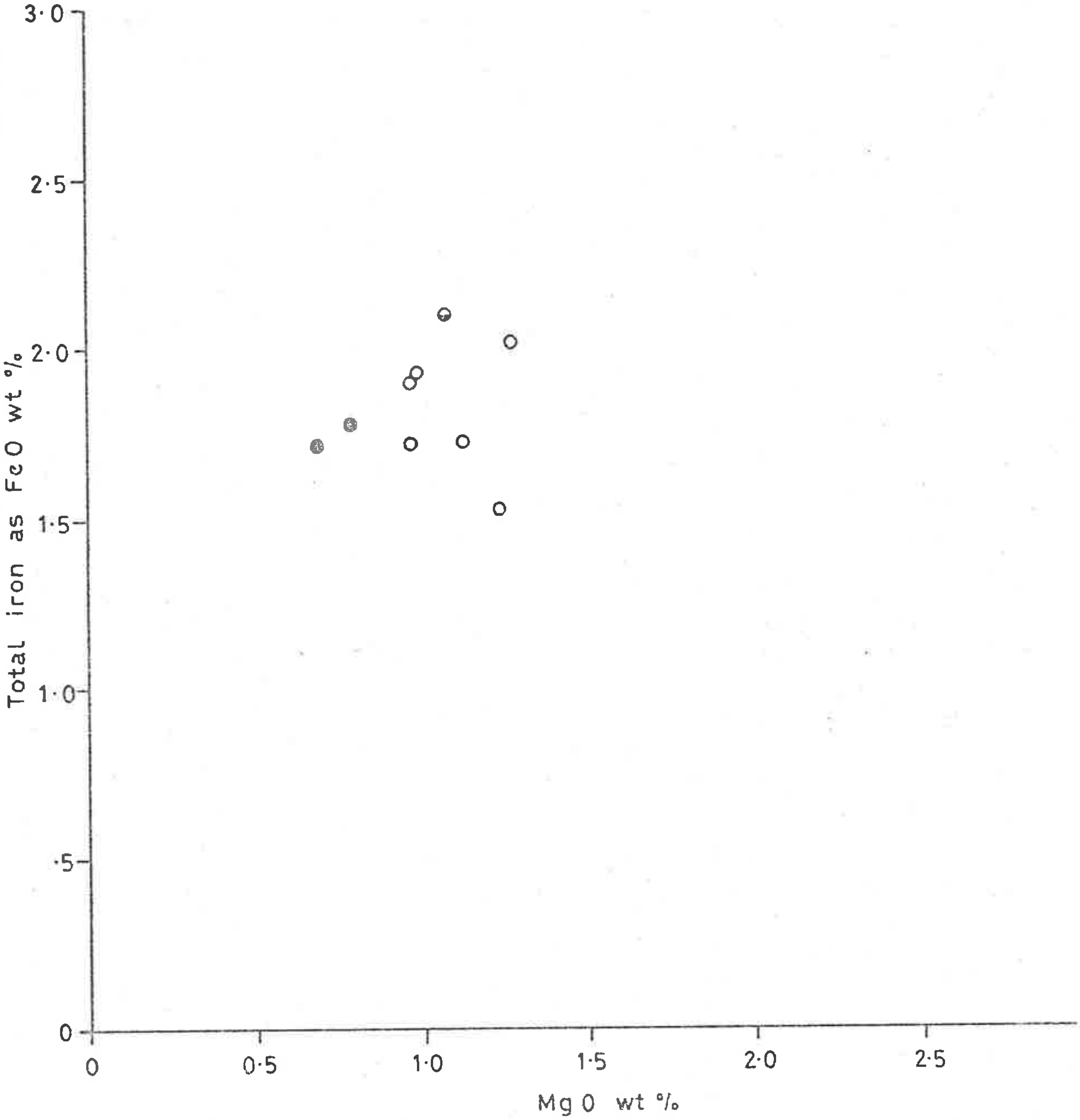
3·0
2·5
2·0
1·5
1·0
·5
0
Total iron as FeO wt %
0
0·5
1·0
1·5
2·0
2·5
Mg O wt %

FIGURE 32

Plot of Ti versus Fe (total) for the Cooke Hill tonalites, the Cooke Hill granodiorites and the Massive granodiorite. Symbols as for Figure 30A

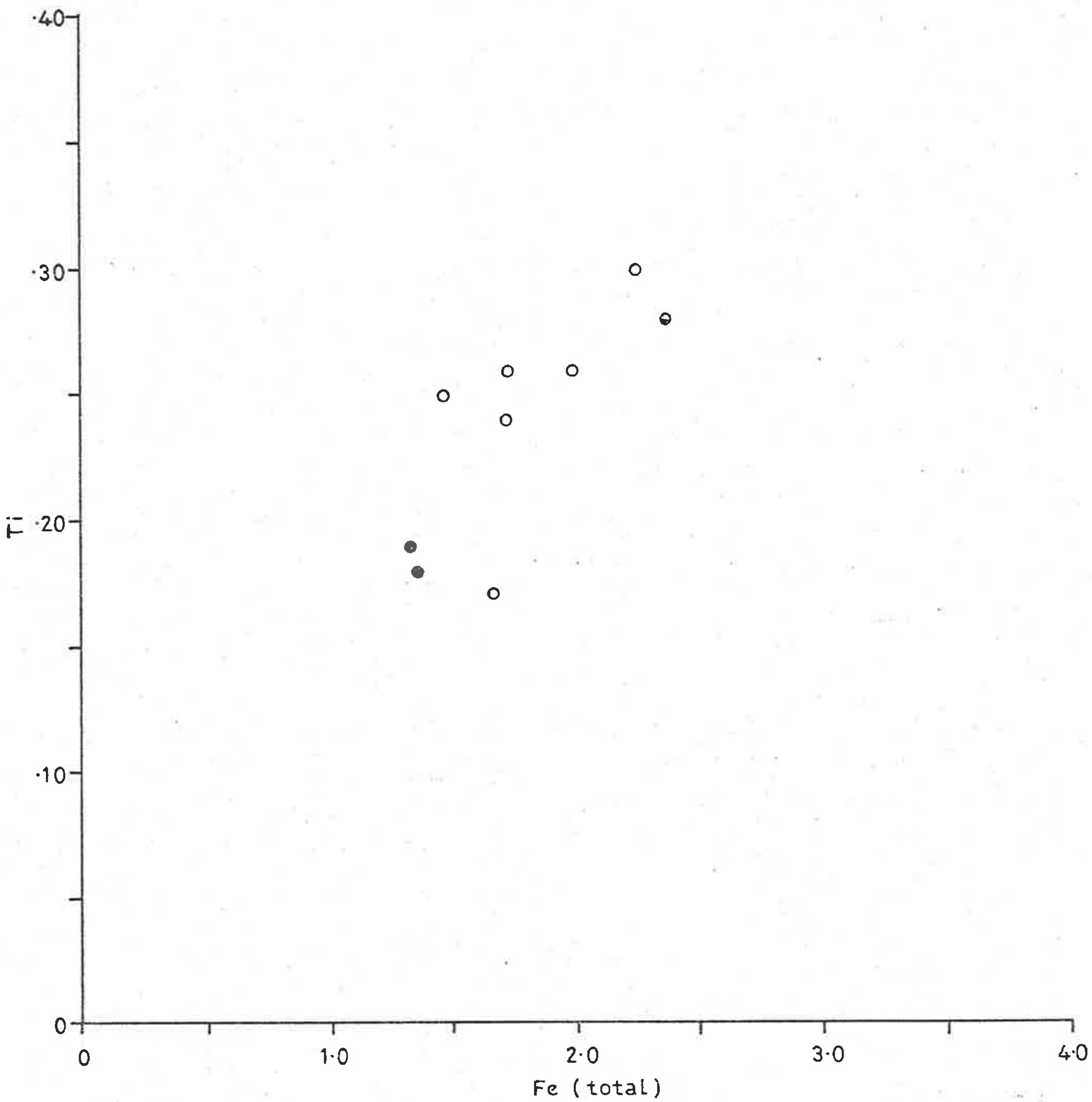
·40
·30
·20
·10
0
Ti
0
1·0
2·0
3·0
4·0
Fe (total)

FIGURE 33

C.I.P.W. normative Q-Ab-Or proportions of the Cooke Hill tonalites, the Cooke Hill granodiorites and the Massive granodiorite projected on to the diagram representing $NaAlSi_3O_8$-$KAlSi_3O_8$-SiO_2-H_2O system at water pressure 500-10,000 bars (after Tuttle & Bowen, 1958; Luth et al., 1964). The fields of granitic rocks (Tuttle & Bowen, 1958; Winkler & Von Platen, 1961) are also shown on the diagram. Symbols as for Figure 30A

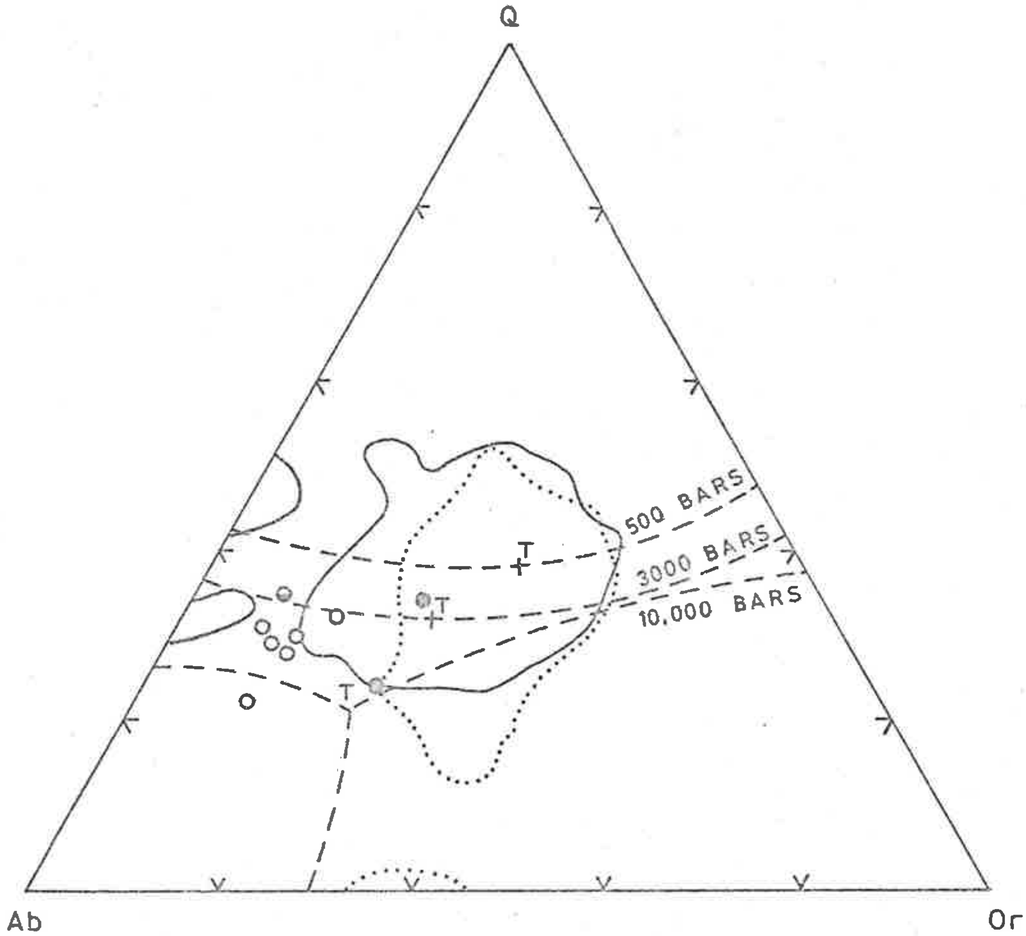

.... Field of 571 granitic rocks containing 80 % or more of the CIPW normative minerals Ab, Or and Q. (after Tuttle and Bowen 1958)

———— Field of 1190 granitic rocks containing the CIPW normative minerals Ab, Or and Q. (after Winkler and von Platen 1961)

FIGURE 34

C.I.P.W. normative An-Ab-Or proportions of the Cooke Hill tonalites, the Cooke Hill granodiorites and the Massive granodiorite projected on to the diagram representing the $KAlSi_3O_8$-$NaAl_3O_8$-$CaAl_2Si_3O_8$-SiO_2-H_2O system with 5,000 bar low temperature trough (after Kleeman, 1965). Symbols as for Figure 30A

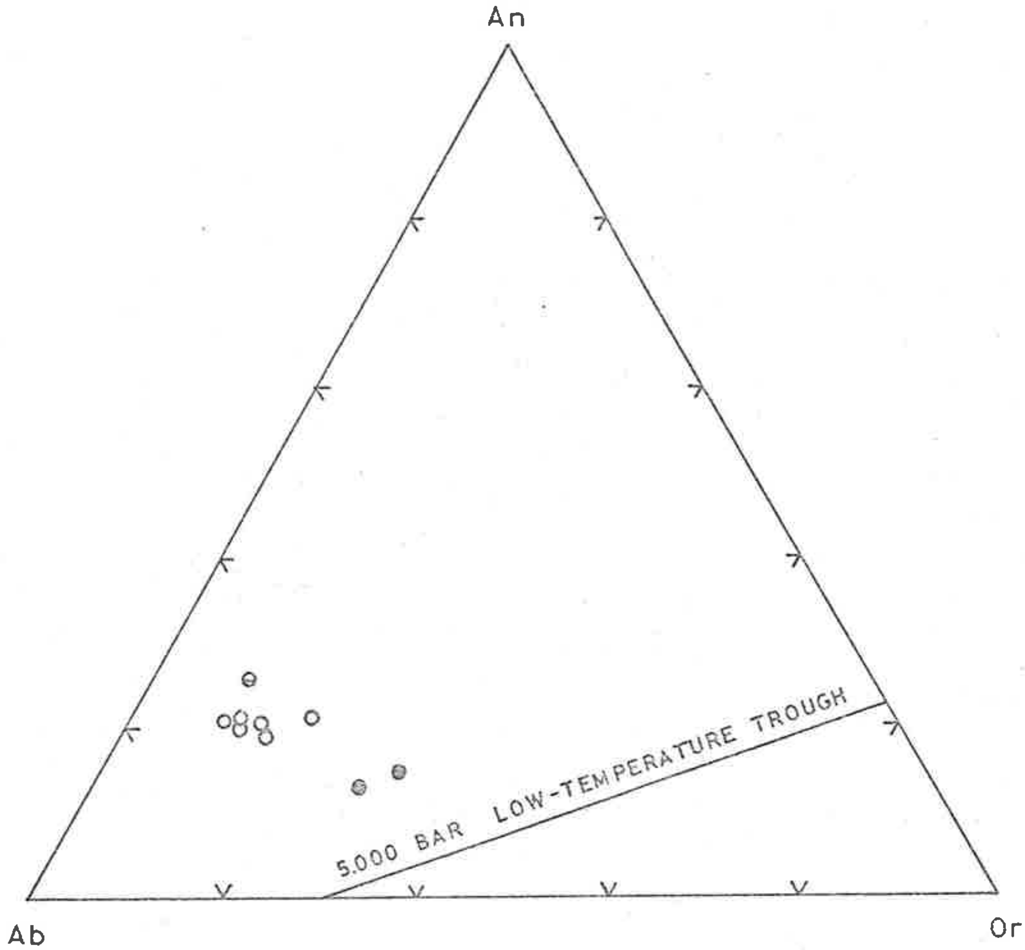
An
Ab
Or
5,000 BAR LOW-TEMPERATURE TROUGH

FIGURE 35

Mineralogical compositions of the Cooke Hill tonalites, the Cooke Hill granodiorites and the Massive granodiorite expressed in terms of quartz (Q), plagioclase (Ab + An) and K-feldspar (Or) after recalculation from the analyses.   Symbols as for Figure 30A

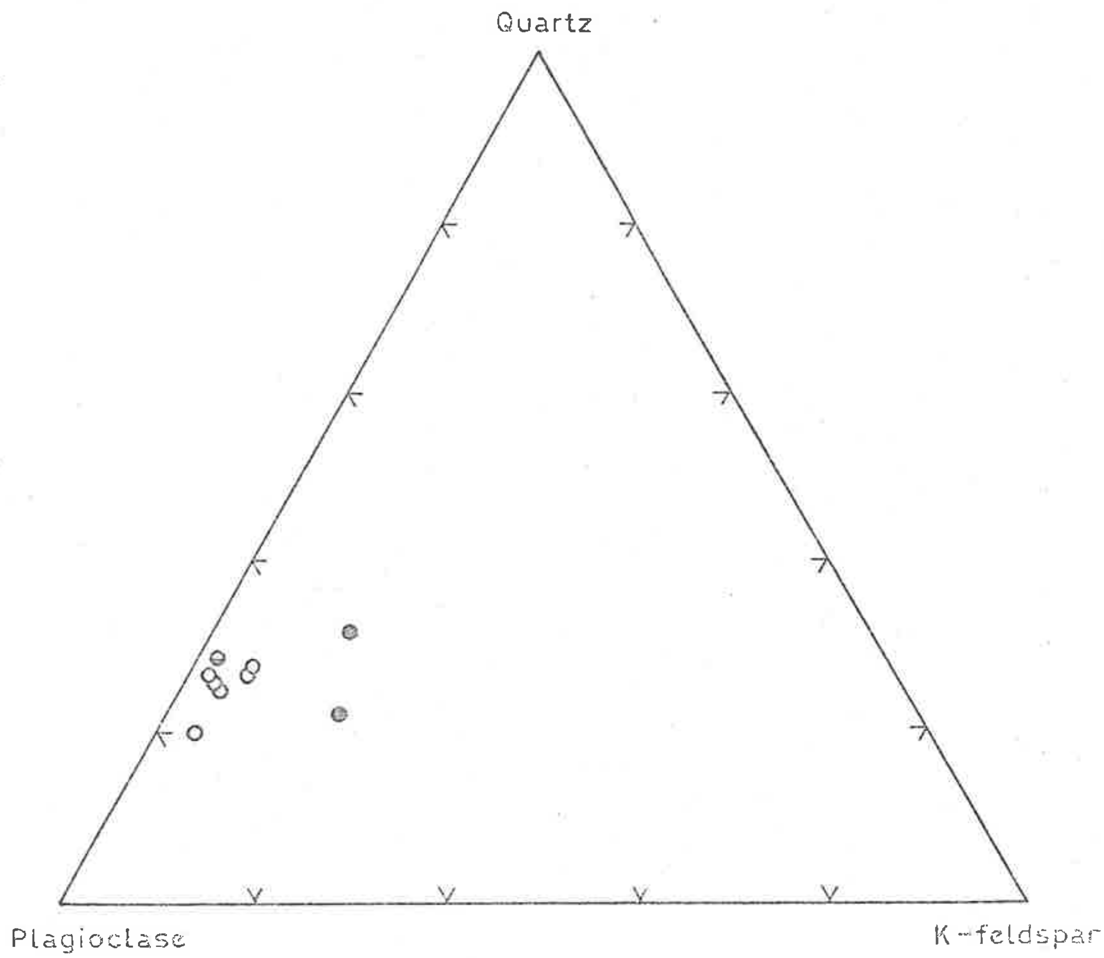

Quartz
Plagioclase
K-feldspar

FIGURE 36

A triangular plot of CaO, Na_2O and K_2O weight percentages of average compositions of the Cooke Hill tonalites, the Cooke Hill granodiorites, the Massive granodiorite, the Palmer granites, the Monarto granite, the Mannum granite, the Swanport granite, the Mannum aplite and the Reedy Creek tonalite. The fields of common igneous rocks are shown by dotted lines (after Nockolds, 1954) and greywacke by solid line (after Condie, 1967). Symbols as for Figure 30A

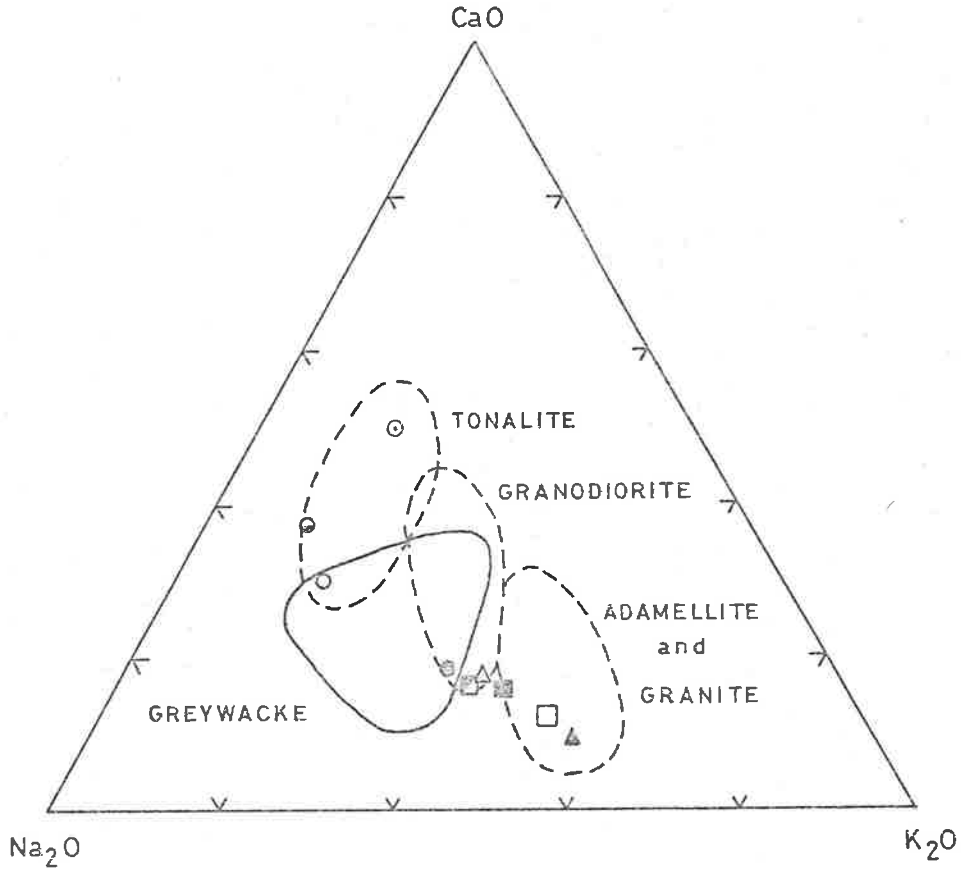
CaO
TONALITE
GRANODIORITE
ADAMELLITE
and
GRANITE
GREYWACKE
Na_2O
K_2O

FIGURE 37

K-Rb relationships for the Cooke Hill tonalites, the Cooke Hill granodiorites, the Massive granodiorite, the Palmer granites, the Rathjen granite gneisses, the Murray Bridge granites and the Mannum granite. Symbols as for Figure 30A.

Logarithmic scale

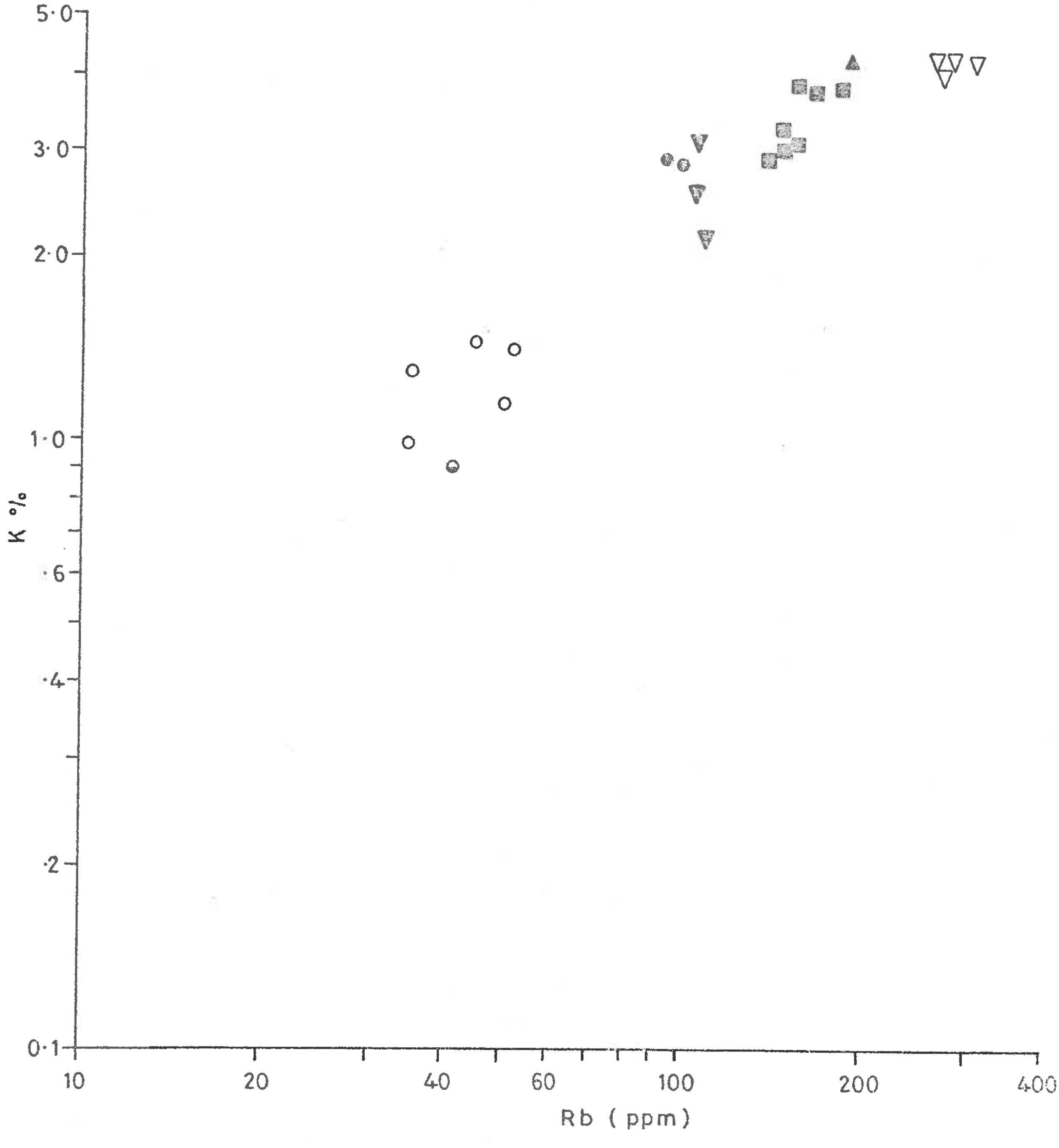

5·0
3·0
2·0
1·0
·6
·4
·2
0·1
K %
10
20
40
60
100
200
400
Rb (ppm)

FIGURE 38

K-Ba relationships for the Cooke Hill tonalites, the Cooke Hill granodiorites, the Massive granodiorite, the Palmer granites and the Rathjen granite gneisses. Symbols as for Figure 30A.
Logarithmic scale

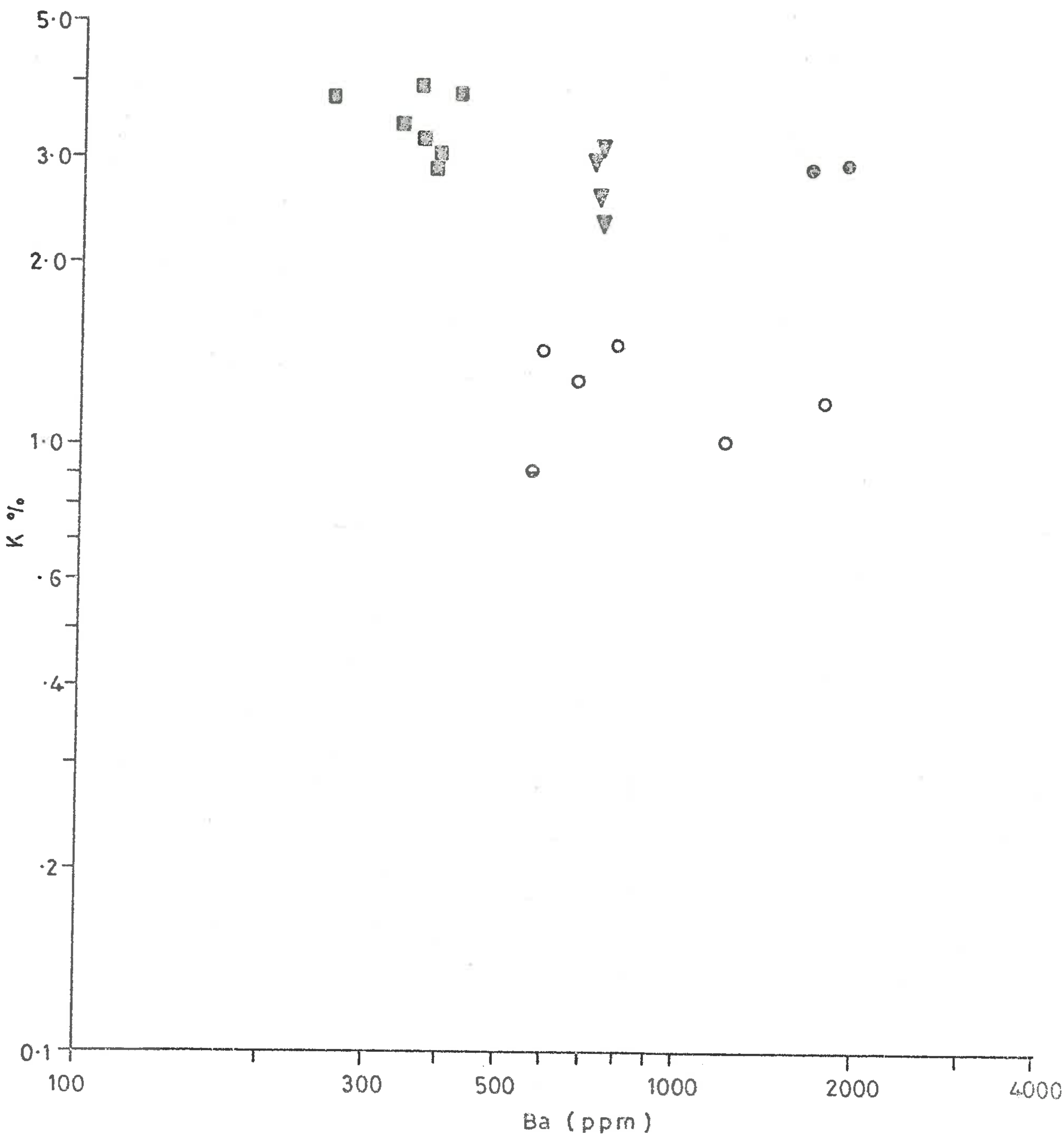

5·0
3·0
2·0
1·0
·6
·4
·2
0·1
K %
100
300
500
1000
2000
4000
Ba (ppm)

FIGURE 39

Ba-Rb relationships for the Cooke Hill tonalites, the Cooke Hill granodiorites, the Massive granodiorite, the Palmer granites and the Rathjen granite gneisses. Symbols as for Figure 30A.

Logarithmic scale

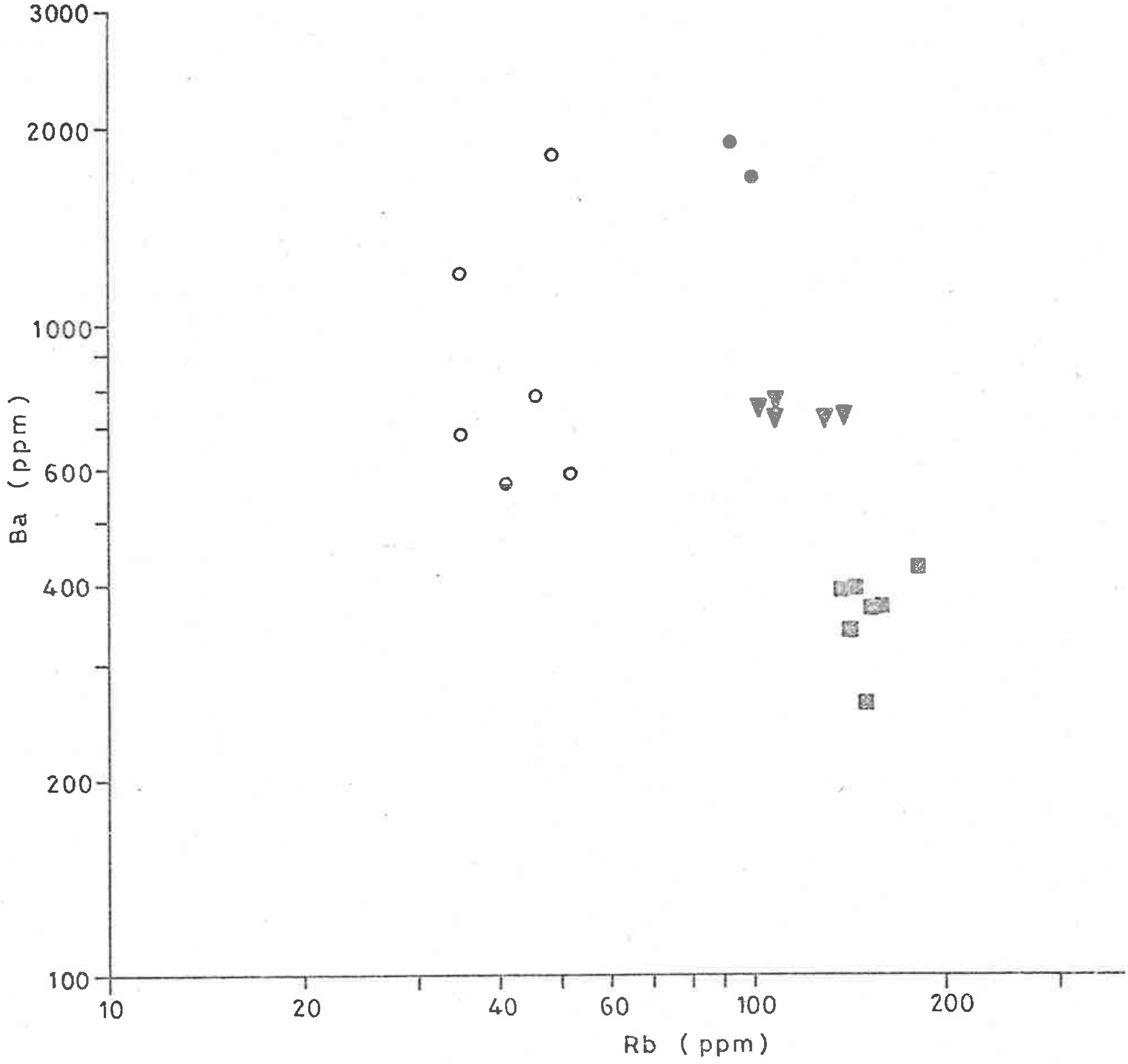

3000
2000
1000
600
400
200
100
10
20
40
60
100
200
Ba (ppm)
Rb (ppm)

FIGURE 40

Ca-Sr relationships for the Cooke Hill tonalites, the Cooke Hill granodiorites, the Massive granodiorite, the Palmer granites and the Rathjen granite gneisses. Symbols as for Figure 30A.

Logarithmic scale

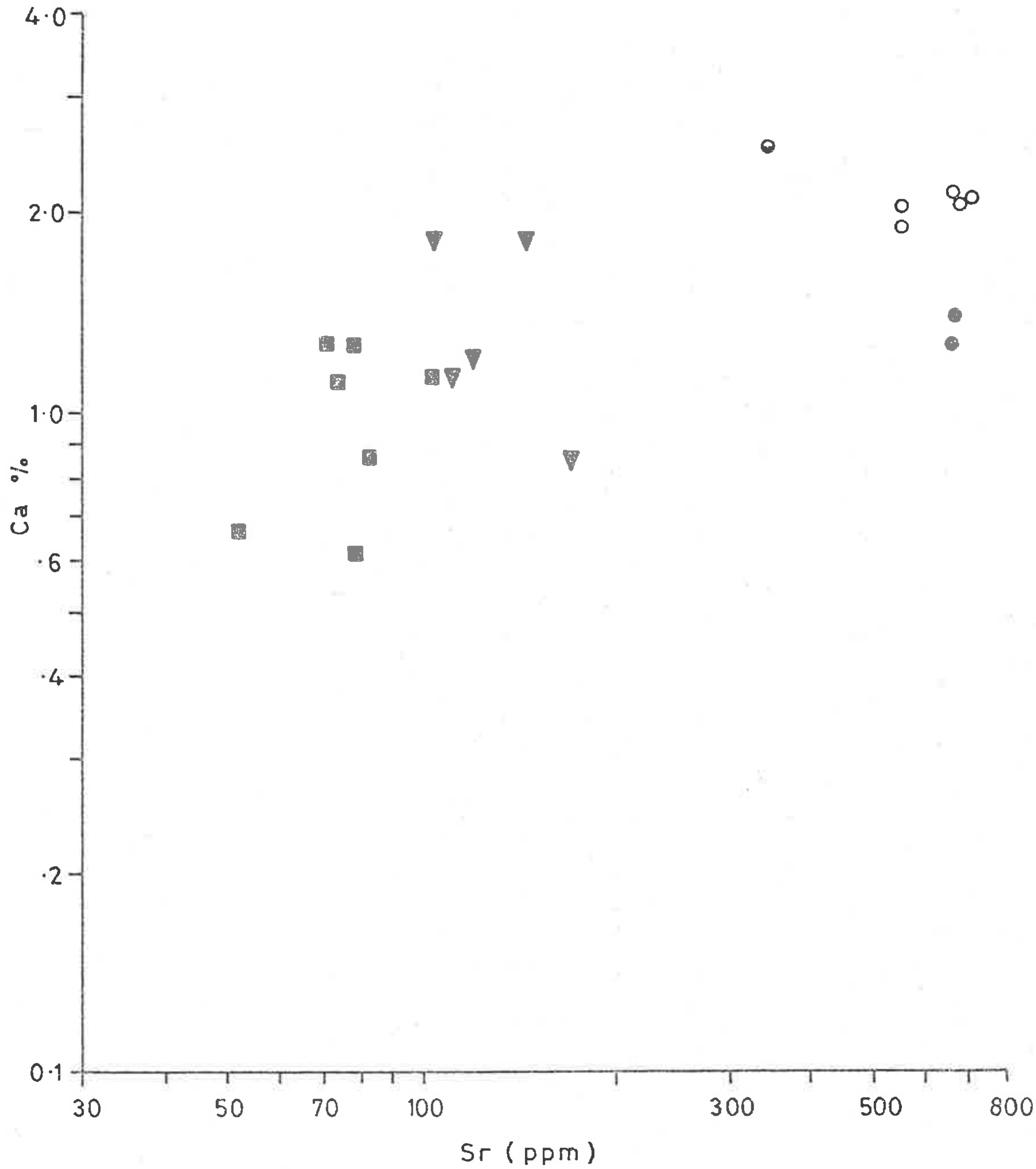
4·0
2·0
1·0
·6
·4
·2
0·1
Ca %
30
50
70
100
300
500
800
Sr (ppm)

FIGURE 41

Plot of atomic ratios of Ca:Mg:Fe (total) for the clinopyroxenes, the clinoamphiboles and the anthophyllite from the calc-schists and the calc-gneisses. Note the composition of the clinopyroxenes lies in the compositional fields of diopside and salite (cf. Deer, Howie & Zussman, 1967, Vol.2, Fig. 1)

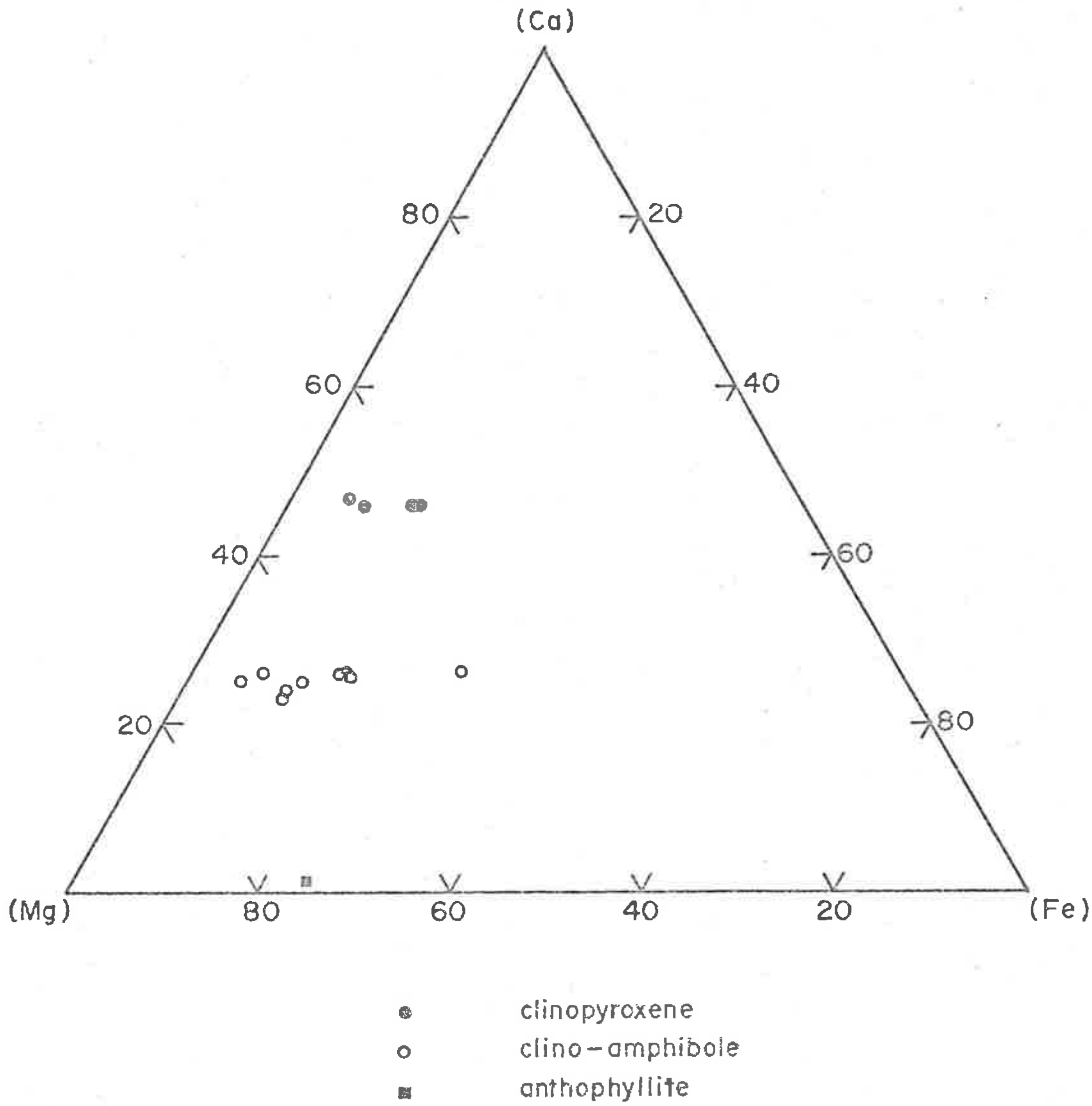

(Ca)
80
60
40
20
20
40
60
80
(Mg)
80
60
40
20
(Fe)
clinopyroxene
clino-amphibole
anthophyllite

FIGURE 42

Plot of tetrahedrally co-ordinated atoms of $(Al)^4$ against (Na + K) of the clinoamphiboles from the calc-schists. Note the composition of the clinoamphiboles lies in the fields of hornblende, actinolite-tremolite and anthophyllite (cf. Deer, Howie & Zussman, 1967, Vol.2, Fig. 71)

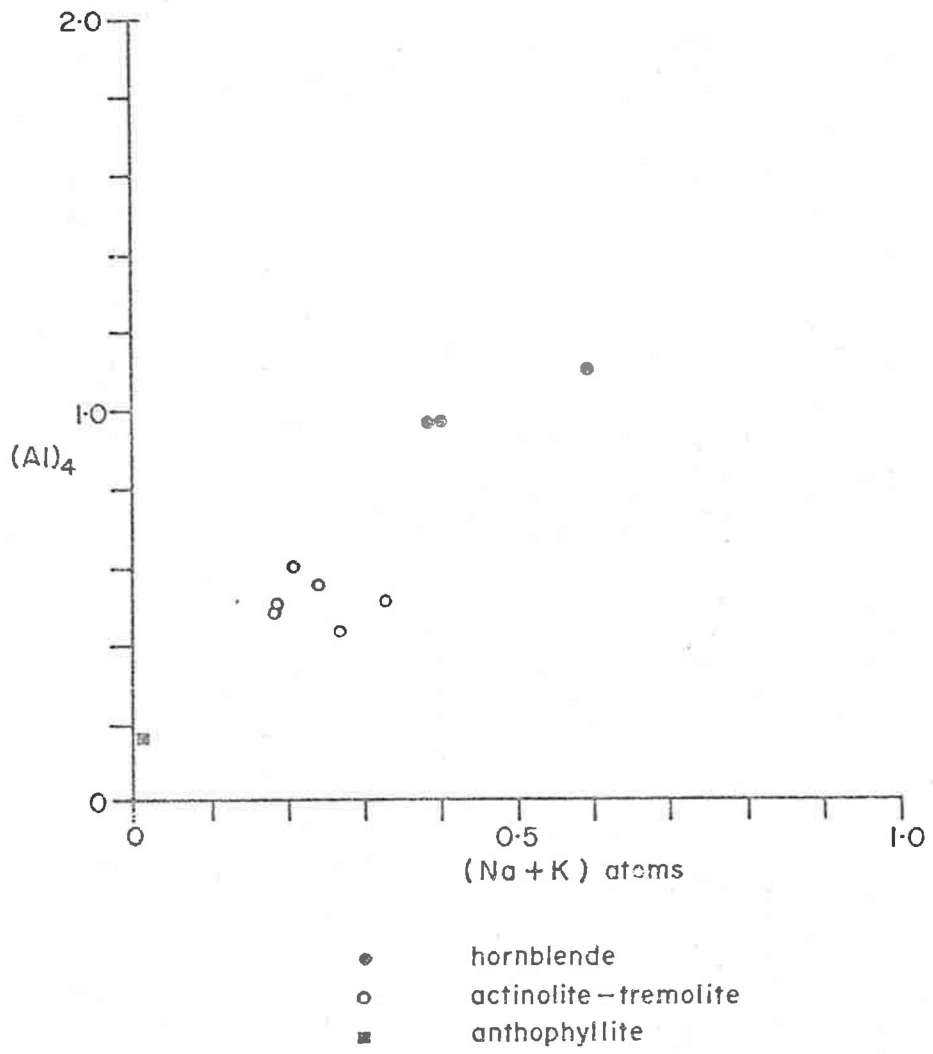
2·0
1·0
(Al)4
0
0
0·5
1·0
(Na + K) atoms
hornblende
actinolite – tremolite
anthophyllite

FIGURE 43

Plots of tetrahedrally co-ordinated atoms of $(Al)^4$ against $((Al)^6 + Fe^3 + Ti)$ of the clinoamphiboles from the calc-schists. Note the composition of hornblende and actinolite-tremolite follows the compositional fields of Deer, Howie and Zussman (1967, Vol.2, Fig. 72)

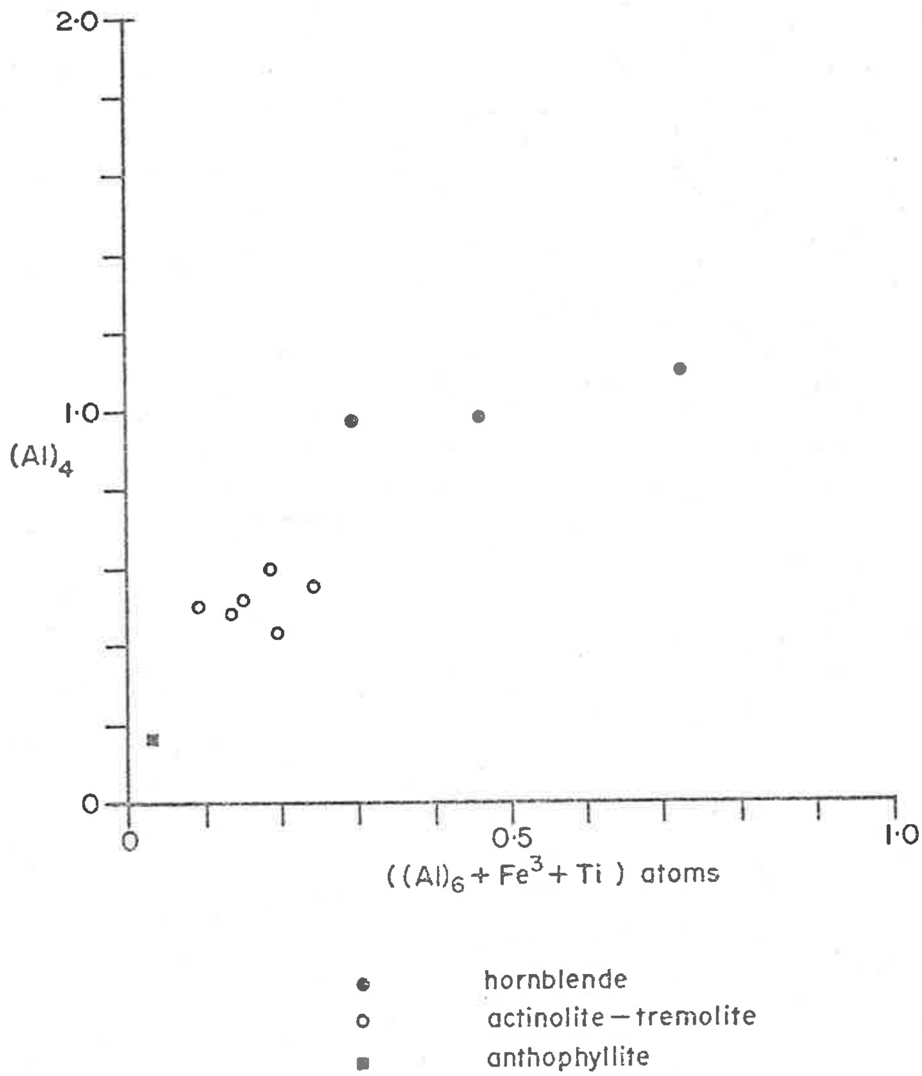
2·0
1·0
(Al)4
0
0
0·5
1·0
((Al)6 + Fe3 + Ti) atoms
hornblende
actinolite – tremolite
anthophyllite

PLATES

PLATE 1

A. Thin biotite rich laminations in quartzo-feldspathic gneiss. Intrusive pegmatite veins are shown in the top and middle part of photo.

SCALE: Pen 12.5 cm.

LOCATION: 172055

B. Compositional banding in quartzo-feldspathic gneiss. S_1 schistosity is parallel to the compositional banding.

SCALE: Bar 10 cm.

LOCATION: 169010

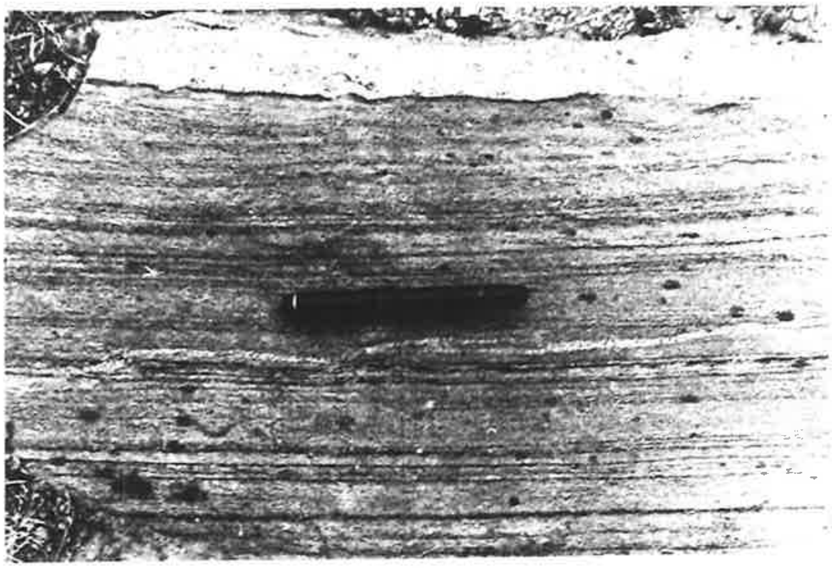

A

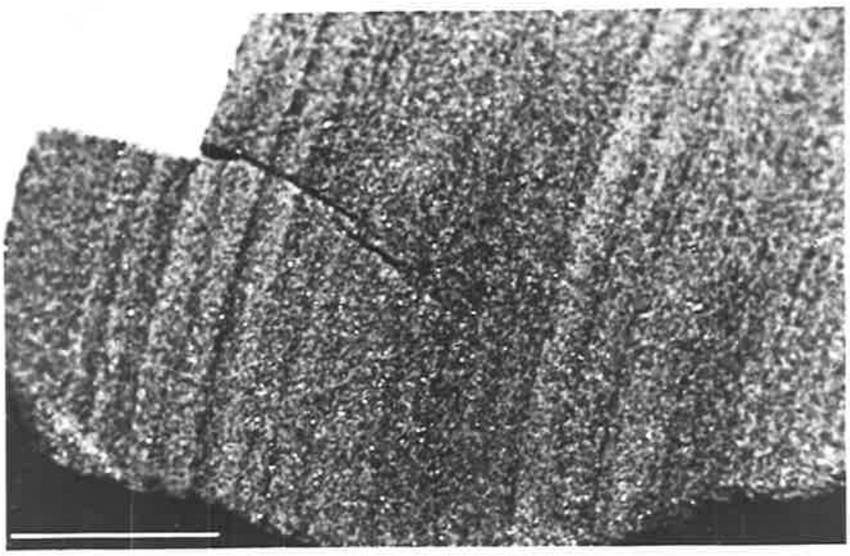

B

PLATE 2

A general view of the mapped area, looking north from the Location 167006, and showing the hills composed of calc-gneisses on the western side and quartzo-feldspathic gneisses on the eastern side of photo. The shallow valley is occupied by the calc-schists.

PLATE 3

A. Intrafolial F_1 folds in quartzo-feldspathic gneiss. Note the thickened hinge of the fold. On the right hand side of photo is a folded pegmatite vein.

SCALE: Length of field: 45 cm.

LOCATION: 186011

B. F_1 similar folds in quartzo-feldspathic gneiss. The axial plane schistosity S_1 is defined by preferred orientation of biotites. Note thickened hinges and thinned limbs.

SCALE: Pencil 15 cm.

LOCATION: 172034

C. Style of similar F_1 folds in quartzo-feldspathic gneiss.

SCALE: Ruler 15 cm.

LOCATION: 155067

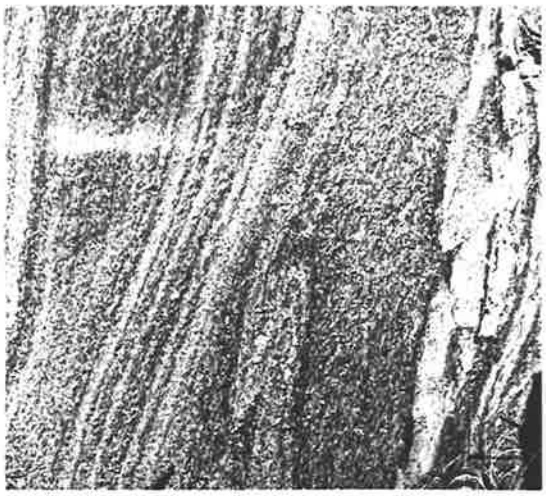

A

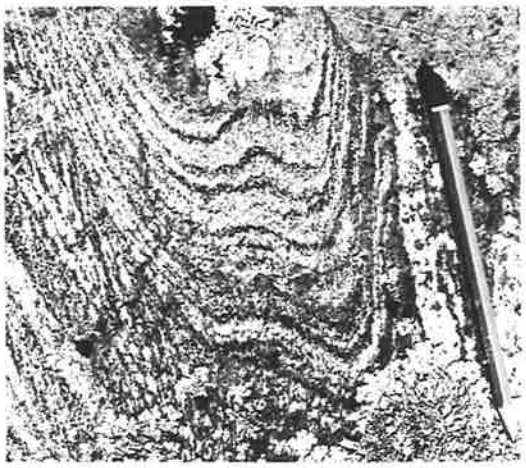

B

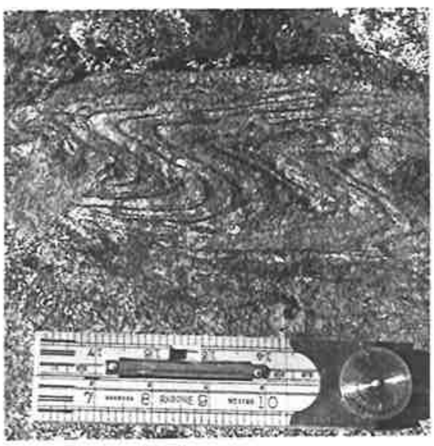

C

PLATE 4

A. F_1 folds in quartzo-feldspathic gneiss. Note the granitic veins are emplaced parallel to axial plane of folds.

SCALE: Ruler 15 cm.

LOCATION 186049

B. F_1 folds in layered quartzo-feldspathic gneiss. Compositional layering has developed parallel to the axial plane schistosity (S_1).

SCALE: Diameter of cap 55 mm.

LOCATION: 157068

C. Style of F_1 folds in interlayered quartz-feldspar rich bands in quartzo-feldspathic gneisses. The axial plane schistosity S_1 is strongly developed in biotite rich layers. A pegmatite vein is emplaced parallel to S_1 schistosity.

SCALE: Ruler 12.5 cm.

LOCATION: 158065

D. F_1 folds in migmatites. Note the style of folding of leucocratic veins with thickened hinges.

SCALE: Pencil 12.5 cm.

LOCATION: 167049

A

B

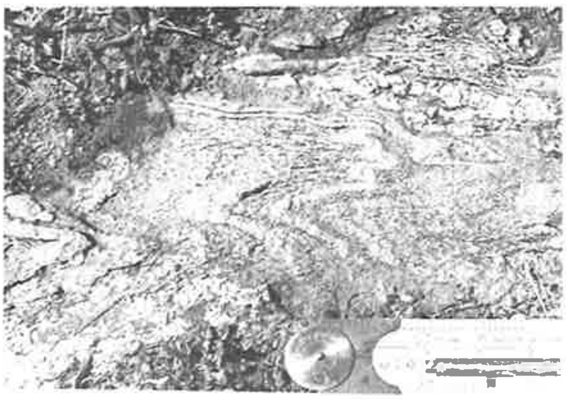

C

D

PLATE 5

A. F_1 folds in interbedded arkosic/pelitic bands. Note the thickening of one limb and thinning in other.

SCALE: Pen 12.5 cm.

LOCATION: 172037

B. Style of F_1 folds in quartzo-feldspathic schist. Note that the quartzo-feldspathic area in the centre of the photograph shows a fold which dies out down the axial plane (towards the bottom left hand corner of the photograph).

SCALE: Diameter of coin is 22 mm.

LOCATION: 185999

C. F_1 folds in migmatised gneisses. Note the development of leucocratic veins along the axial trace of folds.

SCALE: Pencil 9 cm.

LOCATION: 171030

A

B

C

PLATE 6

A. F_1 folds in migmatised gneiss. The leucocratic veins of migmatite appear along the axial trace of folds.

SCALE: Pencil 9 cm.

LOCATION: 159065

B. F_1 folds in quartzo-feldspathic schist. Note the style of folding of quartz veins (white) in the schist.

SCALE: Pen 12.5 cm.

LOCATION: 188003

C. Overturned F_1 folds in a gently folded F_2 structure. Plunge of F_1 folds is perpendicular to the plane of the photograph.

SCALE: Ruler 15 cm.

LOCATION: 167006

A

B

C

PLATE 7

A. Tightly appressed F_1 folds in quartzo-feldspathic gneiss.

SCALE: Ruler 15 cm.

LOCATION: 149071

B. F_1 folds in marble.

SCALE: Ruler 15 cm.

LOCATION: 207067

C. Style of F_1 folding in the calc-schist. Note the development of a quartz pod in the core of folds.

SCALE: Pen 6.5 cm.

LOCATION: 151035

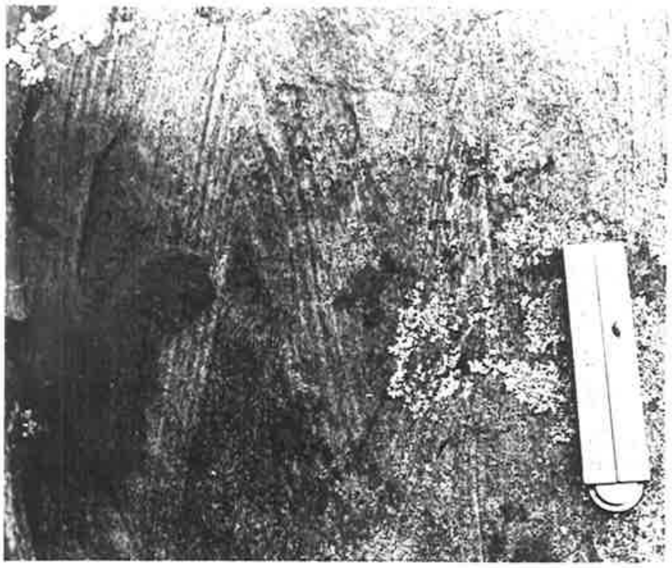

A

B

C

PLATE 8

A. F_2 folds in the migmatite gneiss showing variations from tight angular hinges to broad open type hinges. A coarse leucocratic vein is approximately parallel to S_1 schistosity. Note two felsic veins are emplaced parallel to axial plane of F_2 folds (see bottom centre of photo).

SCALE: Pencil 15 cm.

LOCATION: 187003

B. F_2 folds in quartzo-feldspathic schist.

SCALE: Pencil 15 cm.

LOCATION: 178056

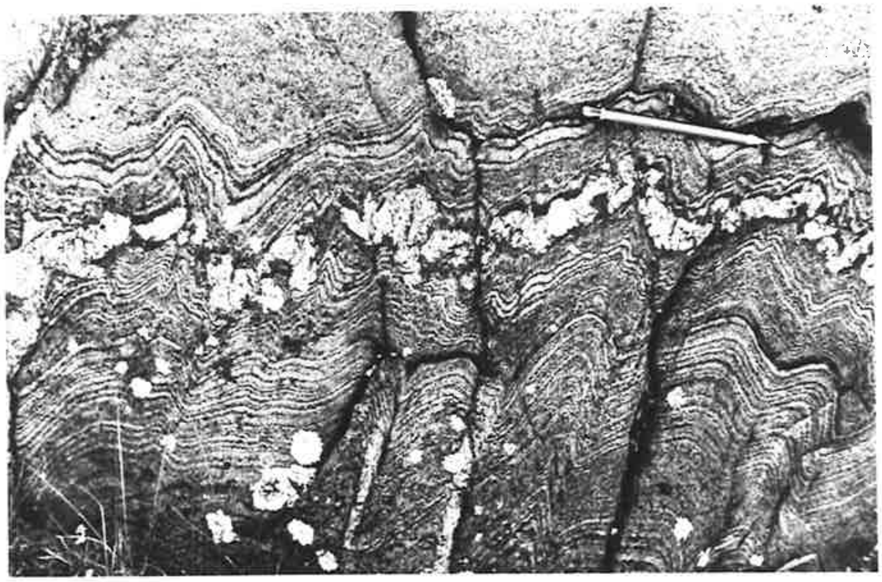

A

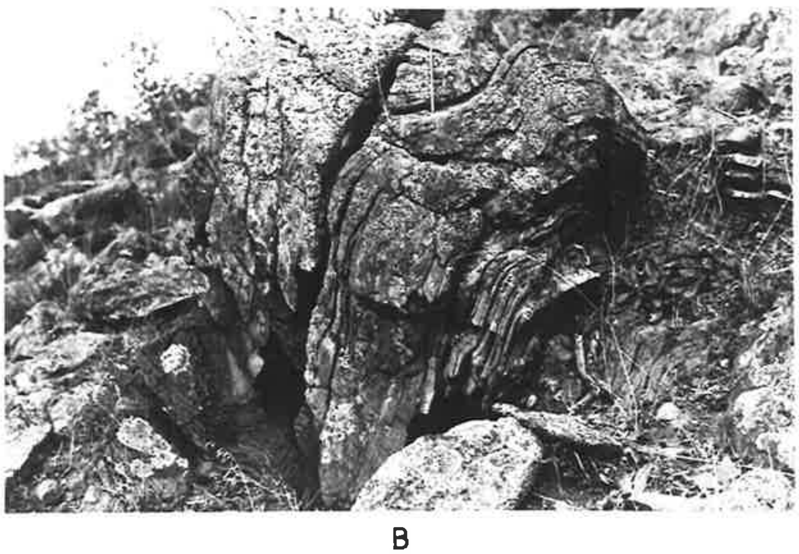

B

PLATE 9

A. F_2 folding in quartzo-feldspathic gneiss with strongly developed axial plane schistosity S_2. Note folded pegmatite veins.

SCALE: Ruler 11 cm.

LOCATION: 178055

B. Style of F_2 folding in quartzo-feldspathic gneiss. Note the variations in degree of folding from chevron type folds on the top left of the outcrop to more open folds in the same lithological band.

SCALE: Pencil 15 cm.

LOCATION: 179040

C. Development of secondary schistosity S_2 in migmatitic gneiss. Note slight fanning of schistosity and the behaviour of pegmatitic veins during folding.

SCALE: Diameter of coin 28 mm.

LOCATION: 171055

A

B

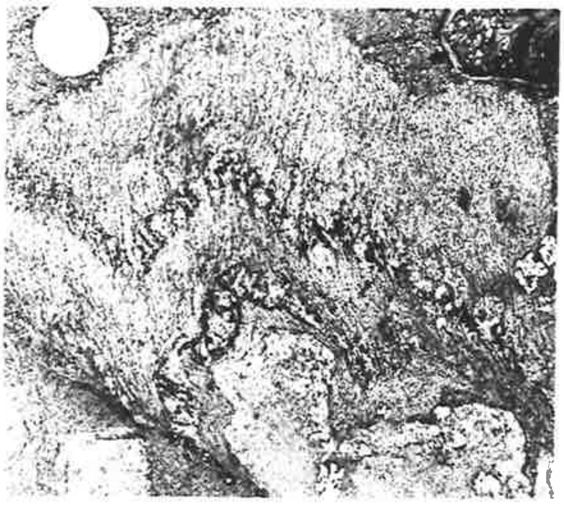

C

PLATE 10

A. Small scale crenulation folds in pelitic bands. The quartz-feldspar rich arkosic bands have a different style of folding.

SCALE: Pen 13 cm.

LOCATION: 163013

B. A hand specimen (A285/501) showing crenulation folds in migmatised pelitic gneiss.

SCALE: Length of field: 13 cm.

C. Style of F_2 folds in coarse grained quartzo-feldspathic gneiss. Micaceous rich laminations show small scale crenulation folds.

SCALE: Pen 12.5 cm.

LOCATION: 166032

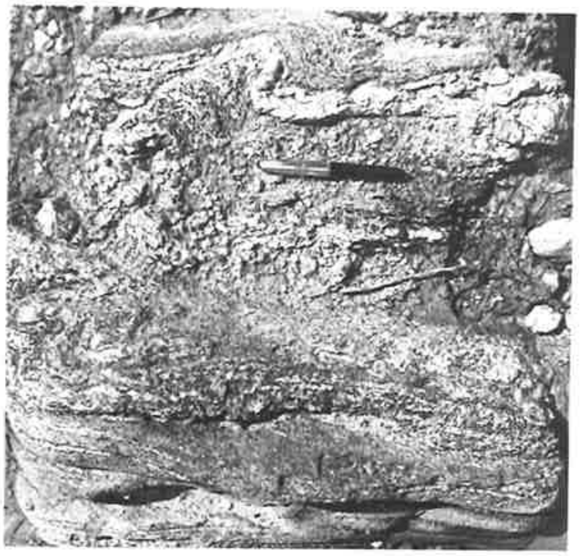

A

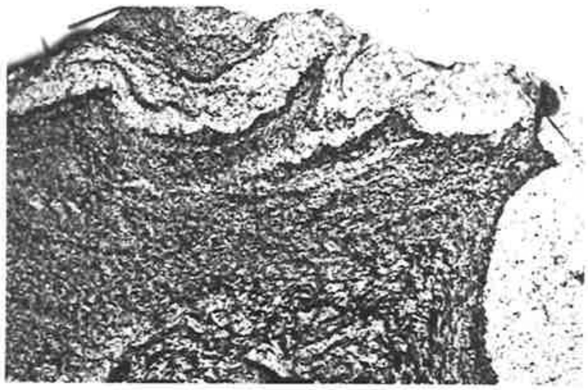

B

C

PLATE 11

A. L_2 lineation - mullion structure on the surface of a folded pegmatite layer.

SCALE: Pencil 15 cm.

LOCATION: 172054

B. L_2 lineation defined by axes of small crenulations in biotite rich layers (S_1).

SCALE: Pencil 15 cm.

LOCATION: 187048

A

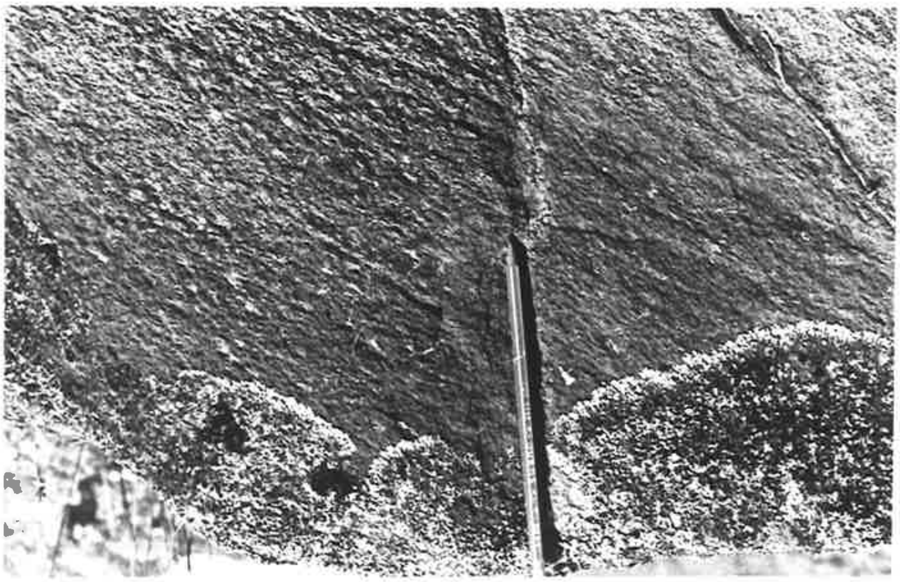

B

PLATE 12

Refolded structures

A. F_1 isoclinal folds (below the ruler) in the western limb of a F_2 anticlinal fold. Crenulation folds are well developed in a micaceous rich band (just below the isoclinal F_1 folds).

SCALE: Ruler 15 cm.

LOCATION: 171018

B. First generation F_1 folds in banded gneiss refolded by F_2 folding. F_1 axial plane trends across the photograph - F_2 axial plane is vertical.

SCALE: Pen 12.5 cm.

LOCATION: 172055

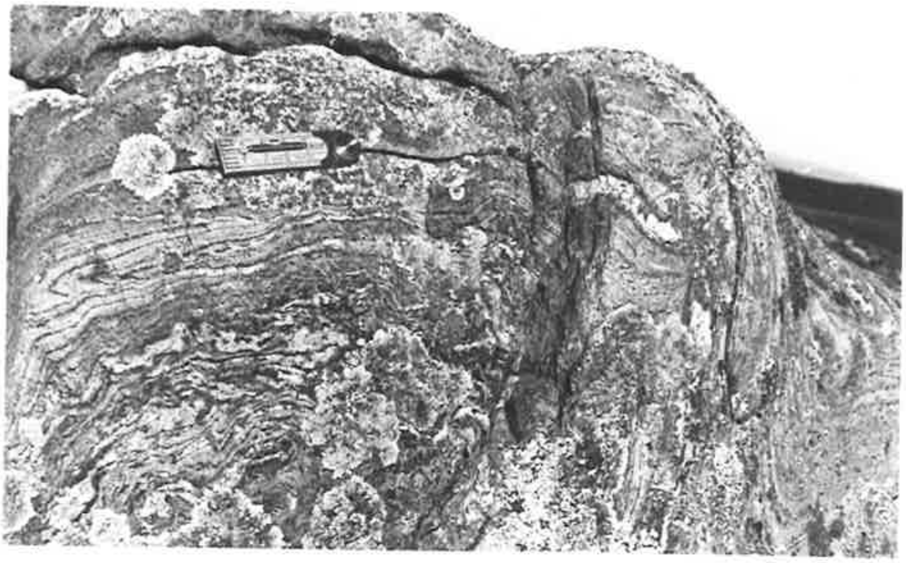

A

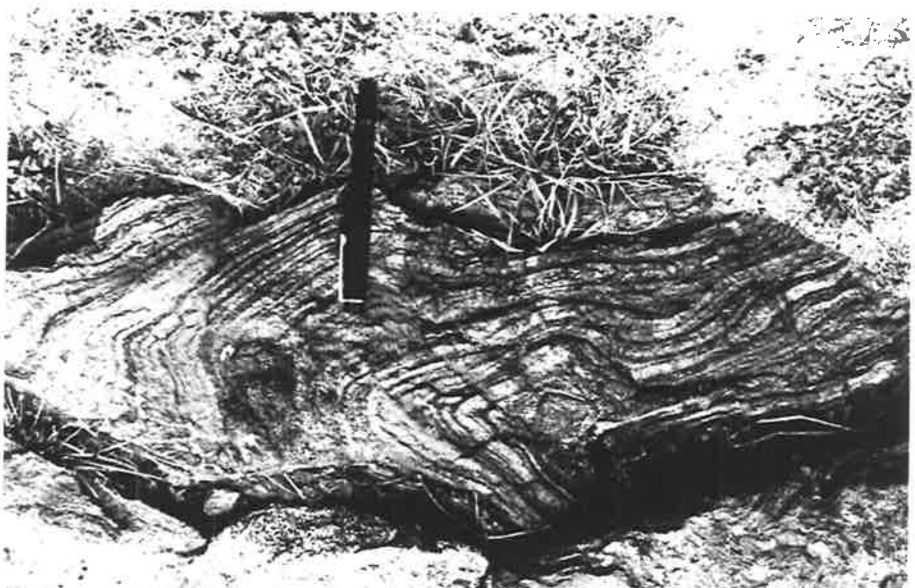

B

PLATE 13

Refolded structures

A. F_1 folds in mica schists and meta-arkose, refolded by F_2 folds. Note the hinge of F_1 folds near the coin. F_1 axial plane is sub-horizontal.

SCALE: Diameter of coin 28 cm.

LOCATION: 166015

B. F_1 isoclinal folds in quartzo-feldspathic gneiss, refolded by gentle warping of F_2 folding.

SCALE: Length of rubber 25 mm.

LOCATION: 182047

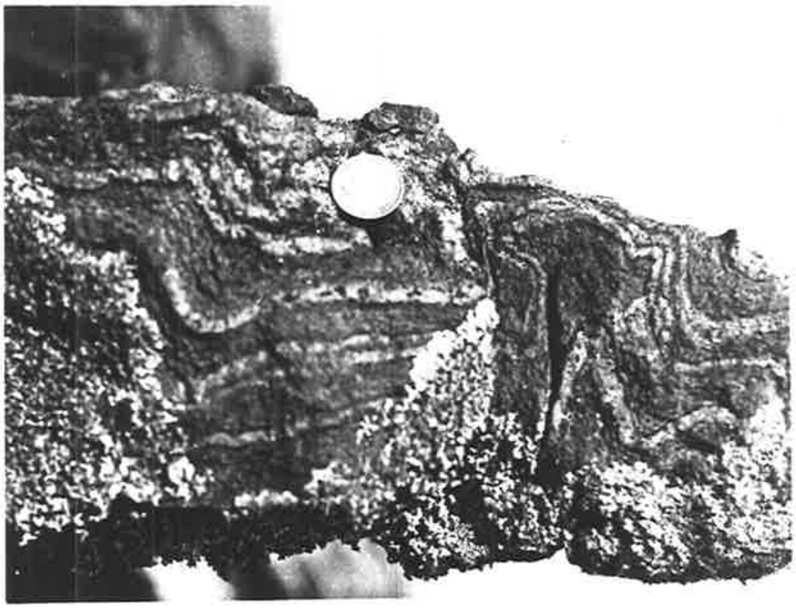

A

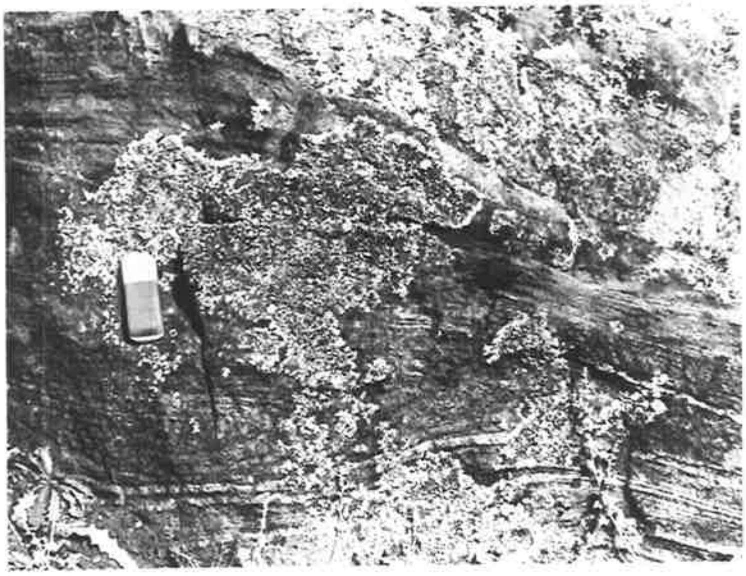

B

PLATE 14

A. Photomicrograph of F_2 folds in quartzo-feldspathic gneiss showing the secondary schistosity S_2 defined by preferred orientation of biotites. Section perpendicular to F_2.

A285/371 Plane pol. light Length of field: 20 mm.

B. Photomicrograph showing two schistosities S_1 and S_2 in quartzo-feldspathic gneiss. Note coarse grained biotites in S_1 and fine grained biotites in S_2.

A285/390 Plane pol. light Length of field: 9 mm.

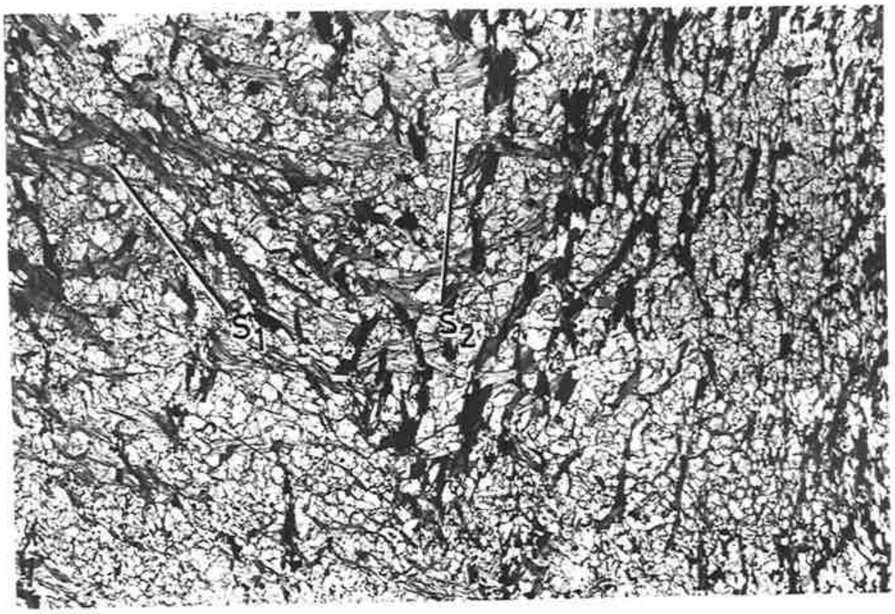

A

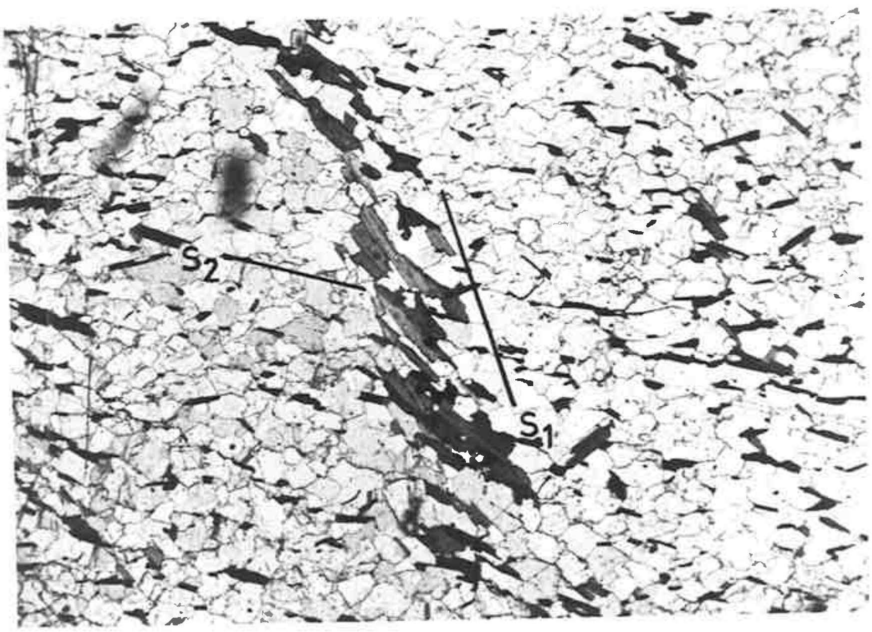

B

PLATE 15

A. A large thin section of quartzo-feldspathic gneiss showing F_1 folds refolded by F_2 folds. The secondary schistosity S_2 is developed parallel to axial plane of F_2 folds.

A285/397 Plane pol. light Length of field: 11 cm.

B. A large thin section of F_2 folds (cut perpendicular to F_2), exhibiting the secondary schistosity S_2, developed in the hinges of folds. Note a granitic vein is emplaced parallel to axial plane of folds.

A285/371 Plane pol. light Length of field: 7 cm.

A

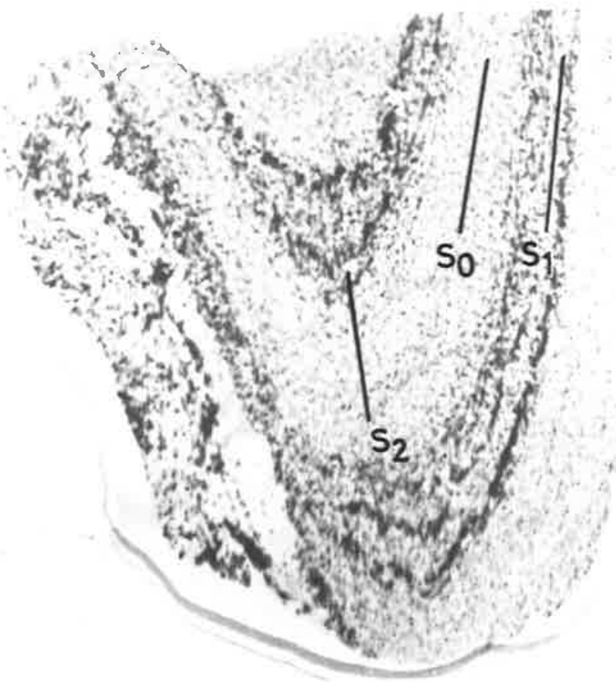

B

PLATE 16

A. Photomicrograph of pelitic schist showing crenulation cleavage (S_2). Note the dimensionally oriented quartz and feldspar along S_1 plane. Section perpendicular to F_2.

A285/200 Crossed polars Length of field: 15 mm.

B. Photomicrograph of anthophyllite schist exhibiting fine and coarse grained layering (S_0) parallel to schistosity S_1. S_0-S_1 planes have been folded by F_2. Section perpendicular to F_2.

A285/159 Crossed polars Length of field: 15 mm.

C. Photomicrograph of F_2 folds in quartzo-feldspathic schist showing secondary schistosity (S_2) in the hinges of folds. Section perpendicular to F_2.

A285/371 Crossed polars Length of field: 15 mm.

A

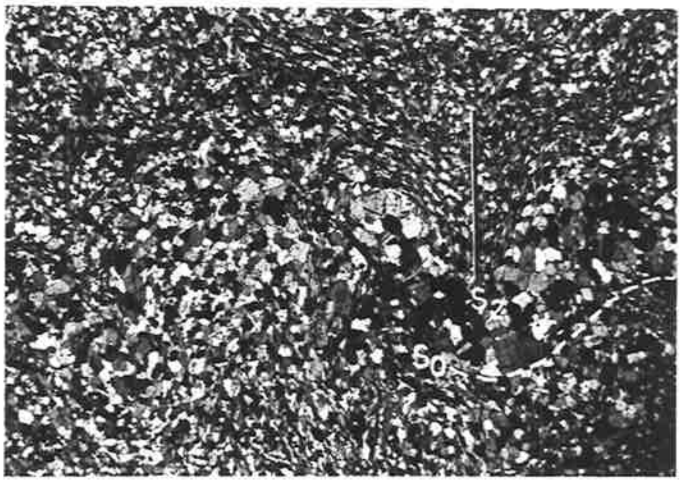

B

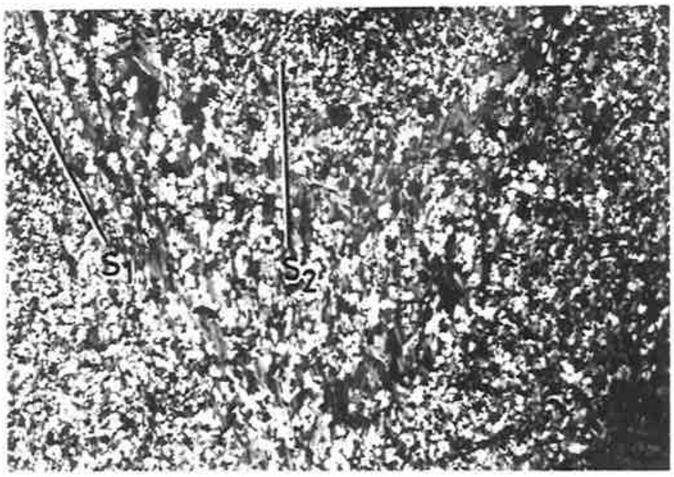

C

PLATE 17

A. Photomicrograph of F_1 folds refolded by F_2 folds. The dark layers are rich in biotite, with the coarse biotite flakes parallel to S_1. The secondary schistosity S_2 is defined by fine biotite plates parallel to axial plane of F_2 folds. Section perpendicular to F_2.

A285/397 Plane pol. light Length of field: 40 mm.

B. Photomicrograph of coarse grained quartzo-feldspathic gneiss exhibiting crenulation folds (F_2). Section perpendicular to F_2.

A285/408 Plane pol. light Length of field: 15 mm.

C. Photomicrograph showing two schistosities, S_1 and S_2 in a quartzo-feldspathic gneiss.

A285/398 Plane pol. light Length of field: 20 mm.

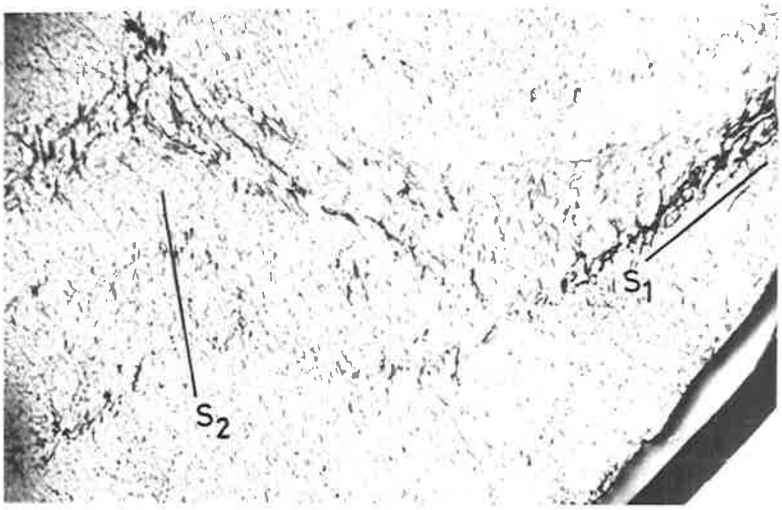

A

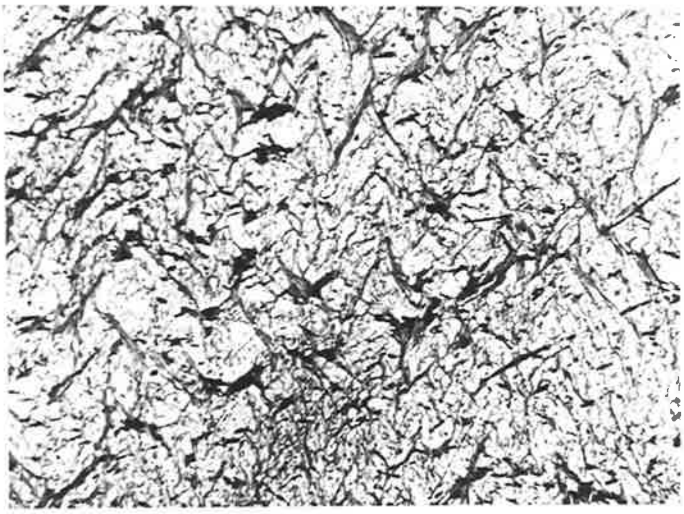

B

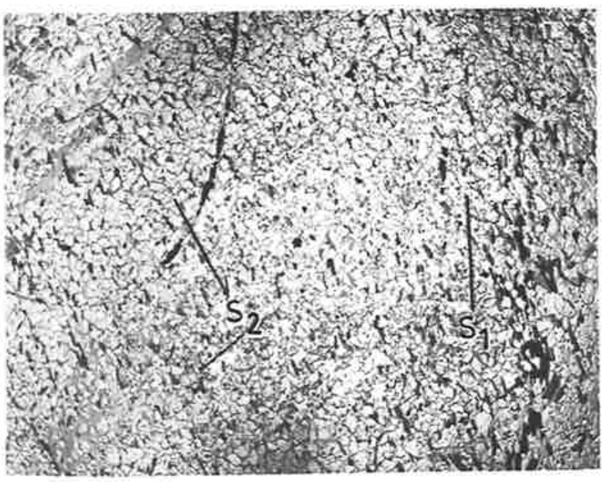

C

PLATE 18

A. Photomicrograph of a muscovite porphyroblast showing kink bands.

A285/379 Crossed polars Length of field: 2.8 mm.

B. Photomicrograph of strongly deformed marble showing kink bands and deformation twinning in calcite grains.

A285/182 Crossed polars Length of field: 9 mm.

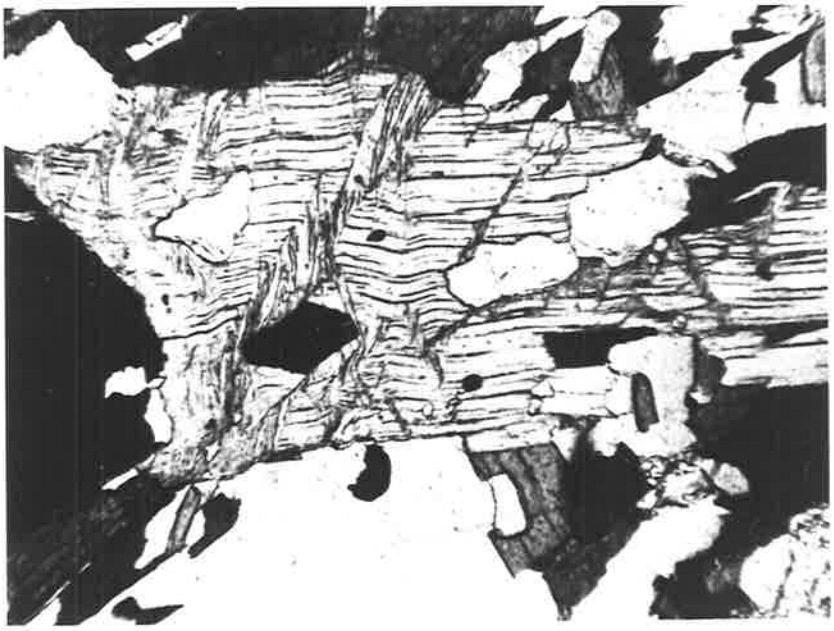

A

B

PLATE 19

A. Photomicrograph of diopside showing deformation twinning. The twinning has been subsequently kinked.

A285/55 Plane pol. light Length of field: 1.5 mm.

B. Photomicrograph of a calcite porphyroblast in marble, exhibiting kink structures and cleavage. A scapolite (S) porphyroblast is seen in the lower right hand corner of photo. Matrix is composed of recrystallised grains of calcite.

A285/690 Plane pol. light Length of field: 1.5 mm.

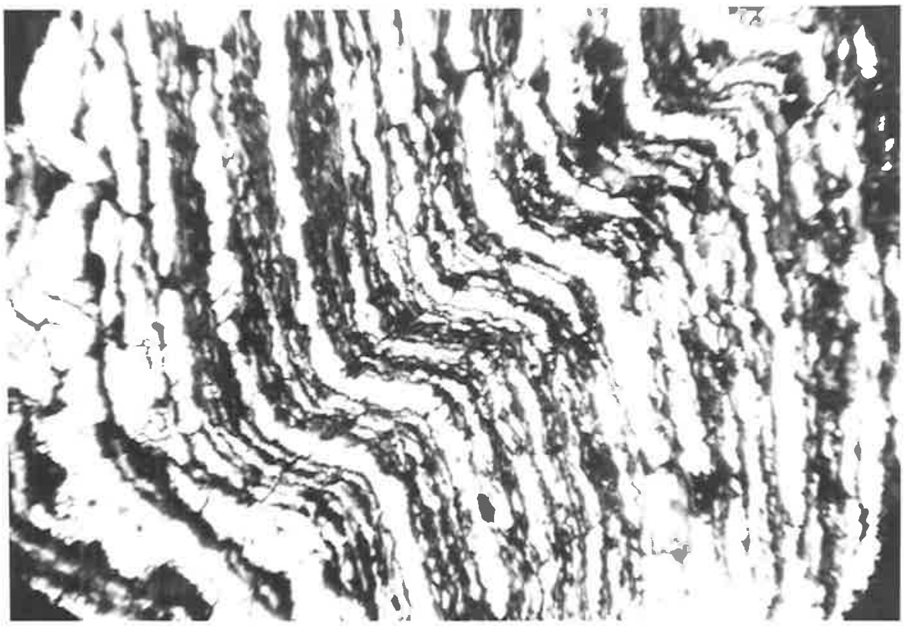

A

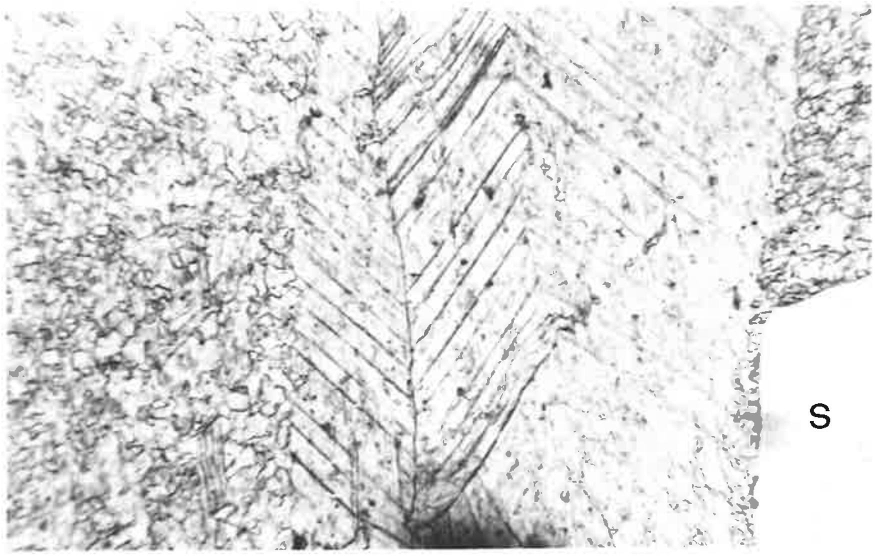

B

PLATE 20

A. Thinly bedded quartzo-feldspathic schist, with alternate dark and light bands.

SCALE: Ruler 6 inches

LOCATION: 198059

B. Photomicrograph of a quartzo-feldspathic schist showing quartz, plagioclase (mostly untwinned) and biotite.

A285/3 Crossed polars Width of field: 2.8 mm.

A

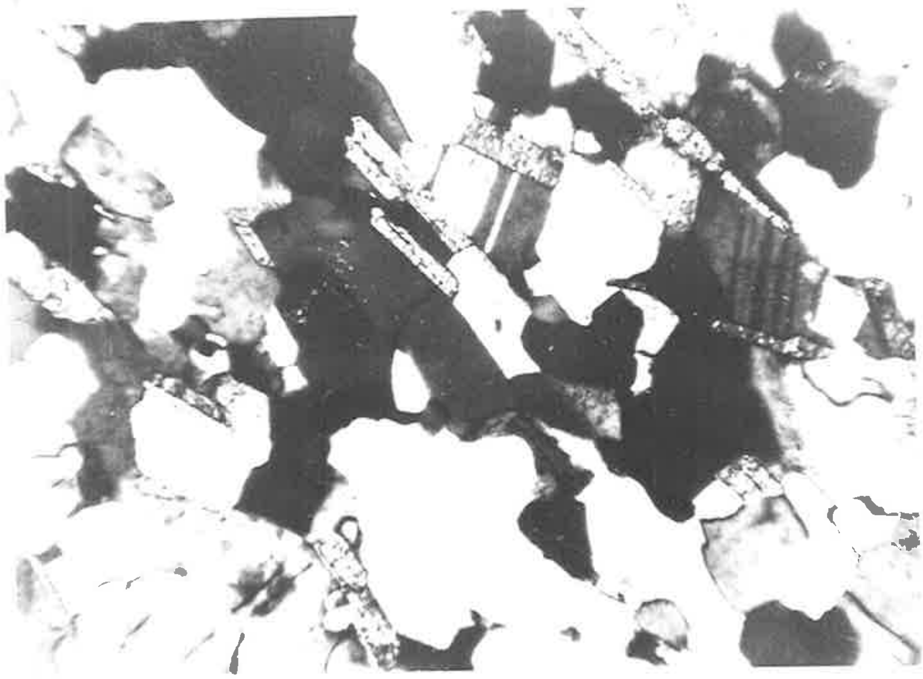

B

PLATE 21

A. Compositional layering in quartzo-feldspathic gneiss with thin biotite rich laminations.

SCALE: Ruler marked in inches

LOCATION: 165032

B. Photomicrograph of quartzo-feldspathic gneiss showing inclusions of quartz in plagioclase.

A285/381 Crossed polars Width of field: 2 mm.

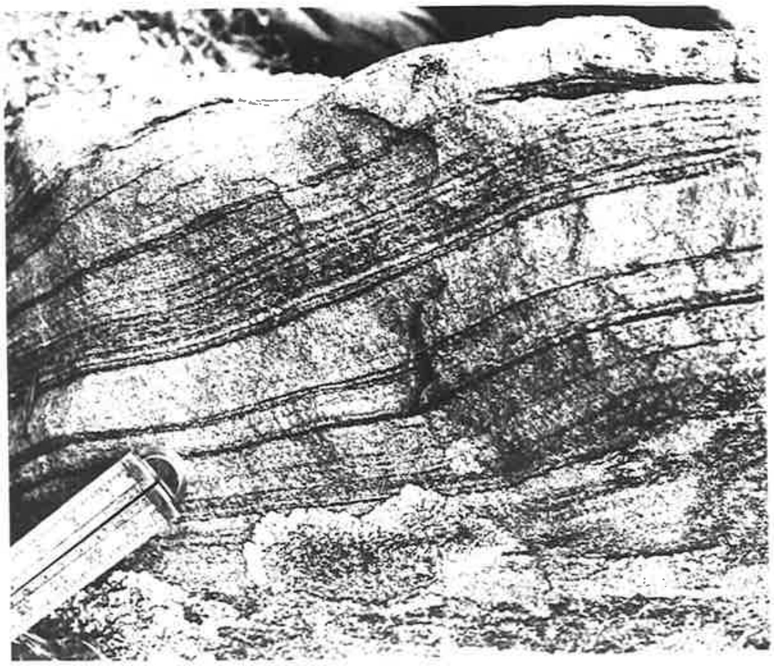

A

B

PLATE 22

A. Photomicrograph showing replacement of plagioclase by biotite in quartzo-feldspathic gneiss.

A285/381 Crossed polars Length of field: 2 mm.

B. Photomicrograph showing coarse biotite in S_1 plane and fine biotite in S_2 plane in quartzo-feldspathic schist.

A285/390 Plane pol. light Length of field: 9 mm.

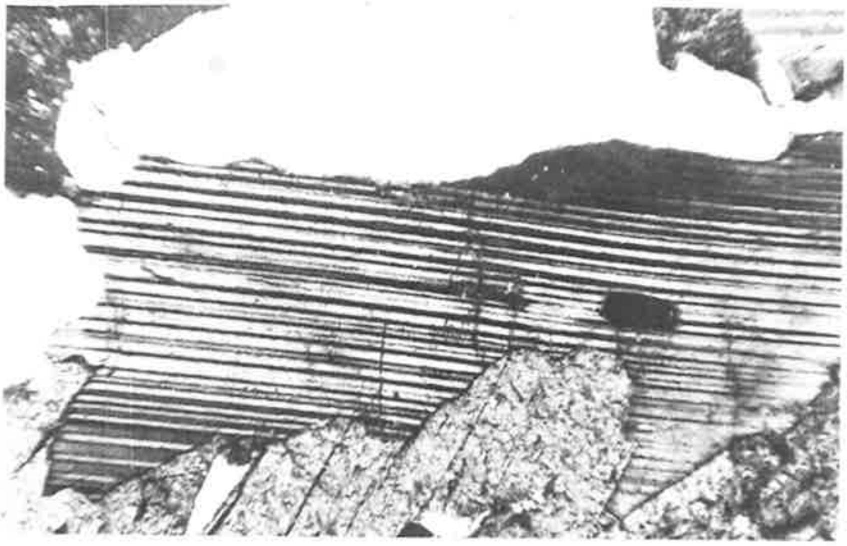

A

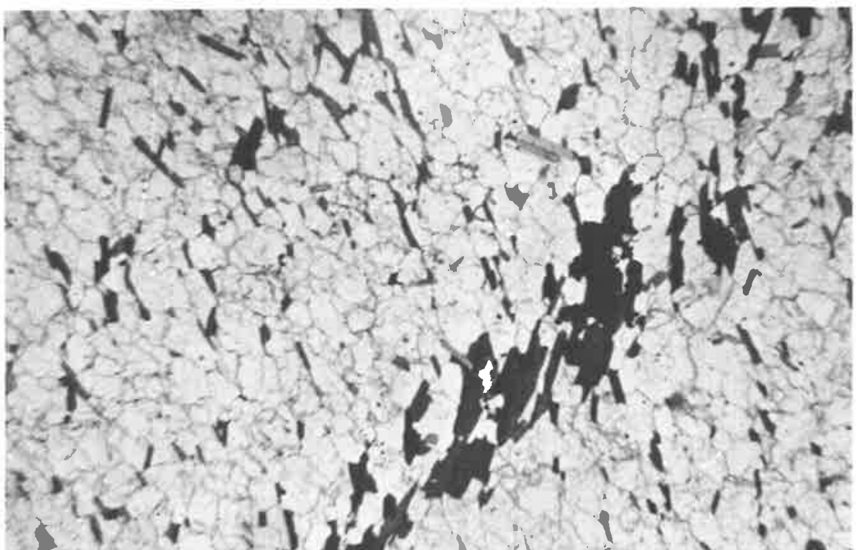

B

PLATE 23

A. Photomicrograph of a semi-pelitic schist, showing post tectonic (F_1) muscovites transecting S_1 schistosity defined by oriented biotites and quartz grains.

A285/281 Plane pol. light Length of field: 1.5 mm.

B. Photomicrograph of sillimanite bearing gneiss, showing fibrolite mats with numerous needles crowded in quartz grains. A biotite flake (dark grey) is seen on the left hand corner of photo.

A285/132 Plane pol. light Scale: x 25

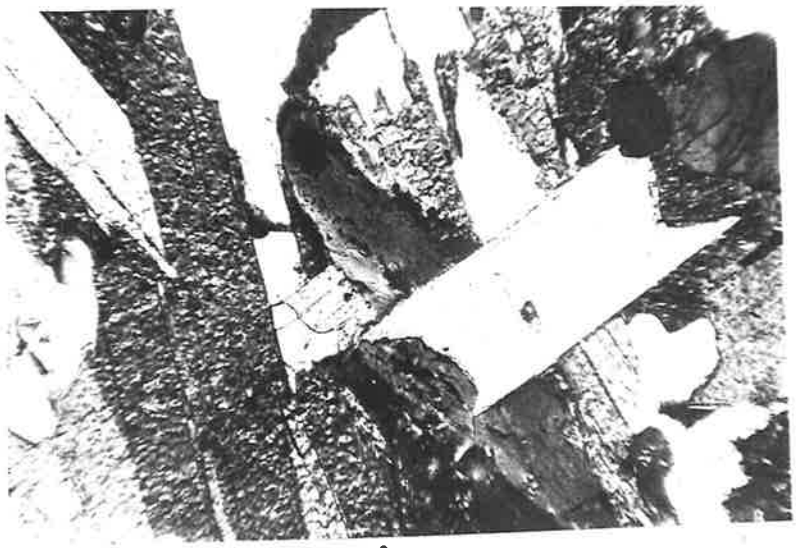

A

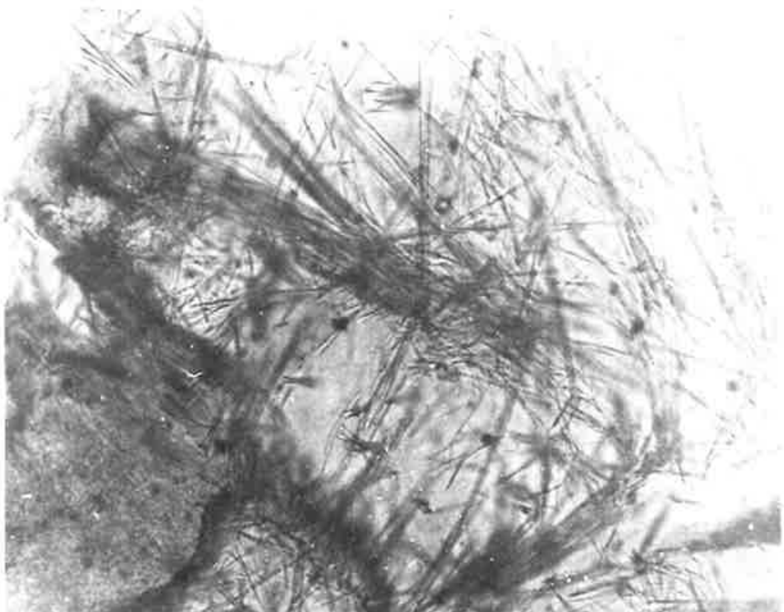

B

PLATE 24

A. Photomicrograph of pelitic schist showing prisms of sillimanite in biotite.

A285/198 Plane pol. light Length of field: 1.5 mm.

B. Aluminous pelitic schist exhibiting the sillimanite (fibrolite) faserkiesel.

SCALE: Ruler 15 cm.

LOCATION: 179033

C. A hand specimen showing nodules of fibrolite in quartzo-feldspathic gneiss. These nodules are elongated parallel to mineral lineation (?L_1).

SCALE: Match 45 mm.

A285/226

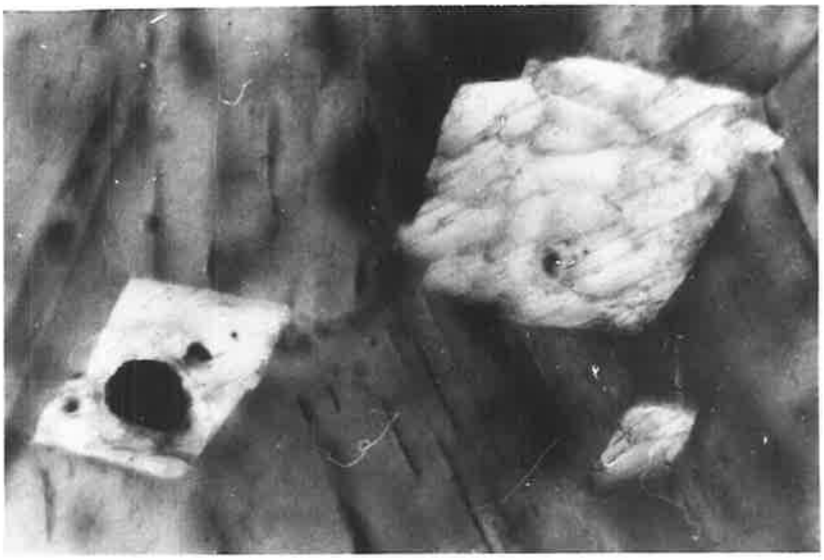

A

B

C

PLATE 25

A Photomicrograph of fibrolitic mats associated with quartz and feldspar grains. Note that the trails of fibrolite needles are enclosed in quartz grains.

A285/130 Plane pol. light Length of field: 1.5mm.

B Photomicrograph of fibrolite nodules in aluminous pelitic schist. The nodules consist of bundles of fibrolite (dark grey) rimmed by skeletal muscovite (light grey) (see Plate 25C). Fibrolitic nodules appear to transect the schistosity S_1 defined by preferred orientation of biotite plates.

A285/349 Plane pol. light Length of field: 9mm.

C Photomicrograph of fibrolite (dark grey) close association with marginal muscovite (light grey).

A285/349 Plane pol. light Length of field: 1.5mm.

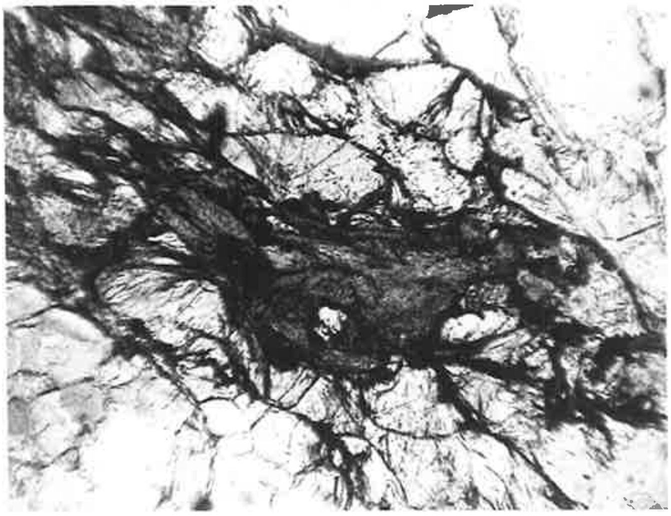

A

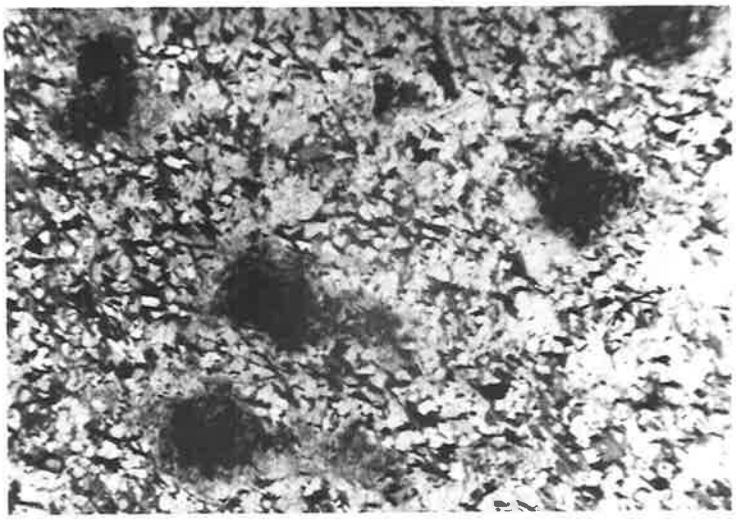

B

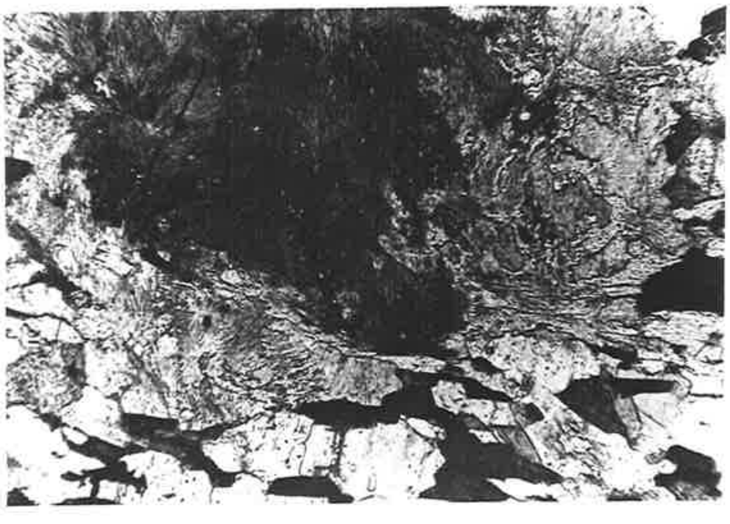

C

PLATE 26

A. Photomicrograph of skeletal muscovite (light grey) is replaced at the marginal part by fibrolites. Note the cleavage planes of the muscovite continue on into the bundles of fibrolite fibres. Numerous needles of fibrolite are crowded in the adjacent quartz grains.

A285/131 Crossed polars Length of field: 2.8 mm.

B. Photomicrograph of fibrolite mats (S) contains iron ores (O) bordering against a biotite flake (B). The quartz (clear white) in the matrix is free of fibrolite needles.

A285/198 Crossed polars Length of field: 1.5 mm.

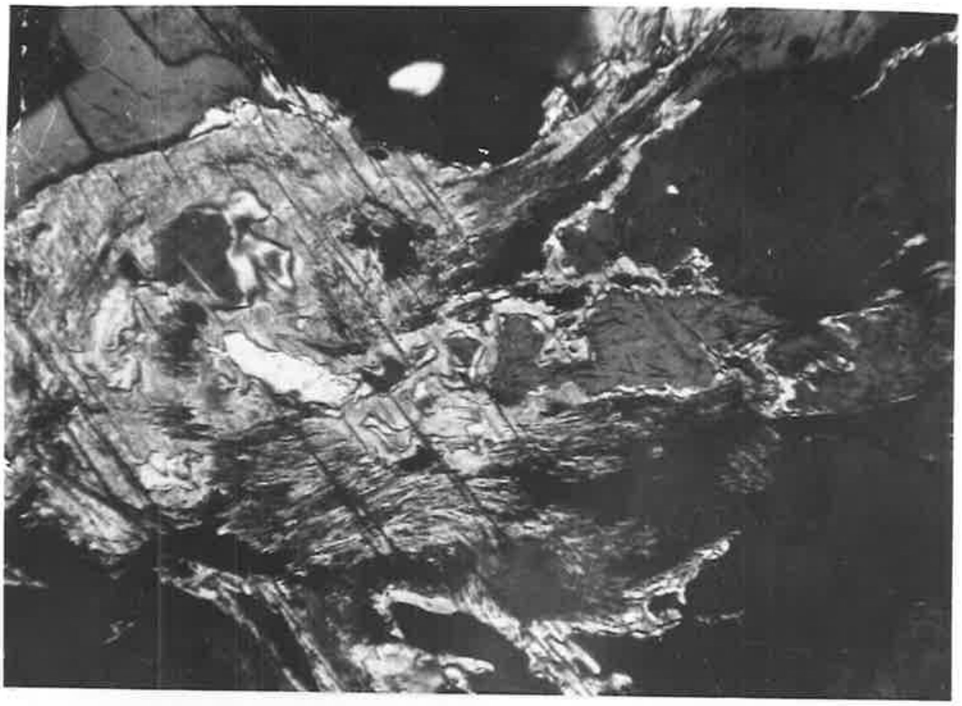

A

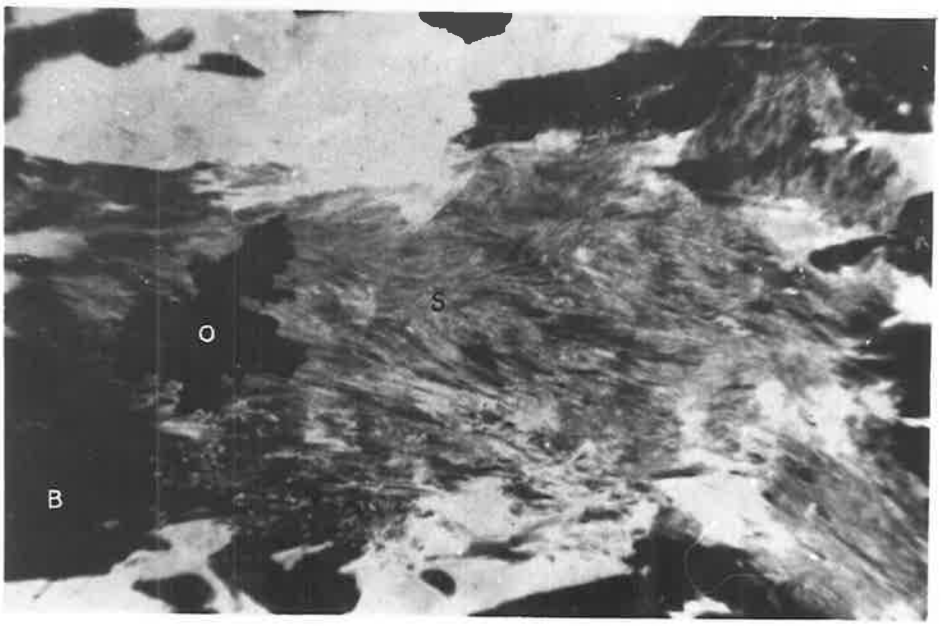

B

PLATE 27

A A hand specimen (A285/583) showing the leucocratic vein of migmatite in the gneissic host rock. Note a thin biotite selvedge at the contact.

SCALE: Length of specimen: 70mm.

B Photomicrograph of migmatite showing the contact of a leucocratic vein and the gneissic host. The preferred orientation of biotite is strongly developed parallel to S_1 in the host rock.

A285/583 Crossed polars Length of field: 9mm.

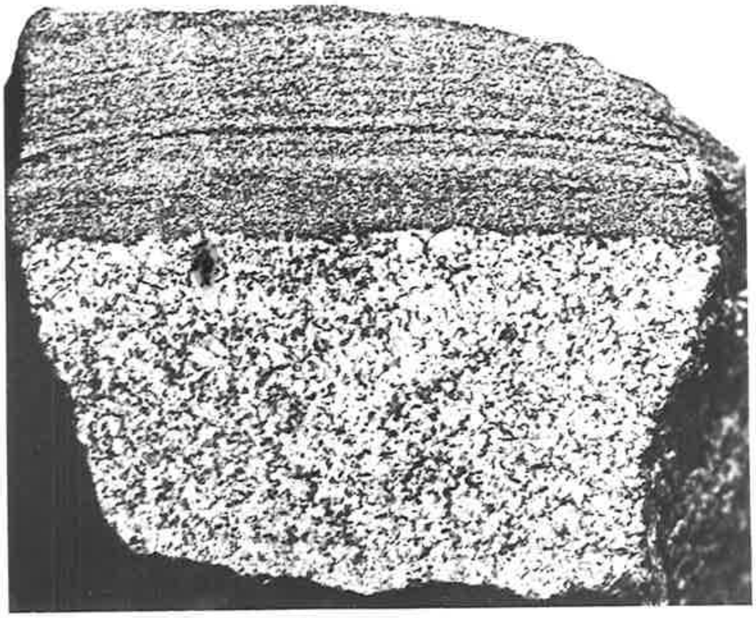

A

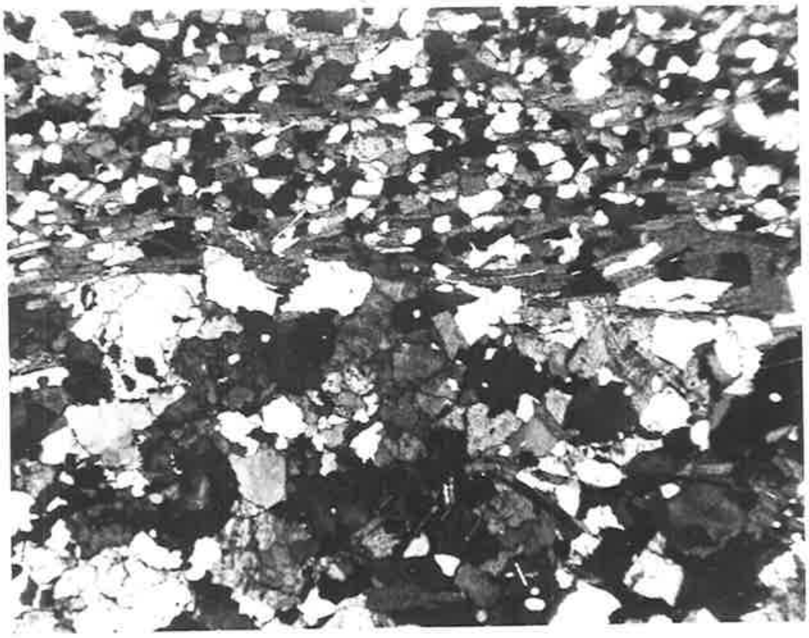

B

PLATE 28

A. Photomicrograph of quartz showing deformation lamellae in the leucocratic vein of migmatite.

A285/474 Crossed polars Length of field: .4 mm.

B. Photomicrograph of a strongly deformed plagioclase showing kink bands (K). The bright areas in plagioclase are muscovite flakes.

A285/474 Crossed polars Length of field: 1.5 mm.

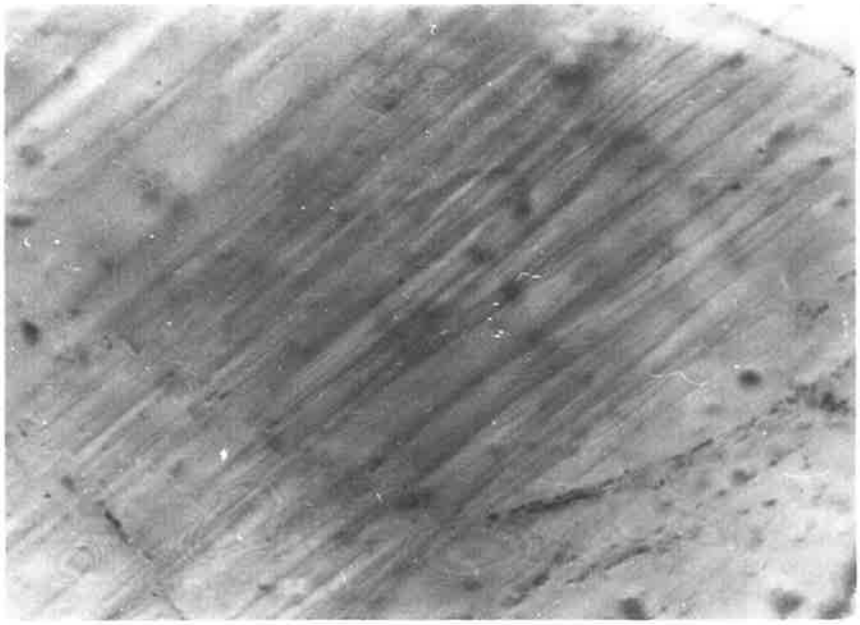

A

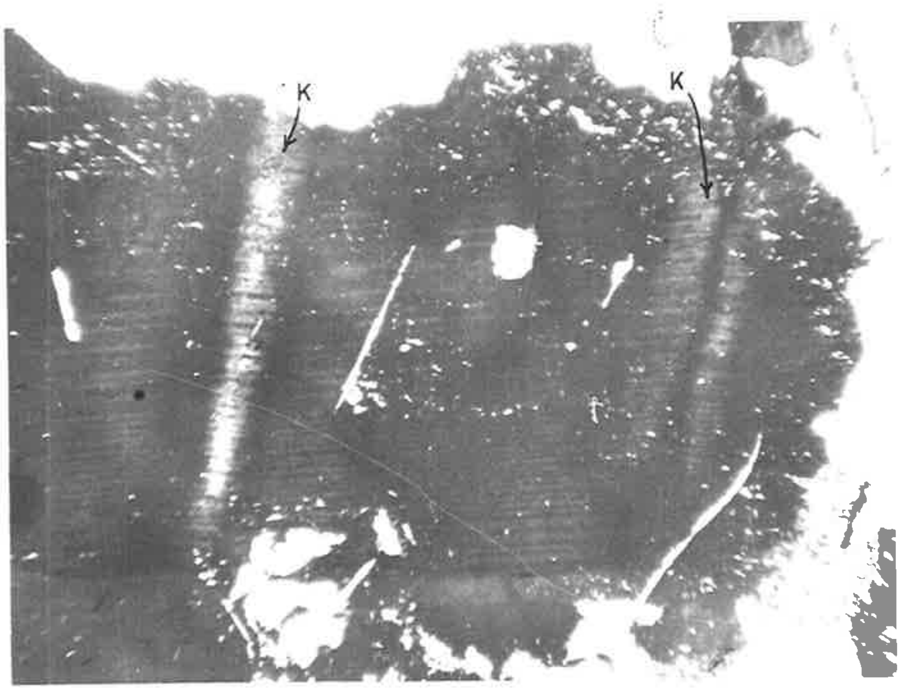

B

PLATE 29

A. A complexly twinned plagioclase grain in the leucocratic vein of migmatite. Note the deformation (glide) twinning and slight bending of twin lamellae.

A285/479 Crossed polars Length of field: 2.8 mm.

B. Photomicrograph of deformed plagioclase in a leucocratic vein of migmatite, showing bending of twin lamellae. Note secondary muscovite replacing plagioclase.

A285/474 Crossed polars Length of field: 1.5 mm.

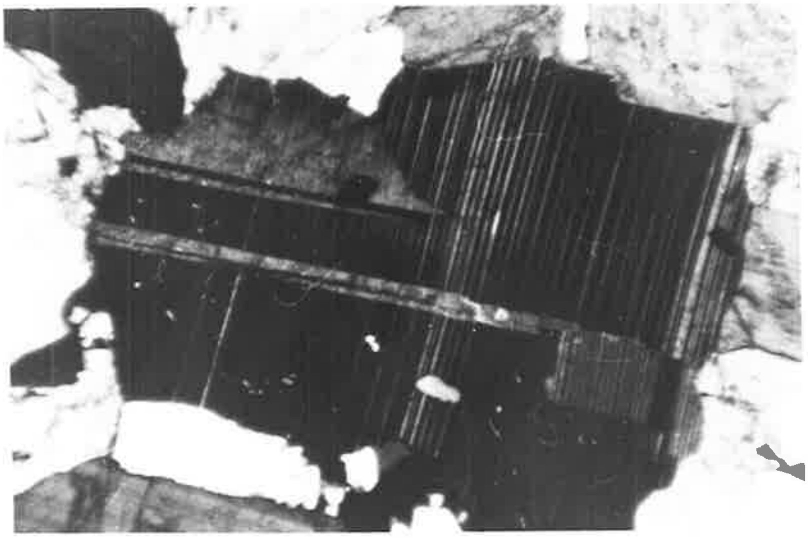

A

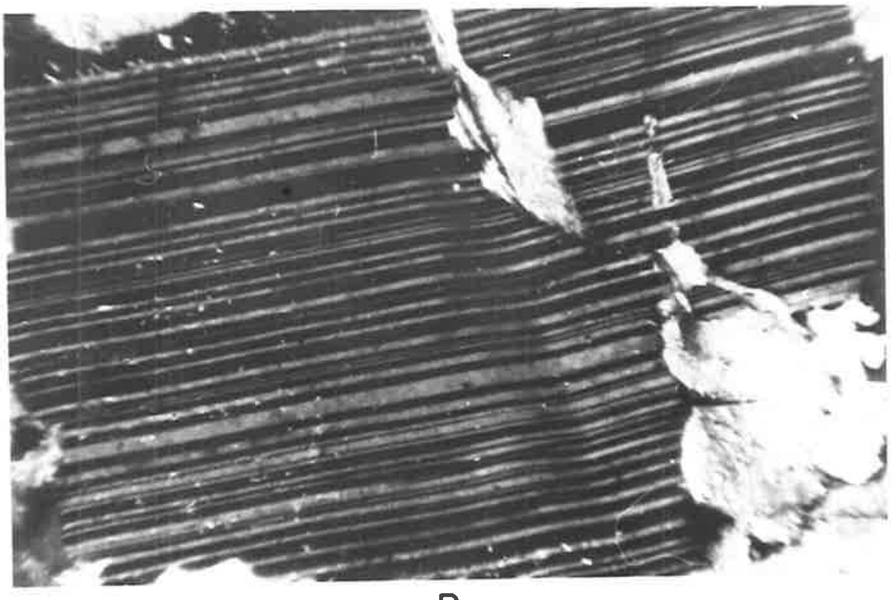

B

PLATE 30

A. Photomicrograph: a megacryst of quartz replacing plagioclase in a leucocratic vein of the migmatite.

A285/496 Crossed polars Length of field: 2.8 mm.

B. Photomicrograph of secondary muscovite replacing microcline in a leucocratic vein of the migmatite. A highly sericitized plagioclase is seen on the top right hand corner of photo.

A285/379 Crossed polars Length of field: 2.8 mm.

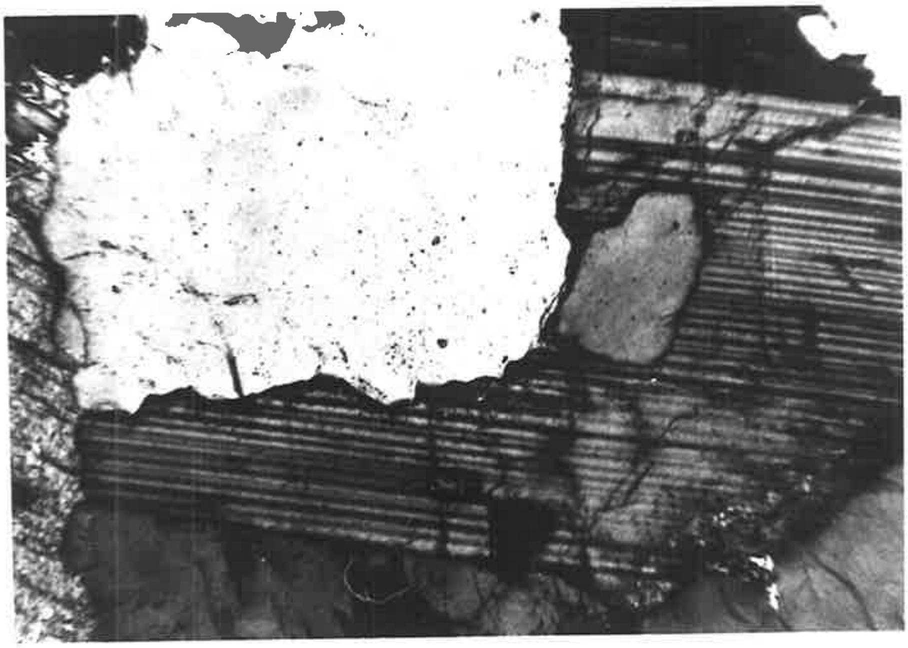

A

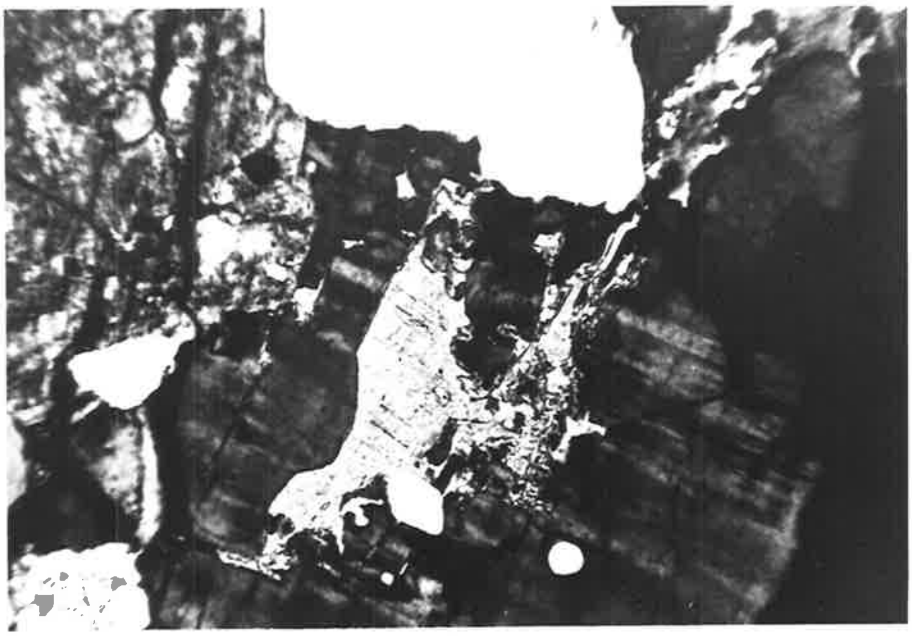

B

PLATE 31

A. Photomicrograph showing post tectonic secondary muscovite replacing plagioclase in a leucocratic vein of migmatite.

A285/496 Crossed polars Length of field: 2.8 mm.

B. Photomicrograph of the gneissic host rock of the migmatite, showing quartz, plagioclase and biotite.

A285/398 Crossed polars Length of field: 2.8 mm.

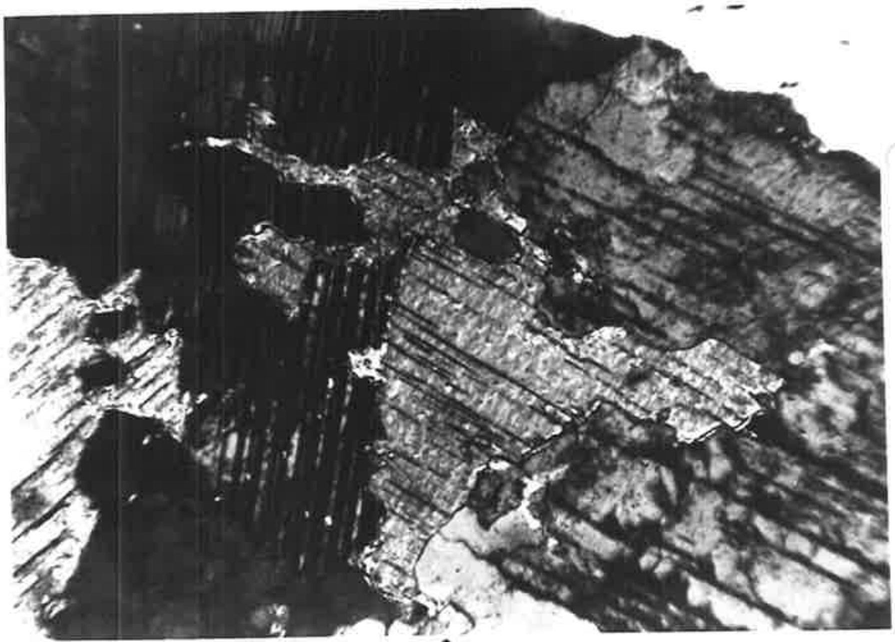

A

B

PLATE 32

A. Photomicrograph of the coarse grained granitic gneiss, showing quartz, plagioclase and biotite. Note small inclusions of biotite in porphyroblastic quartz grain.

A285/531 Crossed polars Length of field: 2.8 mm.

B. Photomicrograph of the medium grained granitic gneiss, showing quartz, plagioclase and biotite.

A285/459 Crossed polars Length of field: 2.8 mm.

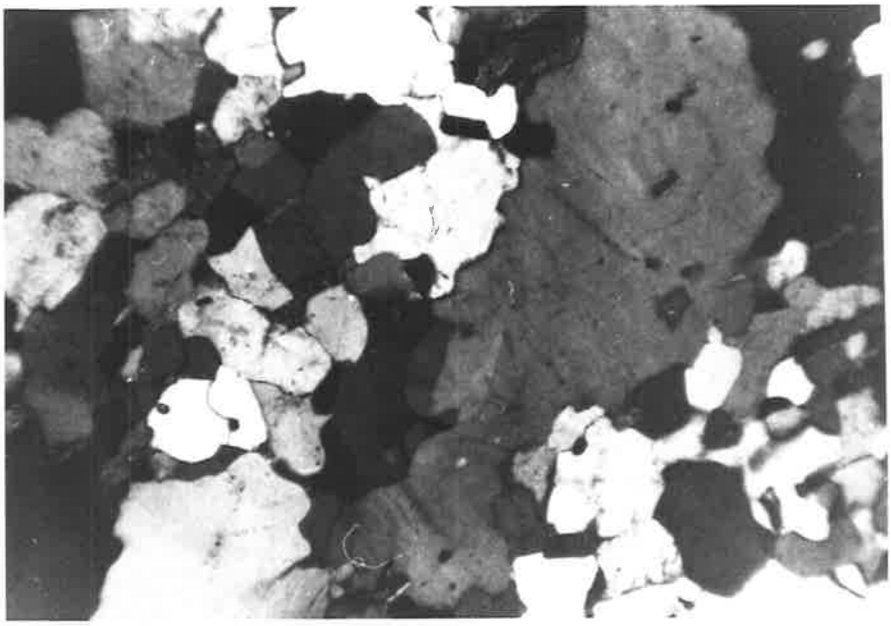

A

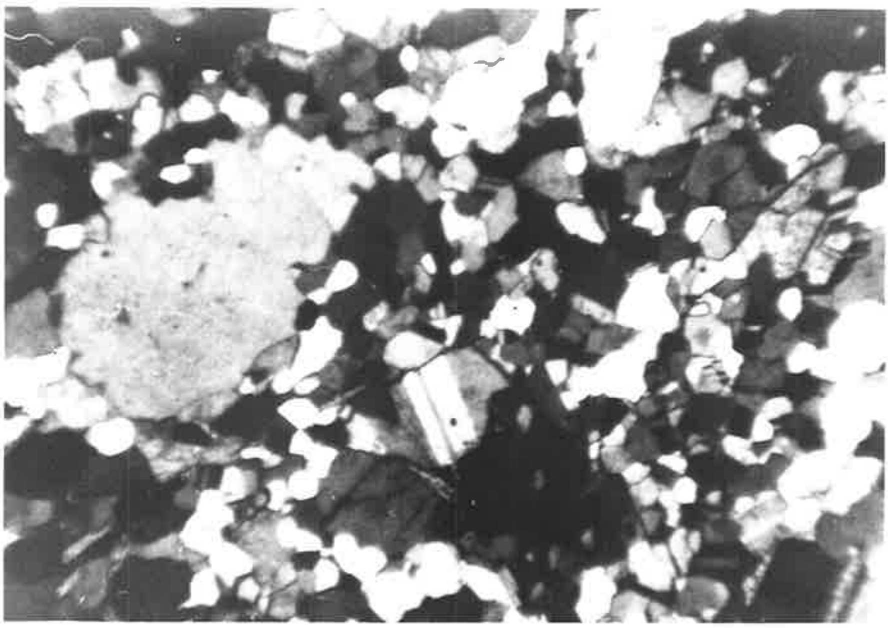

B

PLATE 33

A Photomicrograph of a quartz porphyroblast in the medium grained granitic gneiss, showing deformation lamellae. The white subrounded grains are quartz inclusions of optically different orientation.

A285/293C Crossed polars Length of field: 0.4mm.

B Photomicrograph of a quartz porphyroblast in the medium grained granitic gneiss. Small plates of biotite occur as inclusions in the porphyroblast.

A285/527 Crossed polars Length of field: 0.4mm.

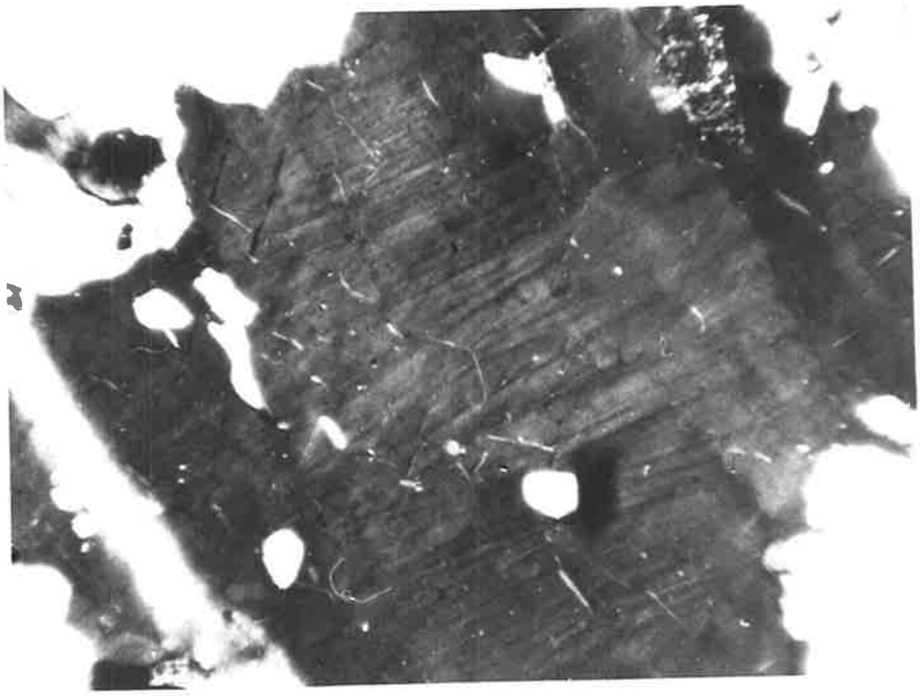

A

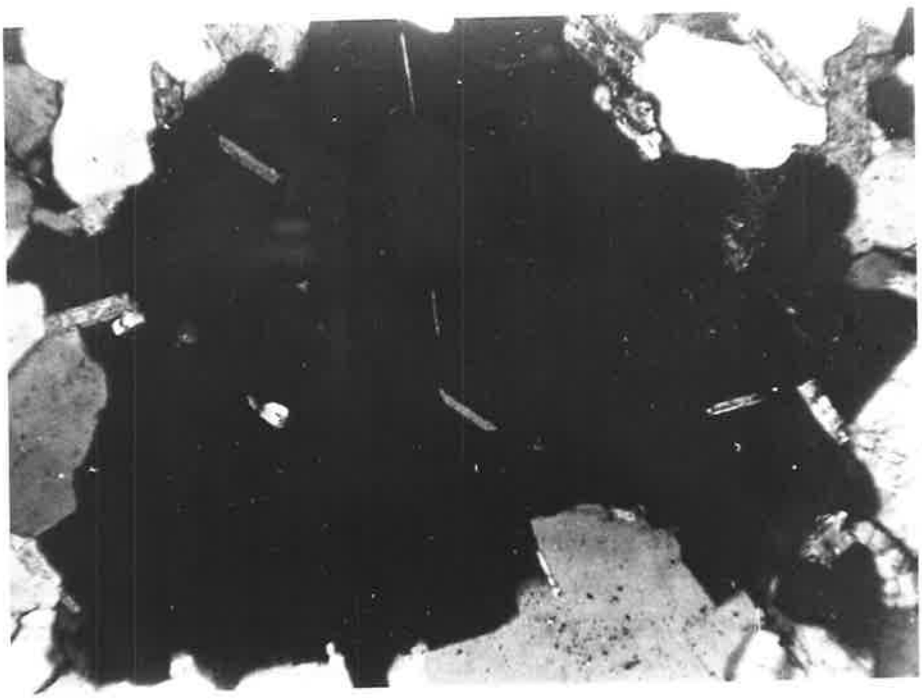

B

PLATE 34

A General view of outcrop pattern of marble.

LOCATION: 197994

B Photomicrograph showing highly deformed marble with deformation twinning and kink bands in calcites. The other minerals are scapolite (white colour), quartz and diopside (high relief, dark grey).

A285/281 Plane pol. light Length of field: 4.5mm.

A

B

PLATE 35

A Photomicrograph of marble (close to the Milendella fault) showing mortar texture due to post-crystallization strain of faulting. A megacryst of diopside with well developed deformation lamellae (e.g. Raleigh & Talbot, 1967), scapolite (white) and sphene (dark grey) are seen in the fine recrystallized matrix of calcite.

A285/690 Plane pol. light Length of field: 1.5mm.

B Photomicrograph of diopside with strongly deformed glide twinning and kinking, probably due to the brittle deformation.

A285/55 Plane pol. light Length of field: 1.5mm.

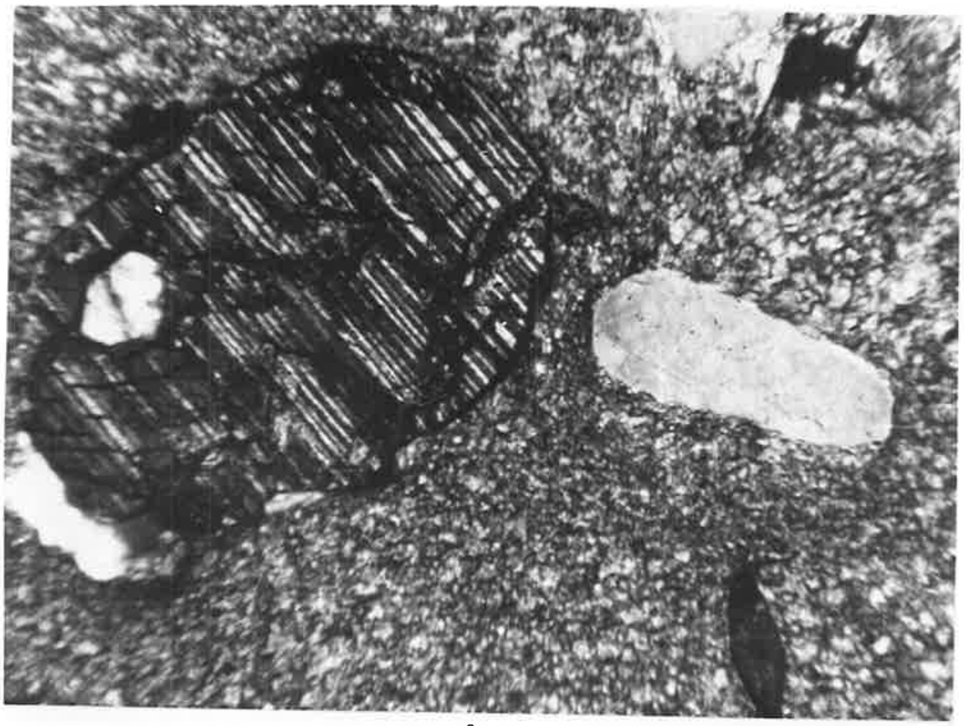

A

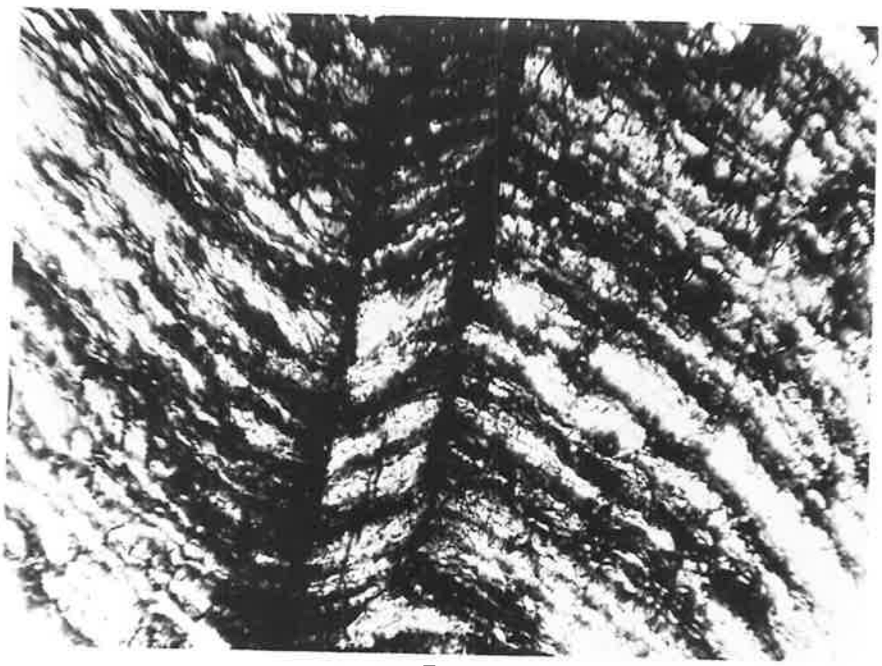

B

PLATE 36

A Photomicrograph of quartz deficient marble with clinohumite (CL) intimately associated with forsterite (FS). The matrix is calcite. Note crystals of spinel (SP).

A285/635 Plane pol. light Length of field: 1.5mm.

B Photomicrograph of marble showing subhedral crystals of spinel (dark grey) in calcite matrix.

A285/635 Plane pol. light Length of field: 1.3mm.

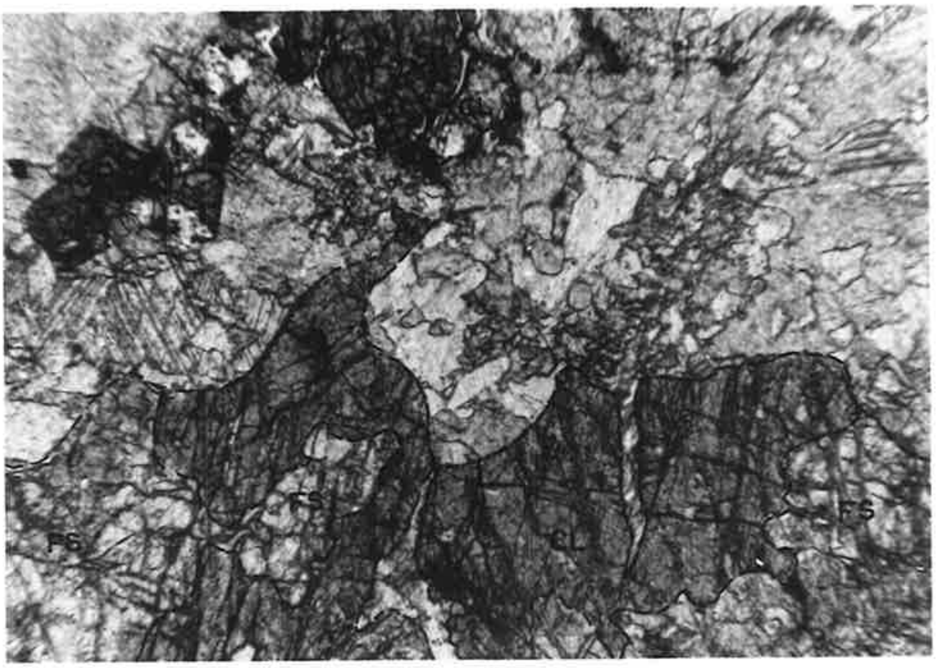

A

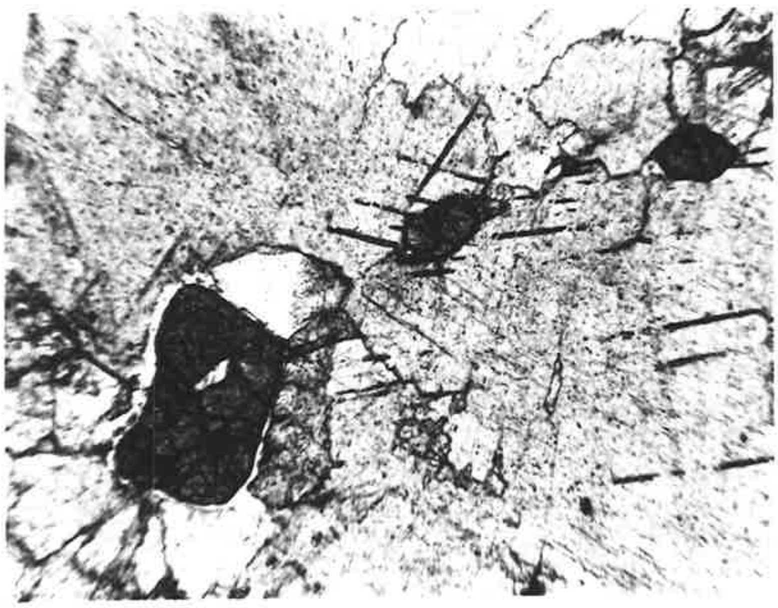

B

PLATE 37

A A general view of outcrop pattern of calc-silicate rocks. Note the prominent uniform thin layerings caused by the alteration of calcite and calc-silicate rich layers.

LOCATION: 196994

B Photomicrograph of diopside with patches of hornblende (dark colour). Note the numerous inclusions of sphene and quartz in diopside. The matrix is composed of scapolite and quartz.

A285/56 Plane pol. light Length of field: 1.5 mm.

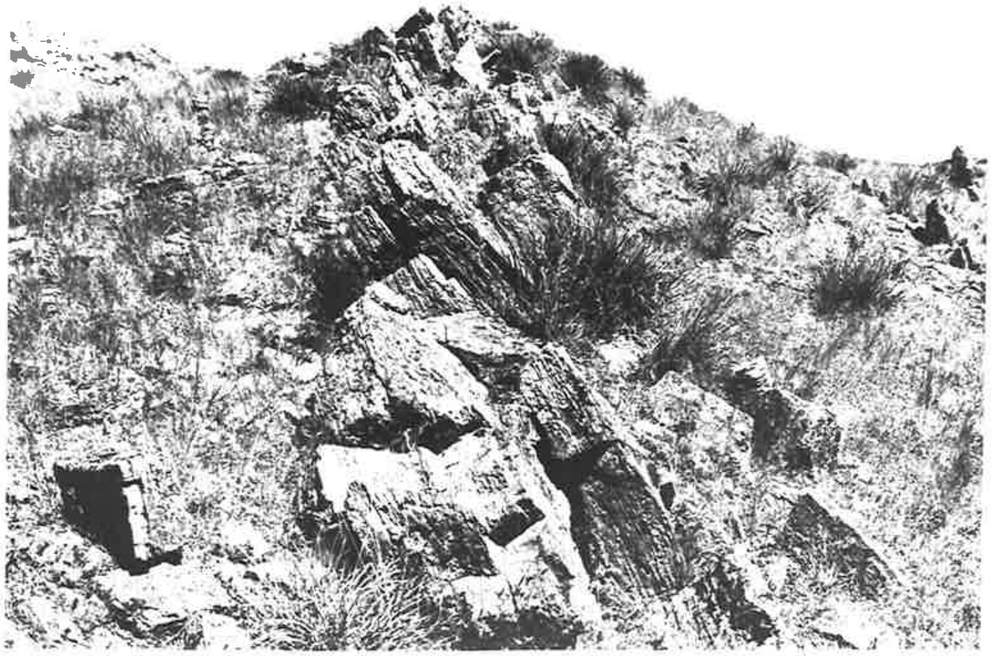

A

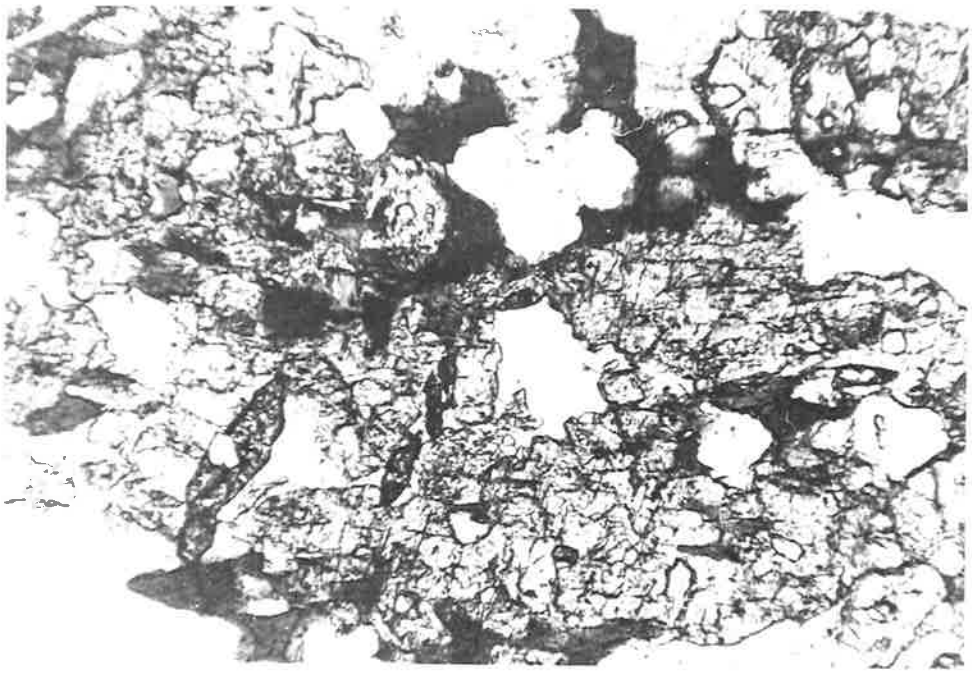

B

PLATE 38

A Photomicrograph of calc-silicate rock containing hornblende. Note inclusions of quartz and sphene. Matrix is mainly composed of quartz, microcline and plagioclase.

A285/357 Plane pol. light Length of field: 2.8mm.

B Photomicrograph of scapolite with a series of parallel partings filled with calcite. Matrix is composed of calcite (light colour), quartz (light grey) and scapolite (white to dark colour).

A285/619 Crossed polars Length of field: 0.5mm.

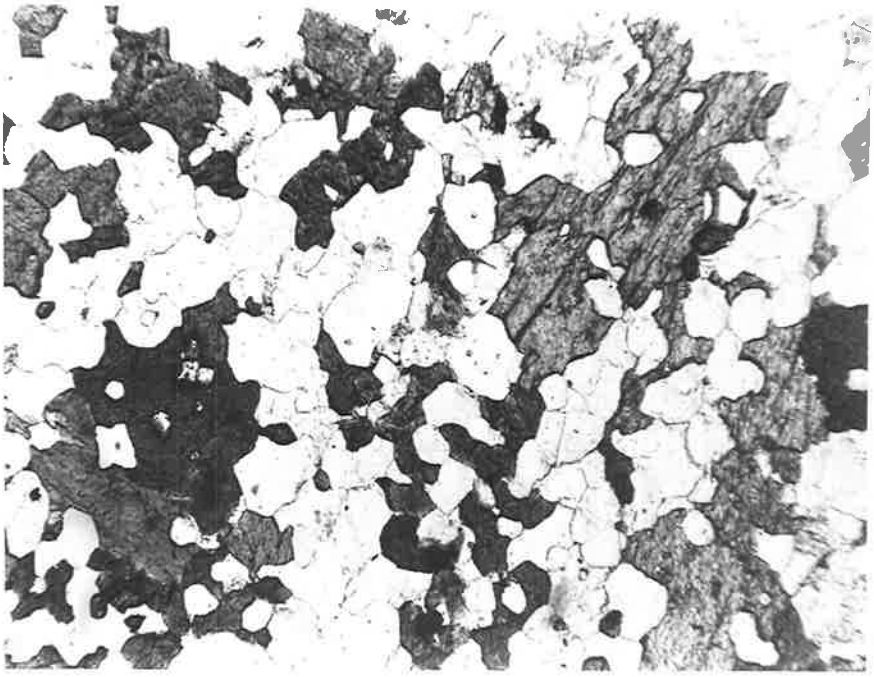

A

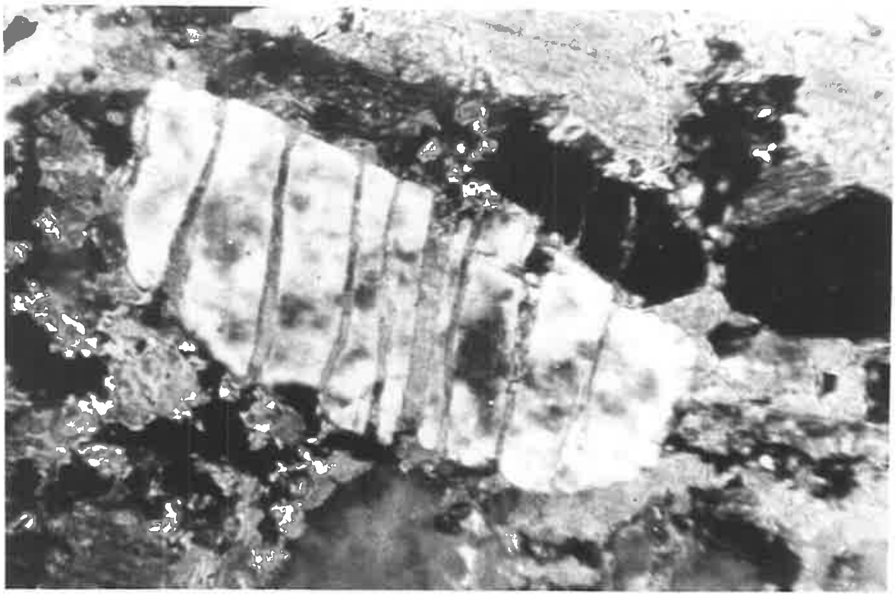

B

PLATE 39

A Photomicrograph of calc-silicate rock showing strongly deformed calcite grains. A scapolite grain is seen in the middle part of photo.

A285/92 Plane pol. light Length of field: 1.5mm.

B Photomicrograph of calc-silicate rock showing well crystallized epidote (dark grey) with scapolite and quartz.

A285/96 Crossed polars Length of field: 1.5mm.

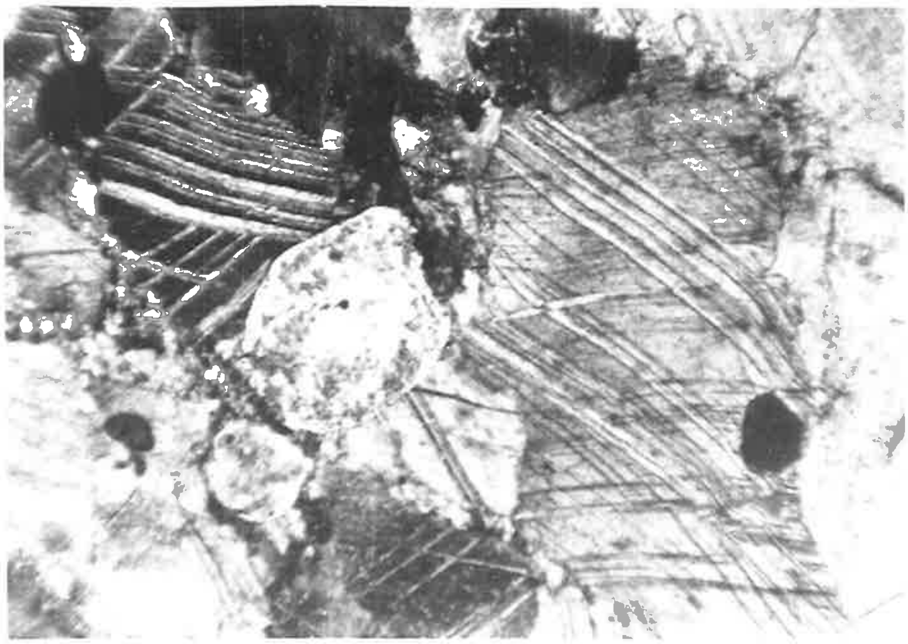

A

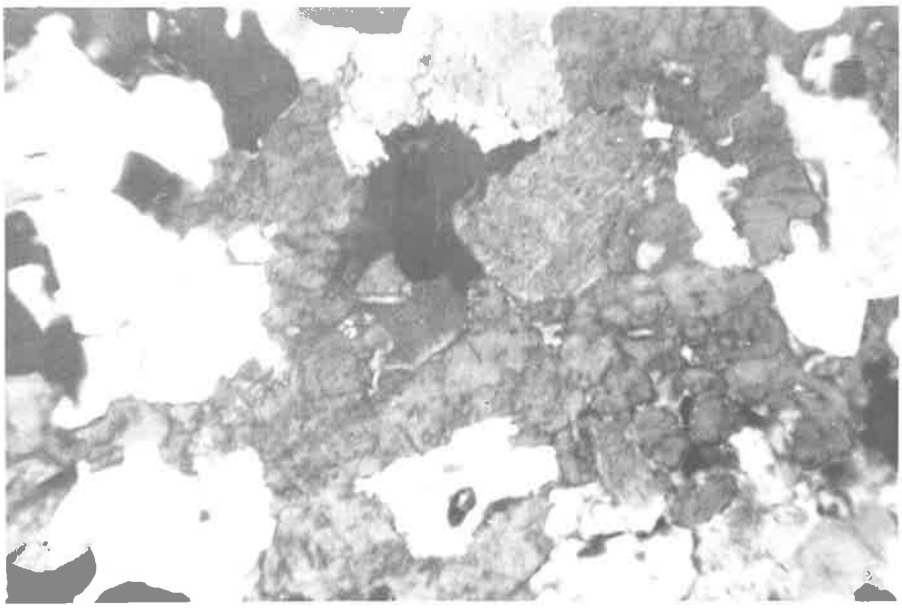

B

PLATE 40

A A general view of the outcrop of the calc-schist.

LOCATION: 162027

B Typical outcrop of the calc-gneiss showing tor-like boulders.

LOCATION: 149021

A

B

PLATE 41

A Photomicrograph of the actinolite schist. Euhedral crystals of actinolite are seen in the central part of photo. The other minerals are quartz and plagioclase (mostly untwinned).

A285/123 Crossed polars Length of field: 1.5mm.

B Photomicrograph of anthophyllite schist. In this section, cut normal to the lineation, the anthophyllite appears as small lozenge-shaped grains.

A285/159 Crossed polars Length of field: 1.5mm.

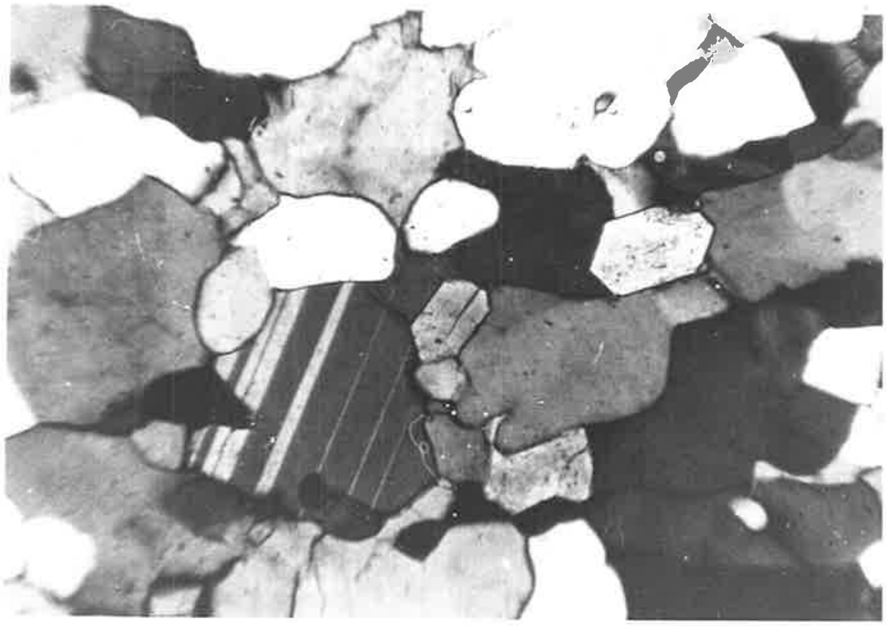

A

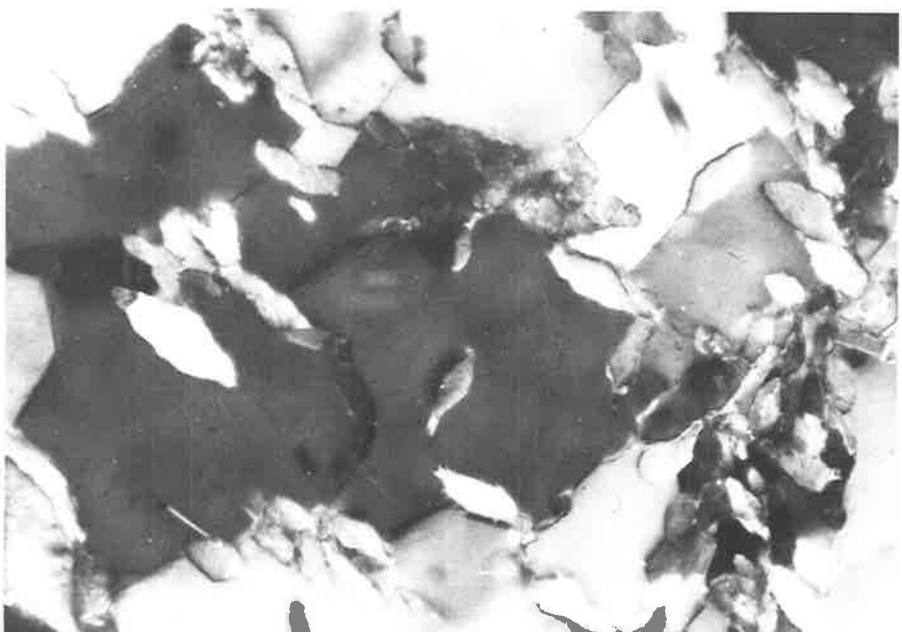

B

PLATE 42

A Photomicrograph of the calc-gneiss showing quartz, plagioclase, diopside (high relief, dark grey) and sphene. Note deformation (glide) twinning in plagioclase.

A285/539 Crossed polars Length of field: 2.8mm.

B Photomicrograph of diopside in the calc-gneiss. Numerous sphene grains occur as inclusions or are closely associated with the diopside.

A285/554 Plane pol. light Length of field: 2.6mm.

A

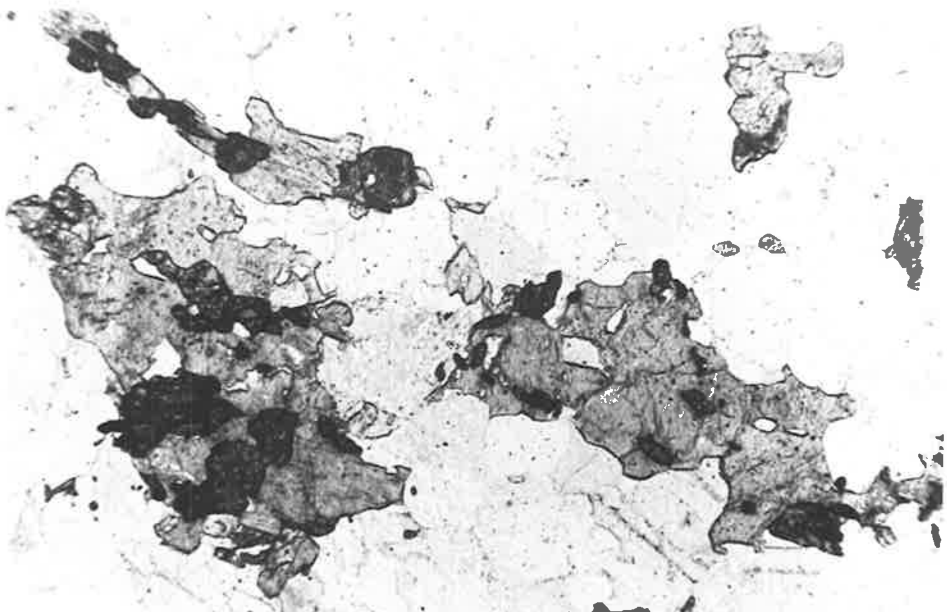

B

PLATE 43

A Photomicrograph of skarn rock: the diopside is surrounded by garnet (black). Note the isolated patches of hornblende (dark colour) in diopside.

A285/674 Crossed polars Length of field: 1.5mm.

B Photomicrograph of skarn rock: the scapolite (white colour) is surrounded by garnet (black). A small grain of diopside (grey) is seen on the right-hand side of photo.

A285/682 Crossed polars Length of field: 1.5mm.

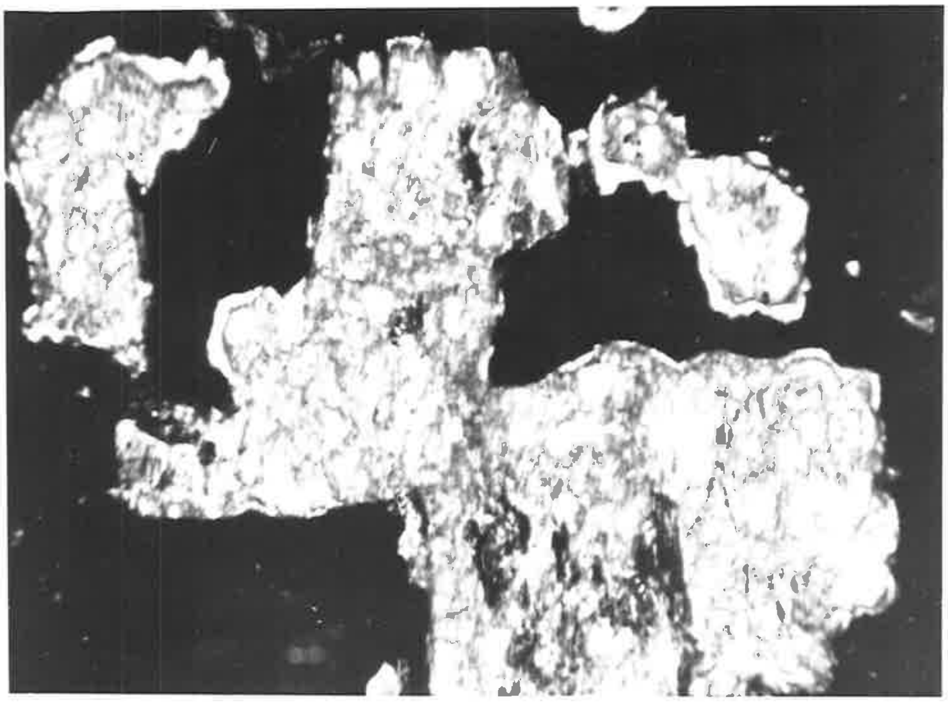

-A

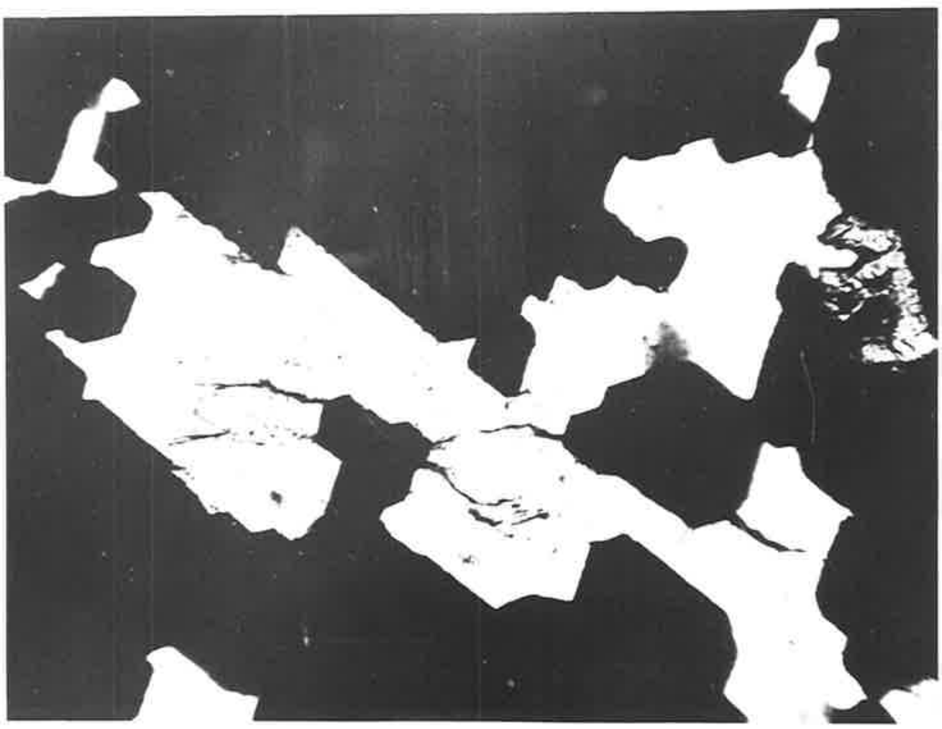

B

PLATE 44

A Photomicrograph of skarn rock showing well crystallized epidote (E), hornblende (H) and garnet (black). Scapolite (clear white) either occurs as inclusions or associated with other minerals.

A285/99 Crossed polars Length of field: 1.5mm.

B Photomicrograph of secondary epidote (dark grey) in the highly altered scapolite (light grey). An unaltered scapolite (dark colour) is seen on the top left-hand corner of photo.

A285/54 Crossed polars Length of field: 1mm.

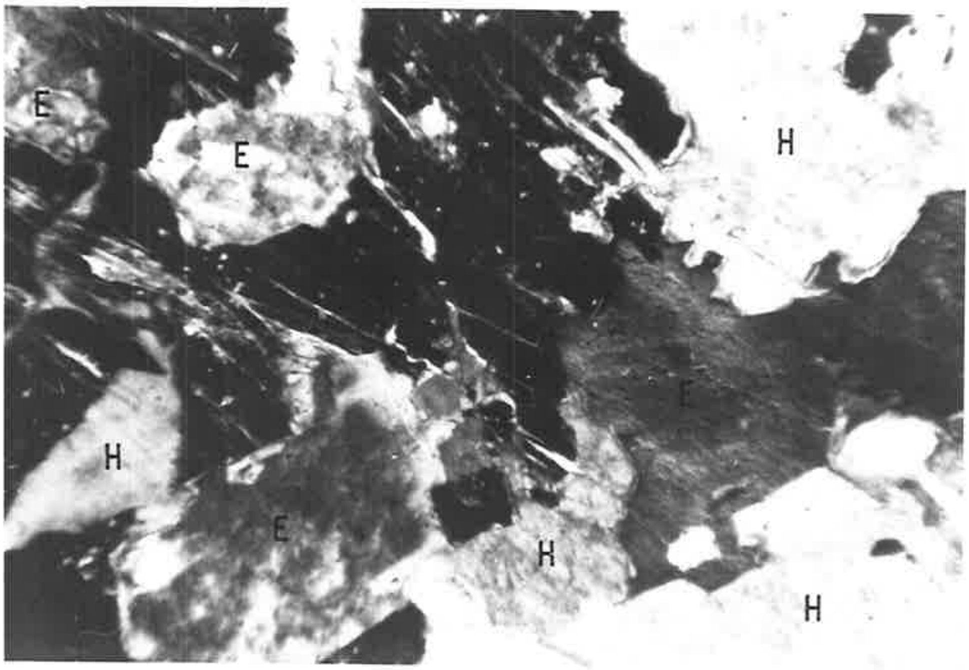
E
E
H
H
E
H
H

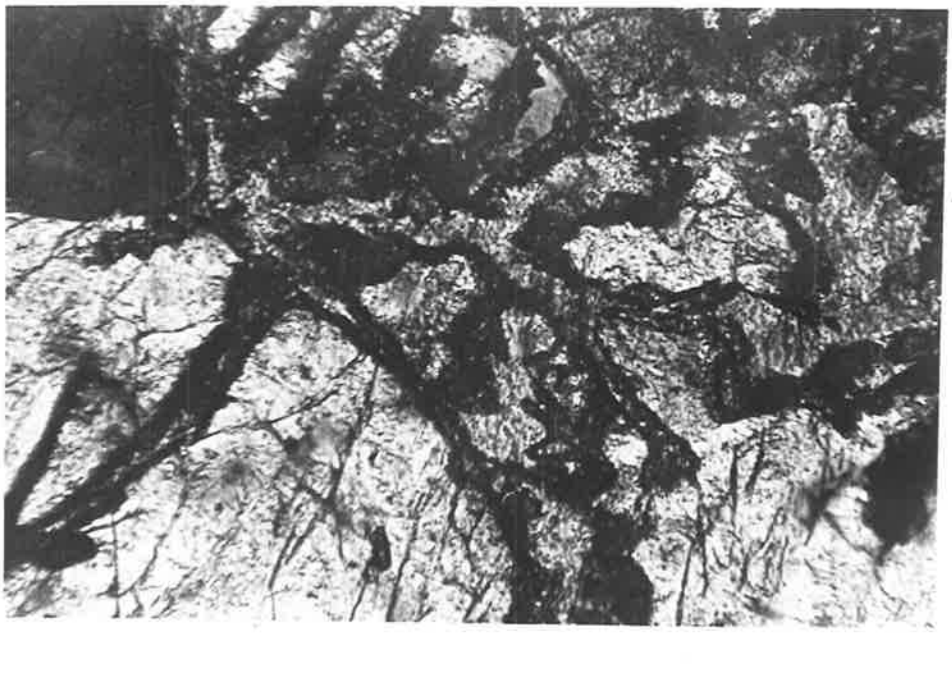

PLATE 45

A Photomicrograph of potash feldspar gneiss showing syntectonic potash feldspar poikiloblasts. Small inclusions in K-feldspar are quartz, plagioclase and biotite.

A285/14 Crossed polars Length of field: 4.5mm.

B Photomicrograph of potash feldspar gneiss. The post tectonic potash feldspar porphyroblast appears to displace the S_1 schistosity during its growth.

A285/445 Crossed polars Length of field: 9mm.

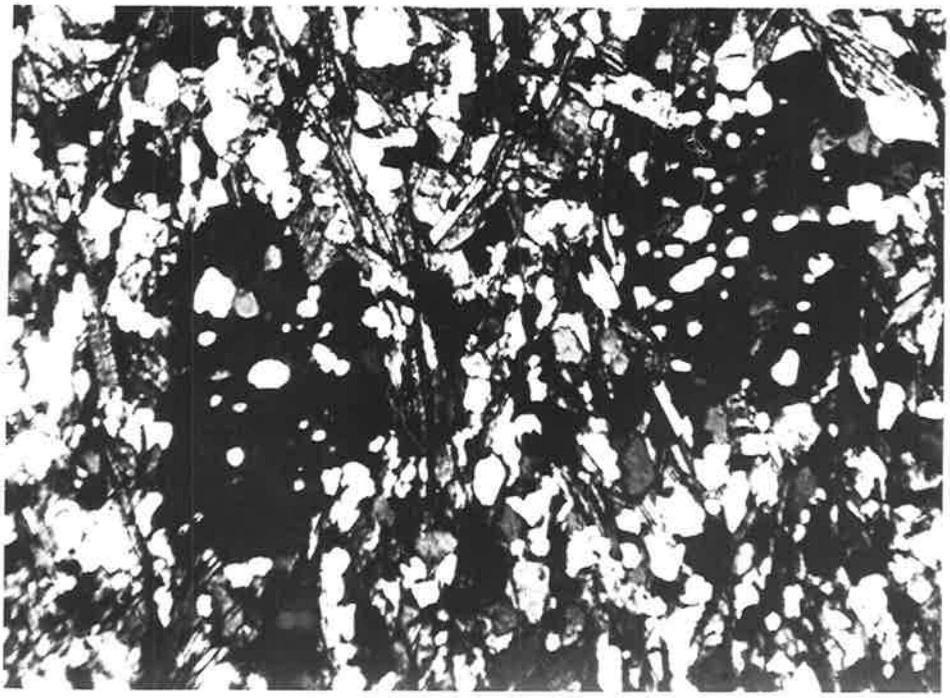

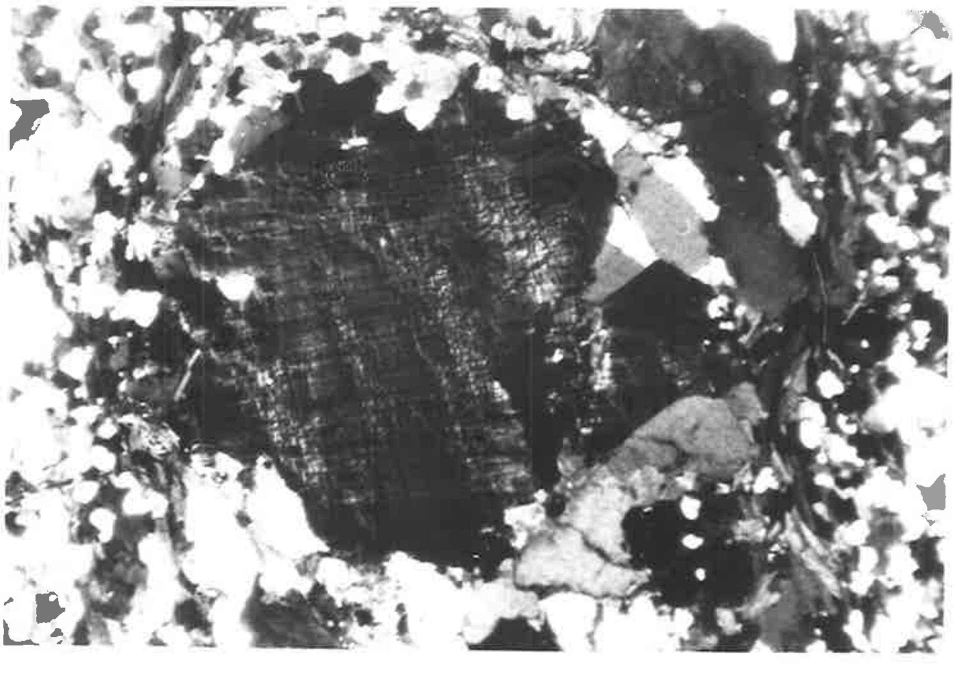

PLATE 46

A Photomicrograph of helicitic potash feldspar containing S_1 (defined by preferred orientation of biotite plates) at a high angle to S_2. Note the fine hair perthite in K-feldspar porphyroblast.

A285/14 Crossed polars Length of field: 2.8mm.

B Photomicrograph of syntectonic (F_1) potash feldspar poikiloblast (white colour) in the gneiss. Inclusion in potash feldspar are quartz, plagioclase and biotite.

A285/445 Crossed polars Length of field: 9mm.

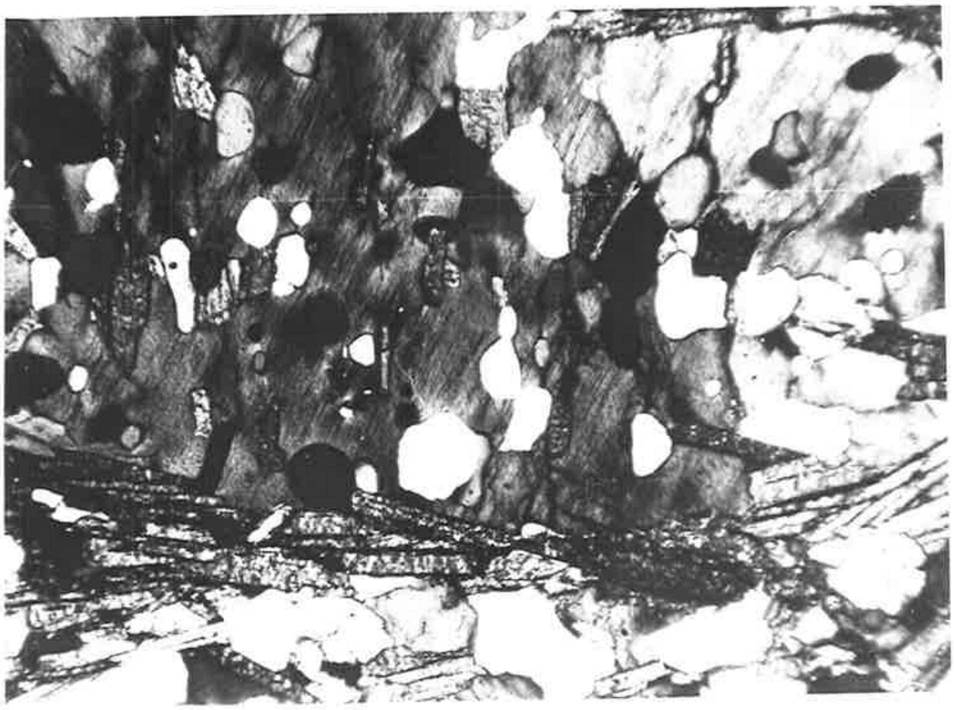

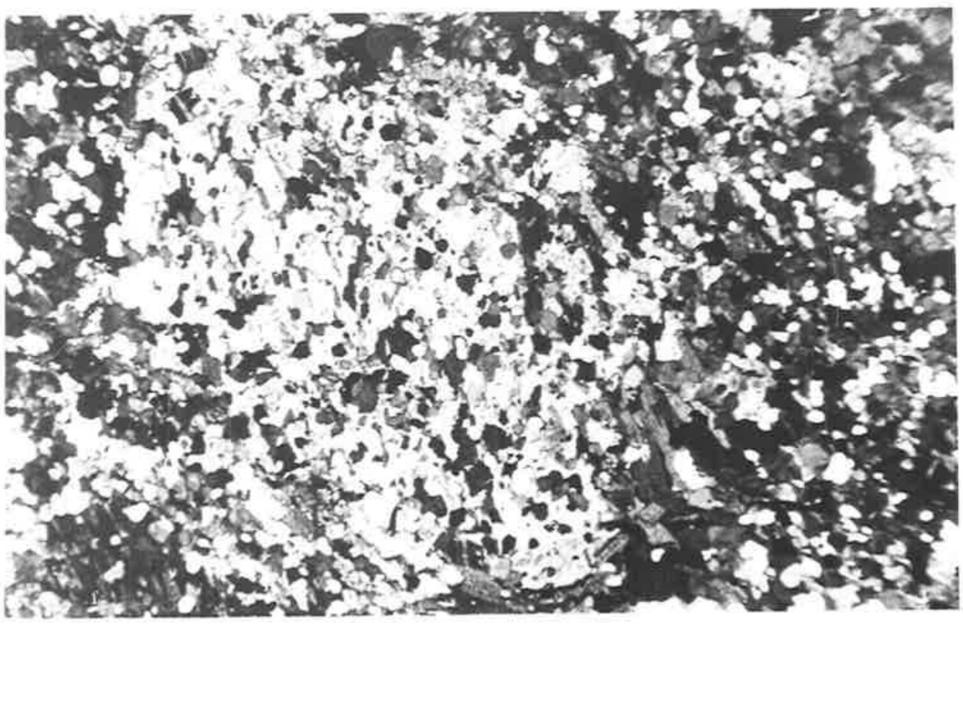

PLATE 47

A Photomicrograph of mica schist. Ovoid porphyroblasts of muscovite appear to transect the S_1 schistosity which is defined by fine plates of biotite and muscovite.

A285/84 Crossed polars Length of field: 9mm.

B Photomicrograph of porphyroblastic muscovite in mica schist. Note the inclusions of quartz and biotite in porphyroblastic muscovite.

A285/73 Crossed polars Length of field: 2.8mm.

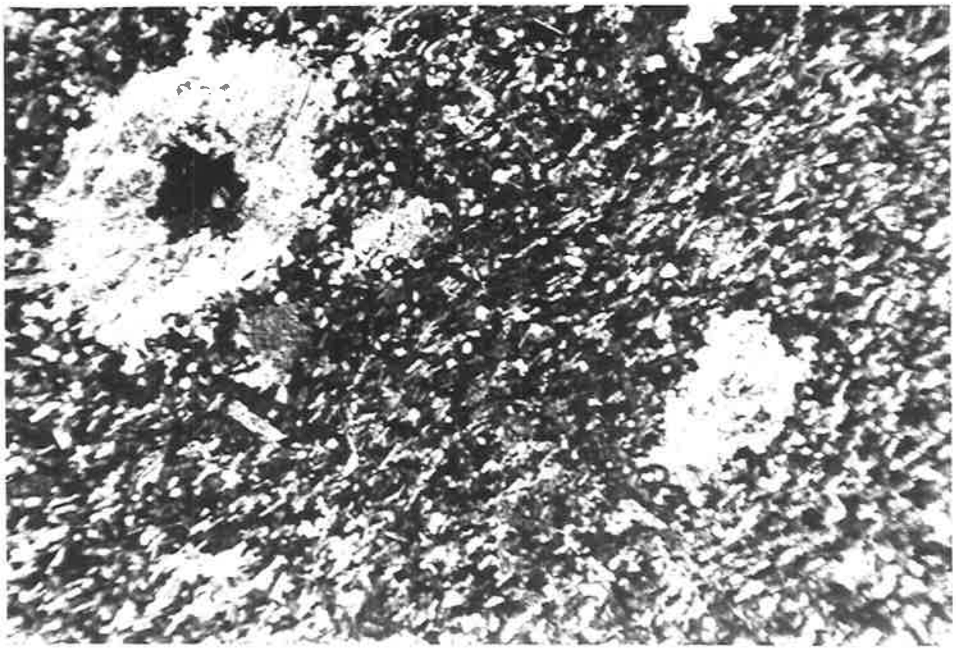

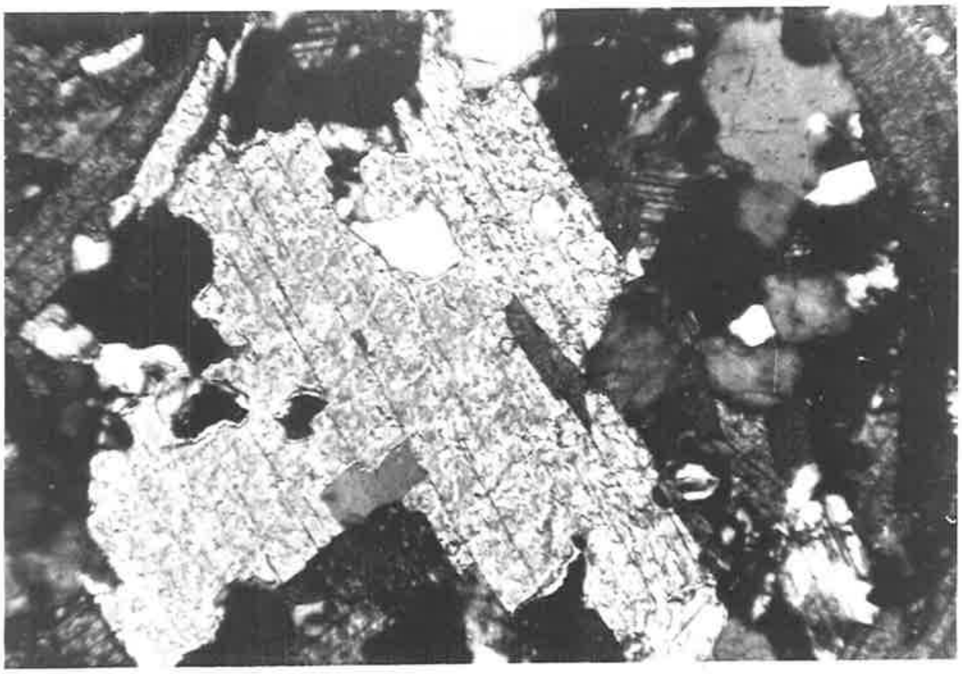

PLATE 48

A A general view of the Cooke Hill tonalite: tor-like boulders form the typical outcrop pattern.

SCALE: Hammer 3 foot long

LOCATION: 193065

B Xenoliths of quartzo-feldspathic gneiss in the Cooke Hill tonalite.

SCALE: Ruler 15cm.

LOCATION: 179042

A

B

PLATE 49

A Photomicrograph of a granitized rock near a Cooke Hill tonalite dyke. The highly altered plagioclase and quartz are the main constituents of the rock.

A285/294C Crossed polars Length of field: 9mm.

B Photomicrograph of altered plagioclase in the granitized rock. Sericitization and muscovitization is generally more common in the core of plagioclases.

A285/294C Crossed polars Length of field: 2.8mm.

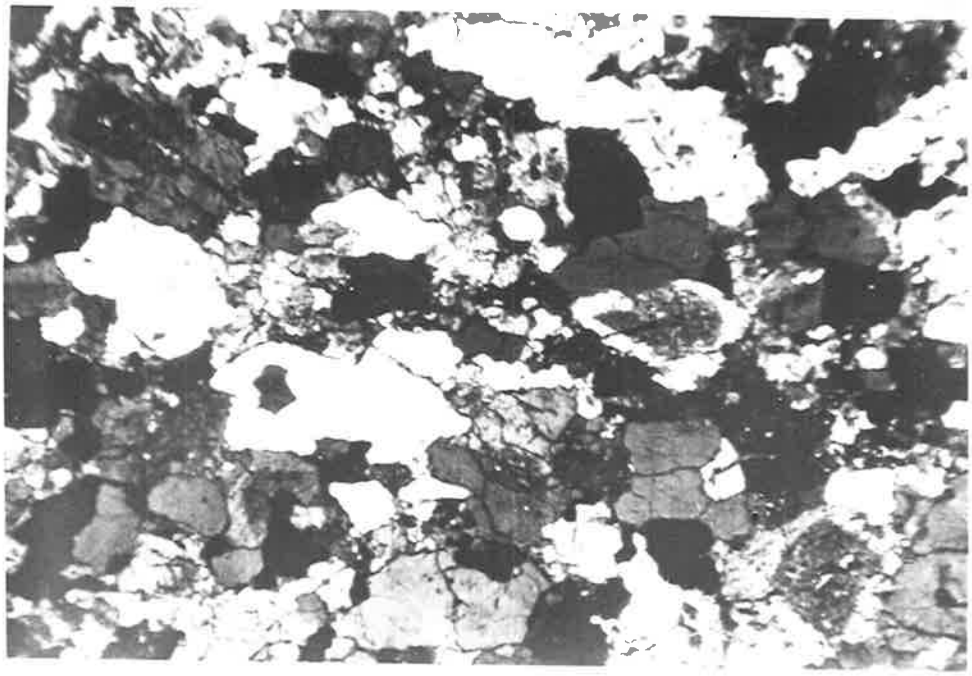

PLATE 50

A Photomicrograph of the Cooke Hill tonalite. The quartz, plagioclase and biotite are the main minerals shown in the photo.

A285/75 Crossed polars Length of field: 2.8mm.

B Photomicrograph of the Cooke Hill granodiorite showing quartz, plagioclase, potash feldspar and biotite.

A285/232 Crossed polars Length of field: 2.8mm.

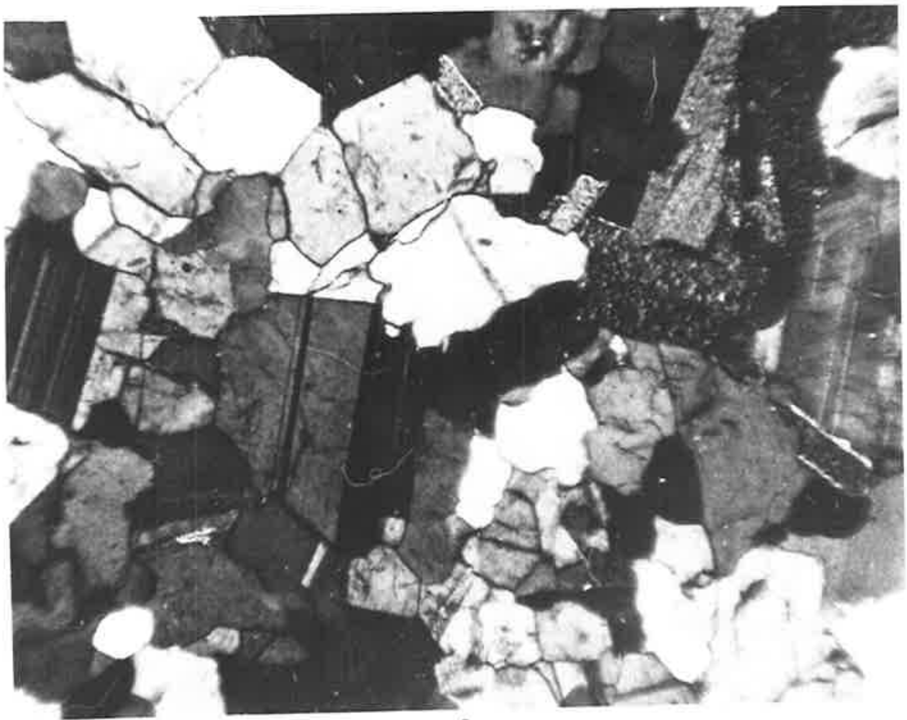

A

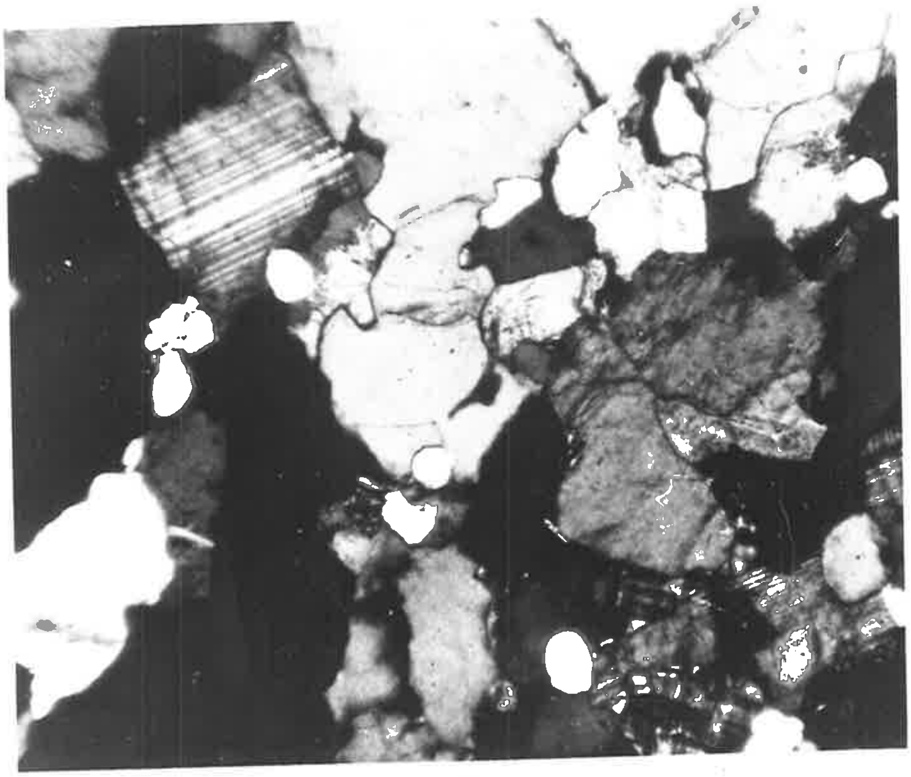

B

PLATE 51

A Photomicrograph showing oscillatory zoned plagioclase in the Cooke Hill tonalite. Note the sericitized core of plagioclase.

A285/188 Crossed polars Length of field: 2mm.

B Photomicrograph showing oscillatory zoned plagioclase in the Cooke Hill granodiorite. Note sericitization and secondary muscovites in the core.

A285/137 Crossed polars Length of field: 2mm.

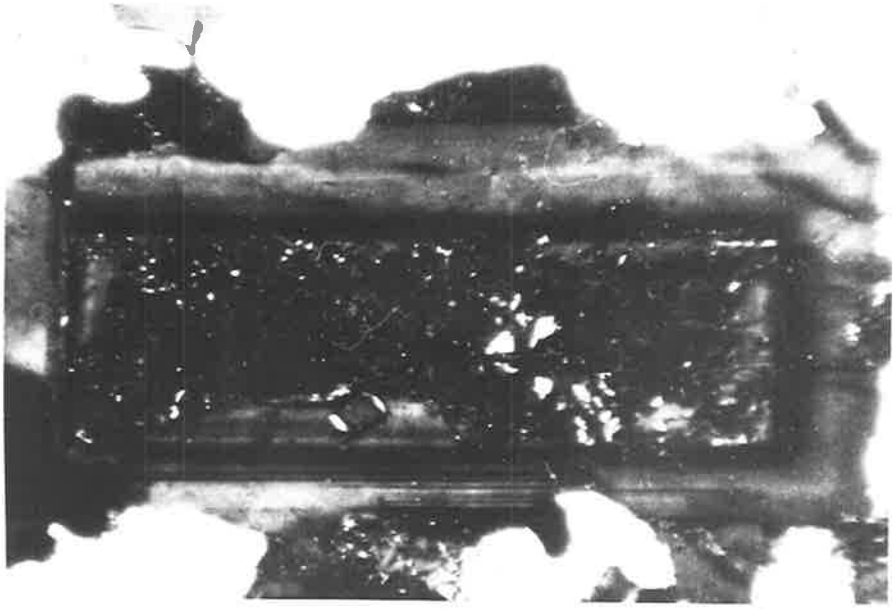

A

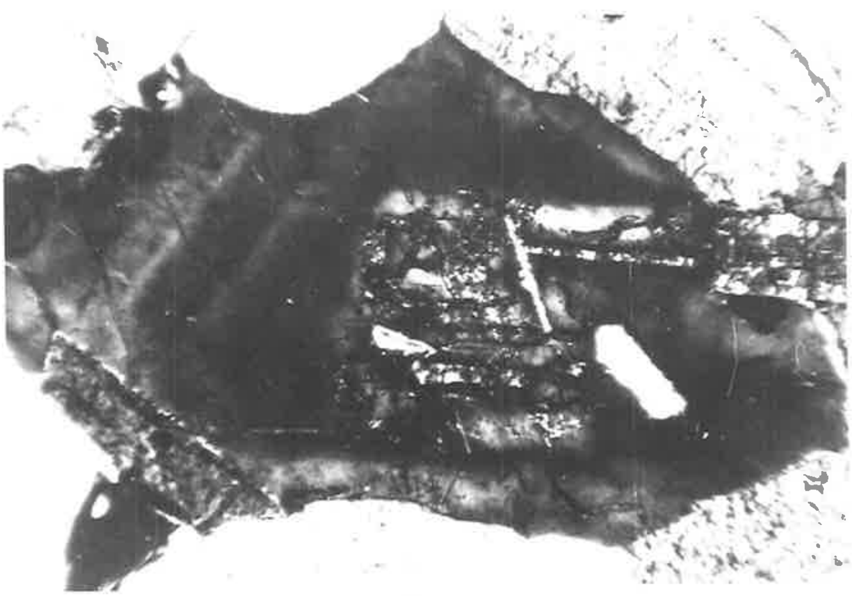

B

PLATE 52

A Photomicrograph of the Massive granodiorite. Note zoning in some plagioclase.

A285/208 Crossed polars Length of field: 2.8mm.

B Photomicrograph of oscillatory zoned plagioclase in the Massive granodiorite.

A285/208 Crossed polars Length of field: 1.5mm.

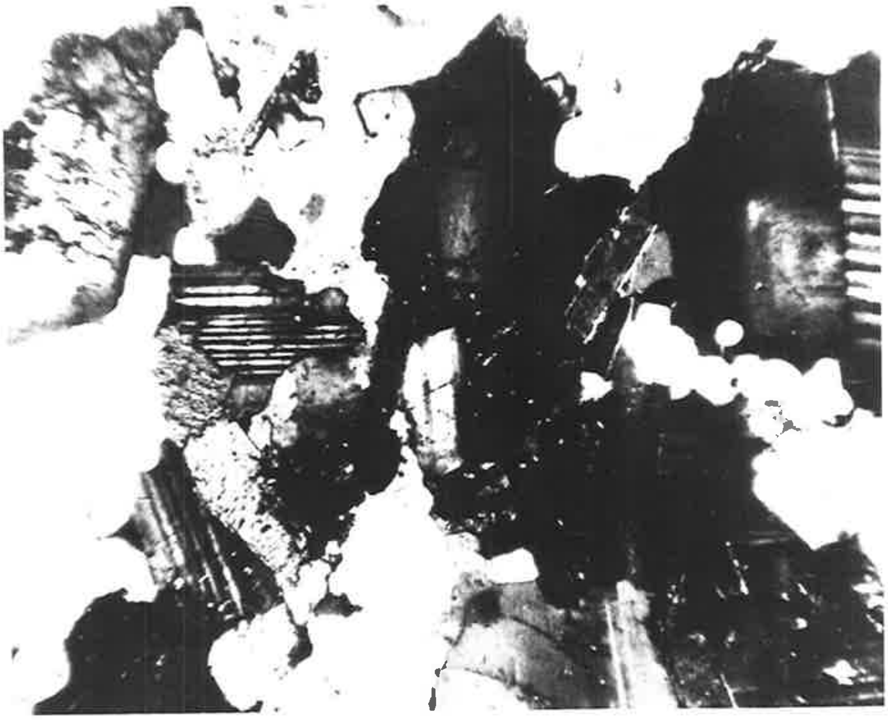

A

B

PLATE 53

A Photomicrograph of foliated pegmatite showing quartz, potash feldspar, plagioclase and small amount of biotite.

A285/221 Crossed polars Length of field: 9mm.

B Photomicrograph of metadolerite with quartz, plagioclase, hornblende (light to dark colour) and biotite (B).

A285/446 Crossed polars Length of field: 2.8mm.

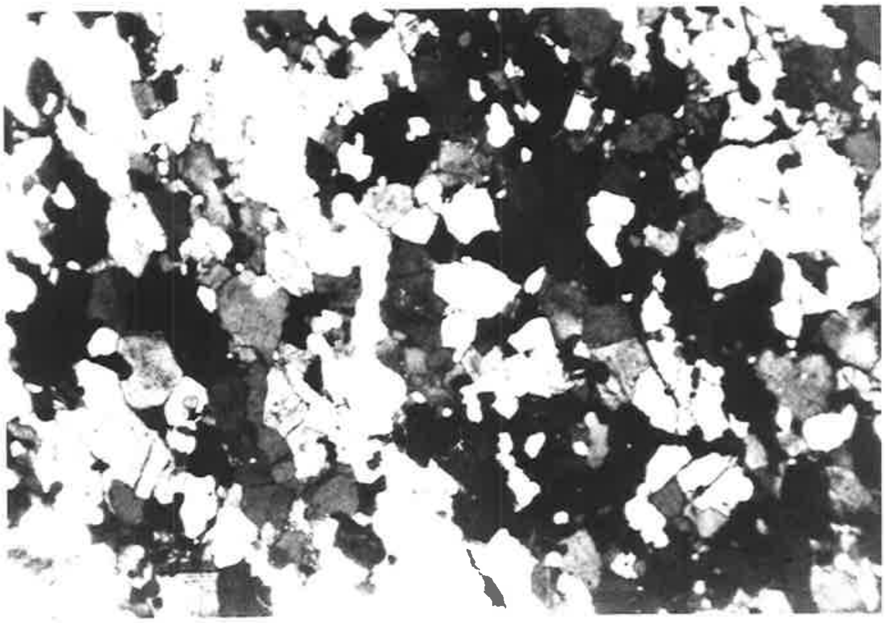


B